

NASA Contractor Report 3935

168p.

# Calculation of Water Drop Trajectories To and About Arbitrary Three-Dimensional Lifting and Nonlifting Bodies in Potential Airflow

Hillyer G. Norment

CONTRACT NAS3-22146  
OCTOBER 1985

Date for general release October 1986

**NASA**

NASA Contractor Report 3935

Calculation of Water Drop  
Trajectories To and About  
Arbitrary Three-Dimensional  
Lifting and Nonlifting Bodies  
in Potential Airflow

Hillyer G. Norment  
*Atmospheric Science Associates*  
*Bedford, Massachusetts*

Prepared for  
Lewis Research Center  
under Contract NAS3-22146



National Aeronautics  
and Space Administration

Scientific and Technical  
Information Branch

1985

## TABLE OF CONTENTS

	<u>Page</u>
SUMMARY	1
INTRODUCTION	3
METHODOLOGY	10
THREE-DIMENSIONAL FLOW	10
PARTICLE TRAJECTORY CALCULATION	15
AERODYNAMIC DRAG ON WATER DROPS	16
FLOW CODE DESCRIPTIONS	18
PROGRAM PBOXC	18
General Discussion	18
Coordinate System	19
Symmetry Planes	20
Surface Description Data for General Nonlifting Sections (IFLAG = 0)	21
Surface Description Data for Lifting Sections - General	24
Surface Description Data for Lifting Sections - Extra Strips and Ignored Elements	26
Surface Description Data for Generated Ellipsoids (IFLAG = 1 or 2)	27
Printed Output	30
Subroutines Required	31
External Storage Units	31
PBOXC Card Input	32
DUGLFT	34
General Discussion	34
Body Surface and Wake Description	34
Semi-Infinite Last Wake Element Option	35
Flow Inlets	35
Off-Body Points	36
Symmetry Planes	36
Uniform Onset Flow (Free Stream Flow)	37
Correction for Compressibility Effects	38
The Kutta Condition: Pressure Equality and Flow Tangency Options	38

	<u>Page</u>
Spanwise Variation of Vorticity: Step Function and Piecewise Linear Options	39
End Conditions for Lifting Sections When the Piecewise Linear Option is Exercised: Parameters NLINE1 and NLINEN	40
Forces and Moments	43
Variable Array Dimensioning	43
Printed Output	45
Unit 18 Output	55
Segmentation Structure	57
Peripheral Storage	59
DUGLFT Card Input	61
SUBROUTINE FLOVEL	66
General Discussion	66
Body Penetration Tests	67
Special Calculations	69
Array Dimensions	70
SUBROUTINE SETFLO	70
PROGRAM FLOPNT	71
General Description	71
FLOPNT Card Input	73
TRAJECTORY CODE DESCRIPTIONS	74
GENERAL UTILITY CODES	74
Subroutine PARTCL	74
Subroutine TRAJEC	74
Function PRFUN	75
Subroutine IMPACT	75
Subroutine DVDQ	76
PROGRAM ARYTRJ	76
General Description	76
Subroutines Required	77
External Storage Units	77
Printed Output	78

	<u>Page</u>
ARYTRJ Card Input	79
PROGRAM CONFAC	80
General Discussion	80
Subroutines Required	81
External Storage Units	81
Printed Output	81
CONFAC Card Input	84
PROGRAM TANTRA	86
General Discussion	86
Subroutines Required	87
External Storage Units	87
Printed Output	88
TANTRA Card Input	89
PROGRAM STEREO	91
General Discussion	91
External Storage Units	93
Printed Output	93
STEREO Card Input	94
VALIDATION	95
PRIOR WORK	95
ADDITIONAL VERIFICATION	96
CALCULATION TIMES	103
IBM 370/3033 Computer	103
CDC 6600 Computer	104
Discussion	105
EXAMPLE PROBLEM	106
GENERAL DISCUSSION	106
THE TEST BODY	106
EXAMPLE PROBLEM CALCULATION	106
CALCULATION TIMES	106
EXAMPLE PROBLEM CARD INPUT	109

	<u>Page</u>
DUGLFT	109
Listing of No. 12 Data Cards for DUGLFT Test Problem	110
FLOPNT	112
EXAMPLE PROBLEM PRINTOUTS	113
DUGLFT	113
FLOPNT	139
APPENDIX A - PRANDTL-GLAUERT COMPRESSIBILITY CORRECTION	141
APPENDIX B - BODY PENETRATION TESTS	145
INTRODUCTION	145
NONLIFTING ELEMENTS	146
LIFTING ELEMENTS	148
APPENDIX C - SPECIAL SOURCE AND DIPOLE CONTRIBUTION CALCULATIONS	150
INTRODUCTION	150
GENERAL	150
SOURCE CONTRIBUTION TERMS	153
DIPOLE CONTRIBUTION TERMS	155
REFERENCES	160

CALCULATION OF WATER DROP TRAJECTORIES TO AND ABOUT ARBITRARY  
THREE-DIMENSIONAL LIFTING AND NONLIFTING BODIES IN POTENTIAL AIRFLOW

by Hillyer G. Norment  
Atmospheric Science Associates

SUMMARY

Computer programs are described by which trajectories of water drops can be calculated to and about three-dimensional bodies of arbitrary shape, which can have lifting surfaces, nonlifting surfaces or combinations of lifting and nonlifting surfaces. External potential airflow about a body is computed at subsonic air speed for any atmospheric conditions. Compressibility effects can be accounted for approximately. Flow into an inlet can be accommodated, provided that the intake flow rate is specified. To calculate water drop trajectories, experimentally derived relations between Reynolds and Davies numbers for water drops of all sizes, from the smallest cloud droplets to large raindrops, are used to represent effects of aerodynamic drag on the particles during integration of the water drop equations of motion, and effects of gravity settling are included. A variable time step numerical integration method is used.

The surface of the three-dimensional body is approximated by plane quadrilateral panels, over each of which a uniform potential source is assumed to be distributed. Source densities, lift vorticity and the resulting potential flow field are calculated by the Hess method. The codes are open-ended in their capacities to accommodate numbers of quadrilateral panels and other geometric complexities needed to define a body surface.

The following seven codes are described:

1. A code used to debug and plot body surface data.
2. A modified version of the Hess lifting code which processes the body data and yields data required to compute flow velocities at arbitrary points in space.

3. A code that computes flow velocities at arrays of points in three-dimensional space.
4. A code that computes trajectories of water drops toward the body from arrays of initial points in space.
5. A code that computes water drop trajectories and water drop fluxes to arbitrary target points.
6. A code that computes water drop trajectories tangent to the body.
7. A code that produces stereo pair plots that include both the body and trajectories.

Code 1 and codes 4-7 are essentially the same as those described in NASA CR 3291. Code descriptions include operating instructions, card inputs and printouts for example problems. The FORTRAN IV source codes are available through COSMIC.

Various tests of simulation accuracy are discussed, and, in general, accuracy is found to be acceptable. Calculated tangent trajectory results are compared with wind tunnel data and reasonable agreement is found. In comparison with the same experimental data, the new calculations show substantial improvement over prior calculations.

## INTRODUCTION

A resurgence of interest in aircraft icing (ref. 1) has stimulated work on computer simulation of icing. Of critical importance to icing simulation are codes that compute trajectories of water drops, and other hydrometeors, to and about aircraft structures. We have recently published, in NASA CR 3291 (ref. 2), a set of codes that compute water drop trajectories about arbitrary three-dimensional nonlifting bodies; the codes described here are similar to, in many cases are identical to, those described there. The new codes do everything the old ones do, plus account for effects on the flow of lift vorticity, if any. Another major difference is that the new codes use variable array dimensioning so that the storage requirements of the code can be tailored to the problem at hand.

We distinguish two major categories of codes: flow codes and trajectory codes. The flow codes process data that describe the three-dimensional body and compute the fluid flow field around that body;\* they are modified versions of the lifting flow codes developed by Hess (ref. 3). The trajectory codes use the flow codes' calculation results to compute trajectories of particles to and about the body. For aircraft icing studies, the body is, of course, an aircraft, the fluid is air and the particles usually are water drops. Table 1 identifies and briefly describes the executive codes in the two categories, and Table 2 does the same for the subroutine and function codes.

As mentioned above, many of the codes are essentially the same as those described in NASA CR 3291 (ref. 2), and these are marked with asterisks in Tables 1 and 2. The user is cautioned to realize that while some of the new code subroutines may have the same names as their functional counterparts in the nonlifting code, it does not follow that they are the same. In fact they should be assumed to be entirely different unless they are marked with asterisks.

---

\*It is immaterial whether we consider the fluid to be stationary and the body in motion, or vice versa, but it is expedient here to consider the body stationary and the fluid in motion.

TABLE 1  
EXECUTIVE CODES

A. FLOW CODES

Code	Description
PBOXC*	Processes and plots data which define the three-dimensional body. Used to debug and plot the body data.
DUGLFT	Processes three-dimensional lifting and/or nonlifting body data and prepares and stores data to be used by SR FLOVEL to calculate flow velocities as needed during trajectory calculations.
FLOPNT*	Computes and prints flow velocities at user-specified arrays of points in space.

B. TRAJECTORY CODES

Code	Description
ARYTRJ*	Computes trajectories, which begin at user-specified arrays of points in space, to and/or about the body.
CONFAC*	Computes trajectories from the free stream to user-specified points in space. Also computes particle concentration factors at user-specified points in space. (Concentration factor is ratio of particle flux at the target point to free stream particle flux.)
TANTRA*	Computes trajectories tangent to the body which are initiated along user-specified lines in the free stream. (Tangent trajectories are those trajectories that barely miss intersection with the body.)
STEREO*	Prepares stereo-pair plots of the body along with particle trajectories.

\*This code is essentially the same as the code of the same name that is described in NASA CR 3291 (ref. 2).

TABLE 2  
SUBROUTINE AND FUNCTION CODES

A. FLOW CODES

Code	Called By	Description
AIJMX	SIGMAL	Computes the matrix, $A_{ij}$ , of dot products of source induced velocities with normal vectors to the on-body elements (ref. 3, eq. (7.12.1)).
BVORTX	CONTRL	Calls PKUTTA or FKUTTA to calculate vortex strength per unit path length around the $k$ th lifting strip, $B^{(k)}$ , for all lifting strips.
CKARRY	CONTRL	Cross checks storage array capacities.
COLSOL	SIGMAL	Solves the linear equation matrices (ref. 3, eq. (7.12.5)) for element source densities.
CONTRL	DUGLFT	Controls flow of the modified Hess code which processes body surface data for use by the flow and trajectory codes.
DATPRS	INPUTL	Translates, scales and rotates about the y axis surface description data immediately after input.
DKEKFK	PISWIS	Calculates $D_k$ , $E_k$ and $F_k$ for use in calculating piecewise linear spanwise variation of $B^{(k)}$ . (ref. 3, eq. (7.11.5)).
FKUTTA	BVORTX	Computes vortex strength, $B^{(k)}$ , for each lifting strip by the flow tangency method.
FLOVEL <sup>†</sup>	TRAJEC* CONFAC* ARYTRJ* FLOPNT*	Returns flow velocity for a given point in space.
HEADER	CONTRL INPUTL NOLIFT LIFT VIJMX PNTVIJ DKEKFK UNIFLO SIGMAL AIJMX NIKMX VELOCITY PRINTL	Writes a printout header.
INPUTL	CONTRL	Inputs surface quadrilateral corner coordinates and controls computation of the geometric properties of the quadrilaterals. Also prints the first major DUGLFT output.
LIFT	INPUTL	Computes geometric properties of lifting quadrilateral elements (ref. 3, sec. 7.2).

TABLE 2, cont.

Code	Called By	Description
MIS1	PKUTTA FKUTTA	Linear equation solver. Used in calculation of vortex strengths, $B^{(k)}$ , of lifting strips.
NEAR	VFMLFT	Computes source and vortex induced velocities from an element in a lifting strip using the near-field equations.
NEARF <sup>†</sup>	VFLIFT <sup>†</sup>	Computes source and vortex induced velocities from an element in a lifting strip using the near-field equations.
NIKMX	SIGMAL	Computes the right hand sides of the $A_{ij}$ matrix, $N_i^{(k)}$ and $N_i^{(\infty)}$ , which are the dot products of the onset flows with the unit normal vectors to the on-body elements. (ref. 3, eqs. (7.12.5)).
NOLIFT	INPUTL	Calculates geometric quantities for quadrilateral elements in a nonlifting section. (ref. 4, sec. 9.2).
PATPRS*	PINPUT*	Translates, scales and rotates about the y axis surface description data immediately after input.
PEADER*	PINPUT*	Writes a printout header.
PICTUR*	PBOXC*	Plots the body surface data.
PINPUT*	PBOXC*	Processes input body coordinate data into quadrilaterals. Produces the non-lifting code "first output" (ref. 4, sec. 9.4).
PISWIS	VMATRIX	Calculates $\vec{V}_{ik}^{(0)}$ and $\vec{V}_{ik}^{(1)}$ according to equation (7.11.2) of reference 3, and calls DKEFK and PSONST to calculate vortex induced onset flows. Used only for piecewise linear spanwise variation of vortex strength.
PKUTTA	BVORTX	Computes vortex strength, $B^{(k)}$ , for each lifting strip by the pressure equality method.
PNTVIJ	VMATRIX	If so requested (for debugging purposes only), prints all source induced velocities, $\vec{V}_{ij}$ , and all vortex induced velocities, $\vec{V}_{ij}^{(F)}$ and $\vec{V}_{ij}^{(S)}$ .
PRINTL	VELOCITY	Prints the final output of the DUGLFT computations.
PSONST	PISWIS	Computes vortex induced onset flows when the piecewise-linear method of spanwise variation of vortex strength is used.
READ1	SIGMAL COLSOL PKUTTA FKUTTA SUMSIG VELOCITY	Reads one singly subscripted array from a peripheral storage unit.

TABLE 2, cont.

Code	Called By	Description
READ3	PNTVIJ STEPFN PISWIS PSONST UNIFLO AIJMX NIKMX PKUTTA VELOCITY	Reads three singly subscripted arrays from a peripheral storage unit.
SETFLO <sup>†</sup>	FLOPNT* ARYTRJ* CONFAC* TANTRA*	Reads DUGLFT output data stored on unit 18 that is required by SR FLOVEL for velocity calculations. If flow velocities are calculated by other than the Hess method, this code must be replaced with a dummy.
SIGMAL	CONTRL	Controls calculation of the element source densities, $\sigma_j^{(k)}$ and $\sigma_j^{(\infty)}$ . (ref. 3, eq. (7.12.5)).
STEPFN	VMATRIX	Computes vortex induced onset flows when the step function method of spanwise variation of vortex strength is used.
STOR18	CKARRY	Store control and quadrilateral geometrical property data on storage unit 18 for use by the flow and trajectory codes. (see SR SETFLO.)
SUMSIG	CONTRL	Computes the combined element source strengths, $\sigma_j$ . (ref. 3, eq. (7.13.1)).
UNIFLO	VMATRIX	Stores uniform onset flow velocities for use in calculating element source densities.
VELOCITY	CONTRL	Computes the final velocity at the centroid of each element, and controls the final printout of the DUGLFT calculation. (ref. 3, eqs. (7.13.2) and (7.13.3)).
VFLIFT <sup>†</sup>	FLOVEL <sup>†</sup>	Controls computation of velocities induced at a point in space by elements of unit source density and unit vortex strength in a lifting section.
VFMLFT	VIJMX	Controls computation of velocities induced at all control points by elements of unit source density and unit vortex strength in a lifting section.
VFMLNF	VIJMX	Computes velocities induced at all control points by elements of unit source density in a nonlifting section.
VFNLF <sup>†</sup>	FLOVEL <sup>†</sup>	Computes velocities induced at a point in space by elements of unit source density in a nonlifting section.
VIJMX	VMATRIX	Controls computation of source induced velocities, $V_{ij}^{\rightarrow}$ , and vortex induced velocities, $V_{ij}^{\rightarrow(F)}$ and $V_{ij}^{\rightarrow(S)}$ , at the centroids of all elements.
VMATRIX	CONTRL	Subexecutive code for computation of induced and onset flow velocities at the centroids of all elements.
WNEAR	VFMLFT	Computes vortex induced velocities from a wake element in a lifting strip using the near-field equations.

TABLE 2, cont.

Code	Called By	Description
WNEARF <sup>†</sup>	VFNLFT <sup>†</sup>	Computes vortex induced velocities from a wake element in a lifting strip using the near-field equations.
WRITE1	AIJMX NIKMX COLSOL PKUTTA FKUTTA SUMSIG	Writes one singly subscripted array on to a peripheral storage unit.
WRITE3	VFMLNF VFMLFT STEPFN PISWIS PSONST UNIFLO	Writes three singly subscripted arrays on to a peripheral storage unit.

B. TRAJECTORY CODES

Code	Called By	Description
CDRR*	PRFUN* PARTCL*	Given Reynolds number, returns Davies number for a sphere. Used for water drops for which Reynolds number is less than or equal to 81.23.
DVDQ*	TRAJEC*	Integrates particle equations of motion for each time step (ref. 7).
FALWAT*	PARTCL*	Returns still-air, terminal settling speed for a water drop. Uses equations of Beard (ref. 13).
IMPACT*	TRAJEC*	Used in runs under control of CONFAC to adjust trajectory initial y,z coordinates to avoid impact on the body on the next trajectory after impaction has occurred. This is a problem-specific subroutine that must be programmed by the user. (See p. 75.)
MAP*	CONFAC*	Controls the iterative calculation of trajectories to a specified target point.
MATINV*	MAP*	Linear equation solver.
PARTCL*	ARYTRJ* CONFAC* TANTRA*	Read particle specification data and returns still-air, terminal particle settling speed and other particle data as required for the particular type of particle. This is a particle type-specific code. The version provided here is for water drops.
POLYGO*	CONFAC*	Calculates area of a plane polygon of N vertices. Provides cross-sectional areas of particle flux tubes which are used to compute concentration factors, concentration ratios and collection efficiencies.
PRFUN*	TRAJEC*	Given the particle Reynolds number, returns the factor which when multiplied by $\vec{v}_p - \vec{v}_a$ yields the first term on the right side of eq. (1). This is a particle type-specific function. The version provided here is for water drops.

TABLE 2, cont.

Code	Called By	Description
STRPNT*	TANTRA*	Specifies a curve in three-dimensional space on which lie the initial points of all trajectories used in computing a tangent trajectory to the body. Also specifies coarse and fine step sizes to be used in traversing the curve in search of the tangent trajectory, and it steps along the curve to define new initial trajectory points under control of TANTRA. The version supplied here uses straight line curves.
TRAJEC*	ARYTRJ* TANTRA* MAP*	Computes particle trajectories. (See p. 75.)
TRANSF*	PRFUN* MAP*	Transforms coordinate system from the "flow system" to the "flux tube system", or reverse. (See pp. 82-83.)
WCDRR*	PRFUN* PARTCL*	Given Reynolds number, returns Davies number for a water drop. Used for case where the Reynolds number is greater than 81.23.

\*This code is essentially the same as the code of the same name that is described in NASA CR 3291 (ref. 2).

†Flow codes associated with SR FLOVEL rather than DUGLFT are so indicated by use of a superscript †.

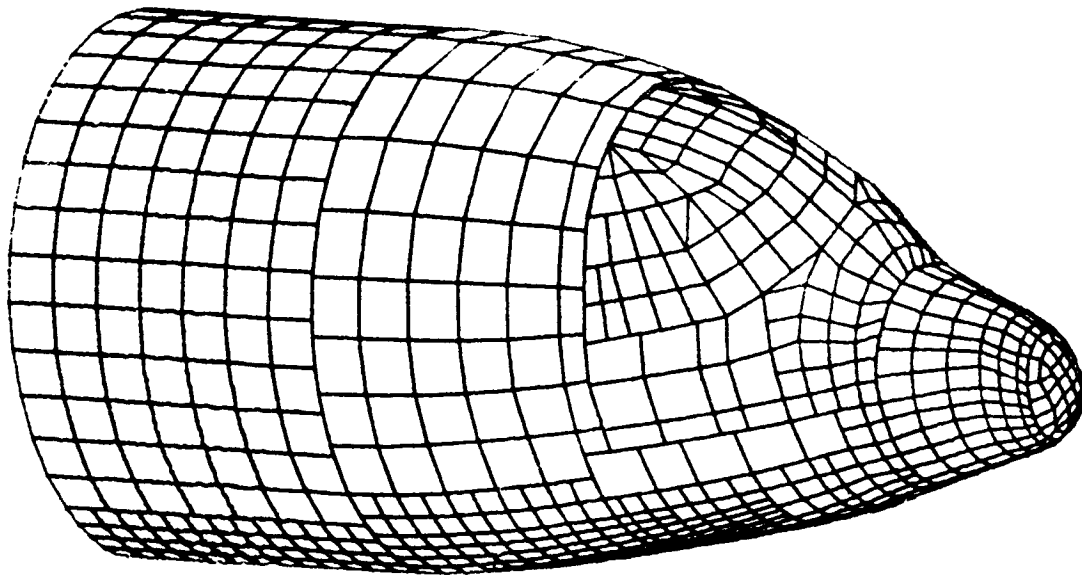
## METHODOLOGY

### THREE-DIMENSIONAL FLOW

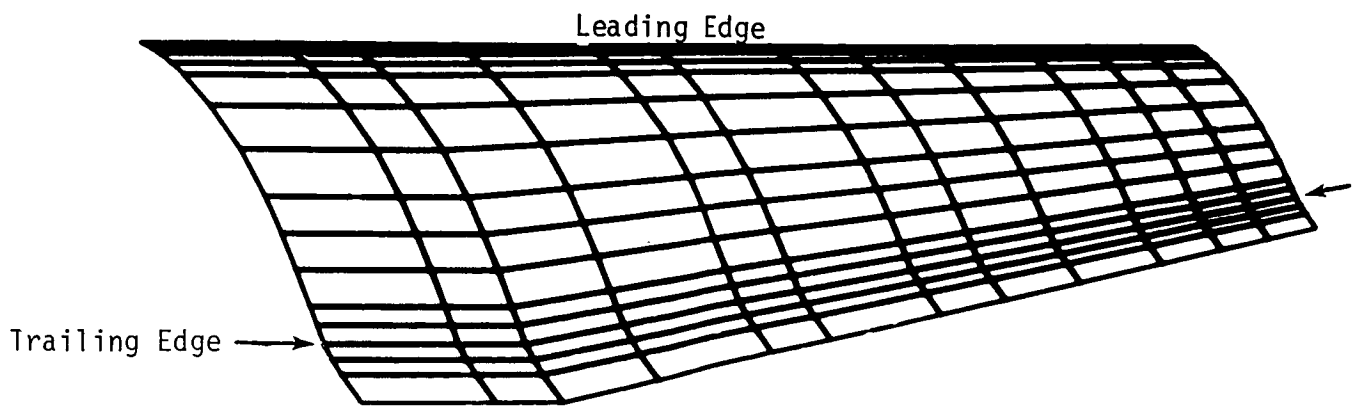
The methods and codes of Hess (ref. 3) and Hess and Smith (refs. 4,5) are used for calculation of lifting and nonlifting potential flow about arbitrary three-dimensional bodies. Lifting bodies (i.e., airfoils) alone, nonlifting bodies alone, or combinations of lifting bodies with nonlifting bodies (e.g., combinations of airfoils and fuselages) can be treated. Effects of flow into an inlet, for example an instrument aperture, can be accounted for provided the intake flow rate, in terms of fraction of free stream air speed, is specified. The method is restricted to subsonic airspeeds, but for free stream Mach numbers greater than 0.5, the Prandtl-Glauert method is used to correct approximately for compressibility effects. Since potential flow is computed, neither viscous effects nor turbulence are treated.

The code requires input of a digital description of the body surface, and for purposes of organizing the data as well as for computing flow, the body surface is partitioned into sections which are designated as either lifting or nonlifting. In either case, the surface is represented by contiguous, plane quadrilateral panels (usually called elements). (See Fig. 1.) For nonlifting sections there are few restrictions on the manner in which the elements can be arranged to represent the surface other than those required for organization. Lifting sections are restricted as follows: each must consist of strips of elements, the strips being oriented parallel to the chordwise direction of the airfoil; each strip must have the same number of elements; and wake elements must be included after the trailing edge of each strip. Details are given below on pp. 20-27. Both lifting and nonlifting portions of the body may be described by more than one section.

Each on-body element (which is in the flow) is taken to be a potential flow source. The source is a distributed one, with the distribution being



a. Forward fuselage of the C130E.



b. Upper surface, including a section of wake, of the C130E half wing.

Figure 1. Examples of digital descriptions of airplane surfaces.

uniform over the surface of the element, and each element, for example the  $j^{\text{th}}$ , is characterized by a unique source density,  $\sigma_j$ . In addition, each strip of elements in a lifting section is characterized by having a unique value of lift vorticity associated with it. This quantity, for example for the  $k^{\text{th}}$  lifting strip,  $B^{(k)}$ , represents vortex strength per unit path length around the strip (see Fig. 4 and its discussion), and it represents the sum of contributions from all panels in the strip. Velocities induced by these vorticities are treated as onset flows. Thus, there is an onset flow from each lifting strip plus the free stream onset flow. It is necessary to compute an independent source density for each of these onset flows for each on-body quadrilateral panel: if there are  $N$  on-body panels,  $K$  lifting strips and one free stream flow,  $N(K + 1)$  values of  $\sigma$  must be computed. Source densities are determined by solving large systems of linear equations that represent the effects of all onset flows on all panels, plus the mutual interactions of all distributed sources, under boundary conditions of zero flux through the centroid (also called control point) of each on-body panel, or specified fraction of free stream flux through each inlet panel.\*

Determination of vortex strengths requires an additional constraint, the Kutta condition, and this is supplied by user-selection of one of two optional methods which are designated as "flow tangency" and "pressure equality." Application of these options is discussed below on pp. 38-39.

Lift vorticity is computed by a novel method developed by Hess (ref. 3). To circumvent problems that have been found to result from use of vortex filaments in prior work, and to ensure that potential flow results from the vorticity distribution and that individual infinitesimal vortex lines either form closed curves or go to infinity, Hess has developed a method by which vortex sheets on the body and wake surfaces can be expressed in terms of dipole sheets on the same surfaces. Hess summarizes the method as follows:

"A variable-strength dipole sheet is equivalent to the sum of:  
(1) a variable-strength vortex sheet on the same surface as the dipole sheet whose vorticity has a direction at right angles to

---

\*An inlet orifice is paneled just as is an impermeable body surface (see Fig. 6).

the gradient of the dipole strength and a magnitude equal to the magnitude of this gradient, and (2) a concentrated vortex filament around the edge of the sheet whose strength is everywhere equal to the local edge value of dipole strength."

Mathematical details are given in Appendix A of reference 3.

For particular body geometry and orientation relative to the free stream, the source densities and vortex strengths are calculated only once, and then these can be used to calculate flow velocity at any space point exterior to the body. The primary functions of the DUGLFT codes are to calculate the  $\sigma_j$  and  $B^{(k)}$  and store these quantities, along with other requisite data, for use by subroutine FLOVEL in calculating flow velocities. Subroutine FLOVEL is called as needed by programs TRAJEC, CONFAC, ARYTRJ and FLOPNT to provide flow velocities for trajectory and flow velocity array calculations.

In calculating each flow velocity, contributions from all quadrilateral elements are summed. There are three sets of algorithms for computing contributions from individual elements: (1) for elements that are close to the calculation point, detailed calculations are used that account for exact element geometries, (2) for elements at intermediate distances multipole expansions are used, and (3) for remote elements the point source approximation is used. Mathematical details are given in references 3-5, with emphasis on lifting flow in reference 3 and emphasis on nonlifting flow in references 4 and 5. The reader is strongly urged to study these references closely before attempting to use this code. Reference 6 consists of a code users manual for the lifting flow calculations described in reference 3.

Calculation accuracy is discussed below in the section on Validation (p. 95). Of course accuracy also depends on the fineness of resolution of the element description of the body, and naturally some compromise is called for. The smaller the elements the finer the resolution, and the fewer of them for which the most exacting of the three algorithms must be used. On the other hand, the number of elements increases inversely as the square of

their linear size. In past studies on airplanes we have used the following paneling criteria: For those parts of the airplane traversed by particle trajectories, we try to keep the element edges between 6" and 8" in length. Where allowed by simplicity of surface shape, remote elements can be larger. Remote downstream complexities of shape are ignored or treated approximately. For example, if interest is confined to the forward fuselage, then the remainder of the fuselage can be represented as a cylinder of constant cross-section which is extended to approximately five times the length of the nose section (as recommended by Hess and Smith, ref. 5), and the wings can be ignored entirely.

The following are basic requirements of the method that apply to all calculations:

1. A uniform, unit-speed free stream approximately in the direction of the positive x axis.
2. Normalization of all velocities to be consistent with the unit free stream speed.
3. Normalization of all distances by a user-specified characteristic dimension of the body.

Surface point coordinates may be recorded in any convenient units and can be appropriately translated and scaled, to meet requirement 3 above, during processing via use of SR's PATPRS and DATPRS. These subroutines also allow rotation of the body about the y axis to adjust attitude angle.\* The coordinate system used for the calculations is described on pp. 19-20.

The unit free stream speed is assumed by program DUGLFT, and the distance normalization, if required, is done during preliminary data processing as indicated above. For trajectory calculations, the user specifies the true free stream speed and the normalization length, and the codes automatically handle any additional normalizing or scaling that is required.

---

\*Translating, scaling and rotating are controlled via parameters IPROS and data cards 4 and 5 of programs PBOXC and DUGLFT, respectively.

## PARTICLE TRAJECTORY CALCULATION

We assume that the bulk air flow is not perturbed by the particles. Moreover, since particle density is large compared to that of air, we can neglect buoyancy and inertial reaction of the fluid to obtain the three-dimensional, normalized equation

$$\frac{d\vec{v}_p}{d\tau} = \frac{1}{N_F} \left[ \frac{1}{v_s} (\vec{v}_a - \vec{v}_p) \frac{N_D N_{R,S}}{N_{D,S} N_R} - \vec{k} \right] \quad (1)$$

Non-dimensional quantities are:

$\vec{v}_p, \vec{v}_a$	particle and air velocities
$v_s$	still-air, terminal settling speed of the particle
$\vec{k}$	Unit vector in the z (upward) direction
$\tau$	time
$N_D = C_D N_R^2$	Davies number
$N_F = V^2 / (Lg)$	Froude number
$N_R = \frac{\rho \delta}{\eta}  \vec{v}_a - \vec{v}_p  V$	Reynolds number
$C_D$	Particle drag coefficient

Dimensioned quantities are:

$\delta$	particle diameter
$\rho$	air density
$\eta$	air viscosity
$g$	gravity acceleration constant
$V$	free stream airspeed
$L$	a characteristic dimension of the body

Here length is normalized by dividing by  $L$ , velocity by  $V$  and time by  $L/V$ .  $N_{D,s}$  and  $N_{R,s}$  are for still-air, terminal particle settling.

We initiate the calculation far enough upstream to be essentially beyond the influence of the body where we can take  $\vec{v}_p = \vec{v}_a - \vec{k}v_s$ . We compute  $N_R$  from these data, calculate  $N_D$  from  $N_R$  using the relations discussed in the next section, and proceed straightforwardly with a numerical integration of eq. (1). The integration is done via use of the code DVDQ of Krogh (ref. 7). This code uses an Adams-type predictor - corrector algorithm with variable time step. It also tests for computational stability and loss of accuracy via roundoff error. It was tested by Hull, et al (ref. 8), along with a number of other codes and found to be most efficient in terms of numbers of function evaluations (flow velocities) required.

For a particular case, time required for trajectory calculation is largely dependent on the number of elements and the number of velocities required. On the CDC 6600 computer, one nonlifting velocity calculation requires on the order of 0.15 second for a typical problem. The number of velocities required per trajectory varies from about 60 to 300. A typical number of trajectories required is 25. Thus, computing time, even on a large computer, can be considerable. Computing times required for the test problem and validation runs are given below on pp. 103-106.

#### AERODYNAMIC DRAG ON WATER DROPS

Davies (ref. 9) shows that still-air terminal settling of spheres can be generalized in terms of the dimensionless numbers  $N_{R,s}$  and  $N_{D,s}$ . Over the range from the smallest spheres, which settle under viscous flow conditions and obey Stokes law, to spheres much larger than of interest here, and for any Newtonian fluid, a reproducible single-valued relationship between  $N_{R,s}$  and  $N_{D,s}$  exists. Furthermore,  $N_{D,s}$  is independent of settling speed, being a function of fluid and sphere properties only; thus for given sphere and fluid,  $N_{R,s}$  and hence  $V_s$  can be calculated. Polynomials by which  $N_{R,s}$  can be computed as a function of  $N_{D,s}$  were derived by Davies from a composite of many sets of experimental data.

Since the work of Davies it has been found repeatedly that this treatment is applicable to particles of other shapes, provided settling is steady and particle orientation is stable.

For the trajectory calculations required here, the problem must be turned around. In addition to gravity settling, there is a particle velocity component (relative to air) caused by the disturbance of the passing airplane. At any time step in the numerical integration of equation (1),  $\vec{v}_a - \vec{v}_p$  (and hence  $N_R$ ) is known, and  $N_D$  must be determined. For viscous motion (i.e., Stokes flow, where  $N_R < 1$ )  $N_D = 24 N_R$  and equation (1) can be integrated without question. However, for larger  $N_R$  the steady-state drag data determined experimentally for terminal settling must be used to compute accelerative particle motion.

Experimental measurements by Keim (ref. 10) and a theoretical analysis by Crowe, et al. (ref. 11) indicate that if the acceleration modulus,

$$N_A = \delta \left| \frac{dv_p}{dt} \right| / V_p^2,$$

is smaller than about  $10^{-2}$ , steady-state drag coefficients can be used without significant error to compute accelerative motion.  $N_A$  rarely exceeds  $10^{-2}$  in our trajectory calculations.

For water drops small enough to be essentially spherical ( $N_R \leq 81.23$ ) we calculate  $N_D$  from a polynomial function in  $N_R$  derived from Davies data (ref. 9). (Function CDRR) For larger drops ( $N_R > 81.23$ ), which have a flattened, non-spherical shape, we calculate  $N_D$  from polynomials in  $N_R$  derived from the water drop data of Gunn and Kinser (ref. 12). (Function WCDRR).

Still-air, terminal settling speeds for water drops are computed via use of Beard's equations (ref. 13). (SR FALWAT)

Water drops of any size, from submicron to the breakup size at about 8000  $\mu\text{m}$  diameter, can be handled by these methods. However, the user should be aware that computation time goes up as droplet diameter goes down, and the time required for drops of diameter 1  $\mu\text{m}$  or less may be large.

## FLOW CODE DESCRIPTIONS

### PROGRAM PBOXC

#### General Discussion

This program is derived from the Douglas Aircraft Company code BOXC which was developed by Hess and Smith (ref. 4) and is identical to the code described in reference 2. It processes and produces CALCOMP plots of the three-dimensional body surface description data and is used primarily to debug these data. Processing and printing go as far as the "first output" (ref. 4, sec. 9.4). A secondary use is to store the body surface data such that it can be retrieved later and used by PGM STEREO to plot the body along with trajectories stored by one of the trajectory codes.

The surface of a general three-dimensional body is defined in terms of "rows" and "columns", the so-called m and n-lines, of coordinates of points on the surface as described below. The m and n-lines of points are combined by the code to form quadrilateral elements, or panels, such that when considered together they represent a reasonable approximation to the surface (Fig. 1). Adjacent panels should be contiguous, or as nearly contiguous as possible. The data for general bodies may be scaled and translated in the three coordinate directions, and rotated about the y axis (see the next section) prior to processing.

This code also has the capability to generate ellipsoids of prolate, oblate or general shape, with the only restriction being that their major and minor axes lie on the coordinate axes.\*

When the user elects to prepare plots of the body, the code automatically prepares a number of plots, each from a unique viewing angle, the number varying according to symmetry. For an asymmetric body fourteen plots are prepared. These consist of the six views from both directions along each coordinate axis, and the eight plots from 45 degree angles in each octant.

---

\*PGM DUGLFT does not have this capability.

For a body with one plane of symmetry nine plots are prepared, for two symmetry planes six plots, and for three planes four plots. The user is urged to make liberal use of the plots to find errors in the body data.

### Coordinate System

Figure 2 shows an example of a cartesian coordinate system that would be appropriate for description of the body surface and for calculation of flow velocities and particle trajectories. Critical directions are those of the free stream and the gravity vector. During particle trajectory calculations the z axis must be directed vertically upward such that gravity settling of particles is along the negative z axis. The x axis typically is taken to be in the plane that contains the z axis and free stream vector, with its positive direction the same as that of the free stream vector projection on the x axis. The y axis then has the direction required by a right-handed coordinate system.

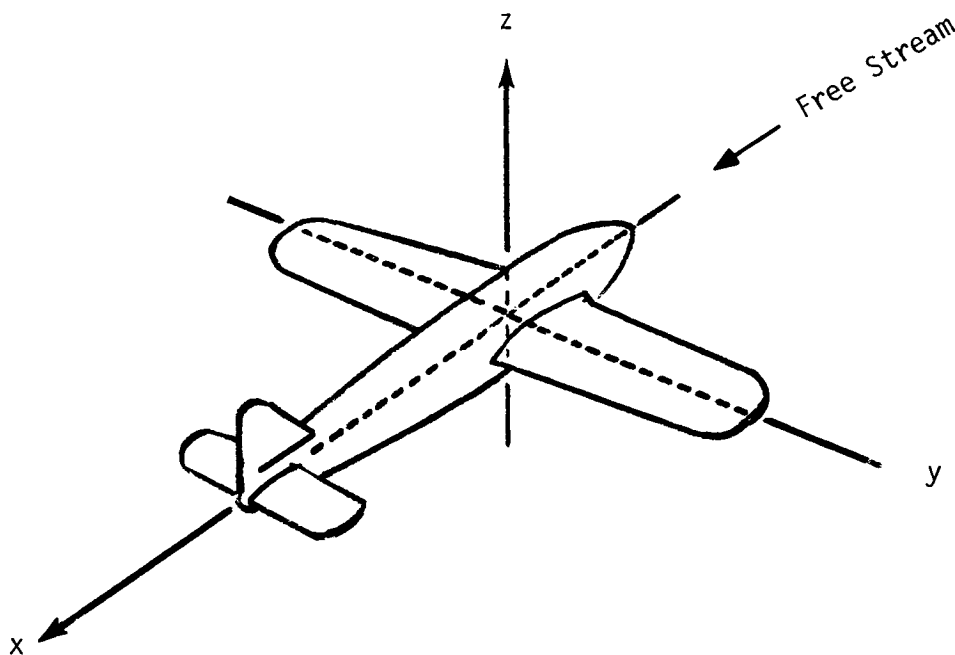


Figure 2. Coordinate system suitable for body surface description and particle trajectory calculations.

For a body such as an airplane, the orientation shown in Figure 2 is the proper one to use in setting up the surface digital description. Any convenient units and any origin can be used since these can be adjusted at data processing time by application of a coordinate translation and scaling capability (SR PATPRS and DATPRS). This capability also allows rotation about the y axis such as to adjust angle of attack. As discussed below on p. 37, angle of attack also can be specified arbitrarily during the DUGLFT calculations, but if particle trajectories are to be computed, the user must keep in mind that the negative z axis must have the direction of the gravity vector.

As noted in the discussion of equation (1), all distances are normalized by dividing by a characteristic dimension of the body. Examples of appropriate characteristic body dimensions are fuselage diameter or airfoil chord length. Therefore, when the coordinate data are scaled by PATPRS or DATPRS, it is appropriate to define the scale factors to be the reciprocal of this characteristic length.

If the body has one or more planes of symmetry, these can be used by the code as reflection planes to generate the complete body from the basic unit structure as described in the next section. However, the origin of the coordinate system must be adjusted (via coordinate translations) such that the symmetry planes are coincident with the  $y = 0$  and  $z = 0$  planes. For example, the symmetry plane of the airplane in Figure 2 must be coincident with the  $y = 0$  plane. More details are given in the next section. Again, the restriction that the z axis must be directed opposite to the gravity vector may complicate matters. For example, if a body normally has a horizontal ( $z = 0$ ) symmetry plane, but for some particular case must be oriented with an angle-of-attack to a free stream that is horizontal relative to the ground, the symmetry could not be used since the z axis would no longer be normal to the symmetry plane.

#### Symmetry Planes

The number of symmetry planes is specified via input parameter NSYM which has allowed values of 0,1,2,3. Only "plus" symmetry planes are

allowed. (See p. 37 for a description of plus and minus symmetry planes.) Symmetry planes are specified and used for reflection according to a fixed procedure: If there is one symmetry plane it is the  $y = 0$  plane. If there is more than one symmetry plane ( $NSYM > 1$ ) the first reflection is always across the  $y = 0$  plane, followed by reflection across the  $z = 0$  plane, which latter is always the second reflection plane. Specification of three symmetry planes (the third symmetry plane is always the  $x = 0$  plane) is used only to restrict the number of perspective view plots, and in generating ellipsoids for the case of  $IFLAG = 1$  (pp. 27-29); surface point coordinates are not reflected across the third plane during calculation of the plots, and a third reflection plane is not allowed by the DUGLFT code.

In summary, the reflection symmetry planes are exercised as follows:

<u>Order of Application</u>	<u>Symmetry Plane</u>
1	$y = 0$
2	$z = 0$

For example, if  $NSYM = 1$ , for each point with coordinates  $(x,y,z)$ , another point with coordinates  $(x,-y,z)$  is created. If  $NSYM = 2$ , for each point with coordinates  $x,y,z$ , three additional points with coordinates  $(x,-y,z)$ ,  $(x,-y,-z)$  and  $(x,y,-z)$  are created.

Only the primary data points should be input if symmetry is to be used. If reflected as well as primary data are input, and both are reflected by symmetry, the calculation results will be in error.

Read the Uniform Onset Flow section, p. 37, before proceeding with use of symmetry planes.

#### Surface Description Data for General Nonlifting Sections ( $IFLAG = 0$ )

The user must examine the body, or drawings of it, and devise a layout plan for subdividing its surface into sections that are compatible with the requirements of m-line, n-line surface point input for lifting and nonlifting

surfaces while providing elements of appropriate size which cover the surface without leaving gaps or introducing unwanted discontinuities. Also a coordinate system must be established, but this can be manipulated at processing time by use of the scaling and translation capability of the code as noted above.

The important thing is to understand the requirements of the m and n-line input. Here we give a brief summary of the requirements; the user is encouraged to carefully study sec. 9.1 of reference 4, and secs. 7.1 - 7.3.1 of reference 3 to obtain a thorough understanding of them.

Points which define the corners of the quadrilateral elements are labeled with integers m and n which identify hypothetical "rows" and "columns" on which they lie. The integers m and n are not input to the computer; they are used for data organization and sequencing only.

To ensure a proper computation, the rows and columns must be organized by the following rule: If an observer is located in the flow and is oriented so that locally he sees points on the surface with m values increasing upward (or forward), he must also see n values increasing toward the right.

The surface of any part of the body may be described by more than one section, each of which must be independent. That is, all quadrilaterals in each section must be closed. Where an edge of a section is contiguous with another, the input for each section must define the common edge, though they need not use the same points on the edge.

Figure 3 illustrates a nonlifting surface description that is subdivided into four sections. Note how the sectioning can be used to change resolution or to deal with structural complexities. Fully general quadrilateral shapes are acceptable in nonlifting sections, including triangles, in which case two points may be coincident or one of the four points may lie on a triangle edge.

Coordinates are punched into cards, one point per card; also in each card is punched the integer parameter STAT which is used to identify the m,n status of each point. All points in a section are ordered in the sequence (m,n):

(1,1), (2,1), (3,1),..., (1,2), (2,2), (3,2),...(1,3), (2,3), (3,3),...

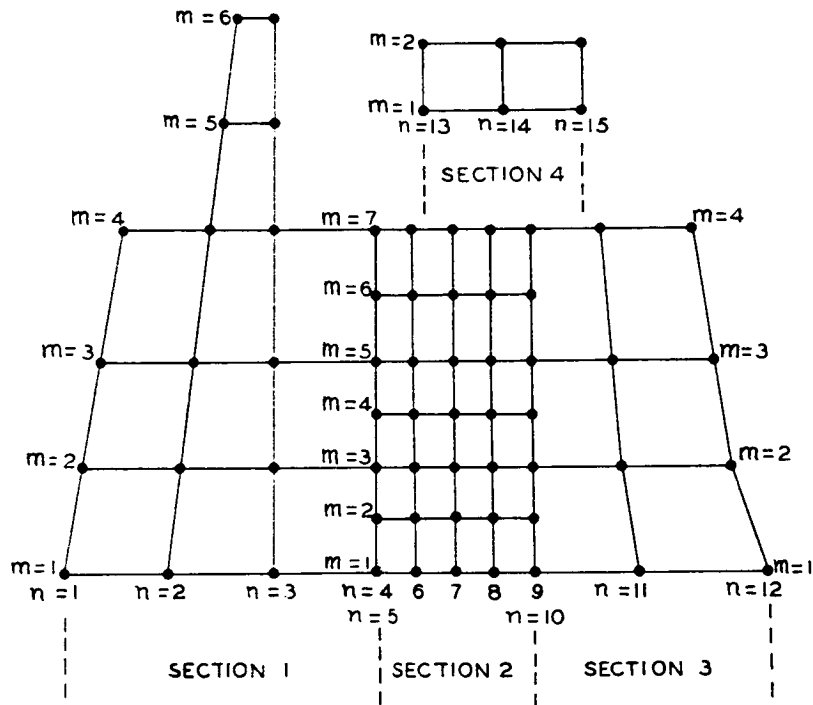


Figure 3. Plan view of the input points on a body divided into sections. (From ref. 4)

The STAT parameters are as follows for each section, whether lifting or nonlifting:

<u>(m,n)</u>	<u>STAT</u>
(1,1)	2
(1,n≠1)	1
all others	0 or blank

For the last card of the last section, STAT = 3.

Input order of sections is immaterial, but within sections, the data must be ordered according to the underlined rule given above.

## Surface Description Data for Lifting Section - General

For lifting sections there are certain restrictions and requirements beyond those for general nonlifting sections. The  $n$ -lines in a lifting section must be approximately parallel with each other, each must have the same number of points, and each must lie roughly in the free stream direction. The code assumes a trapezoidal shape for each lifting element, with the parallel sides of the trapezoids along the  $n$ -lines. (An  $n$ -line is a line along which  $n$  is constant; in this case it is chordwise.) In addition to the elements which define the lifting surface, elements also must be defined for the wake. These wake elements are constructed similar to the body surface elements, the first is contiguous with the body elements along the trailing edge, but they extend aftward of the body to represent an infinitesimally thick vortex sheet wake. Wake elements are assigned vorticity but not source density since, of course, they are not on the body surface.

Figure 4 illustrates how an airfoil surface and wake should be partitioned into elements for a typical situation (i.e., a wing with trailing edge normal to the free stream flow or tapering backward, and a zero or nose-up angle of attack). In any situation  $n$  varies spanwise while  $m$  varies chordwise. For the typical situation, the  $m$  index begins at the trailing edge, proceeds forward along the lower surface, around the leading edge, aftward along the upper surface to the trailing edge and then into the wake. To satisfy the "underlined rule" on p. 22 for organizing input data, it is common practice to define the wing on the starboard side of the airplane with  $n = 1$  at the tip and proceed inward toward the root.

For cases where the trailing edge tapers forward at a significant angle, or negative lift is expected, it would seem best (ref. 3, secs. 6.5 and 8.4) to reverse the above procedure. That is, begin at the trailing edge as before, but traverse the upper surface first, around the leading edge, back across the lower surface and finally into the wake. On a starboard wing, this reverse procedure requires that  $n$  values increase from root to tip, and the code allows this order of input as well as the more usual tip to root order.

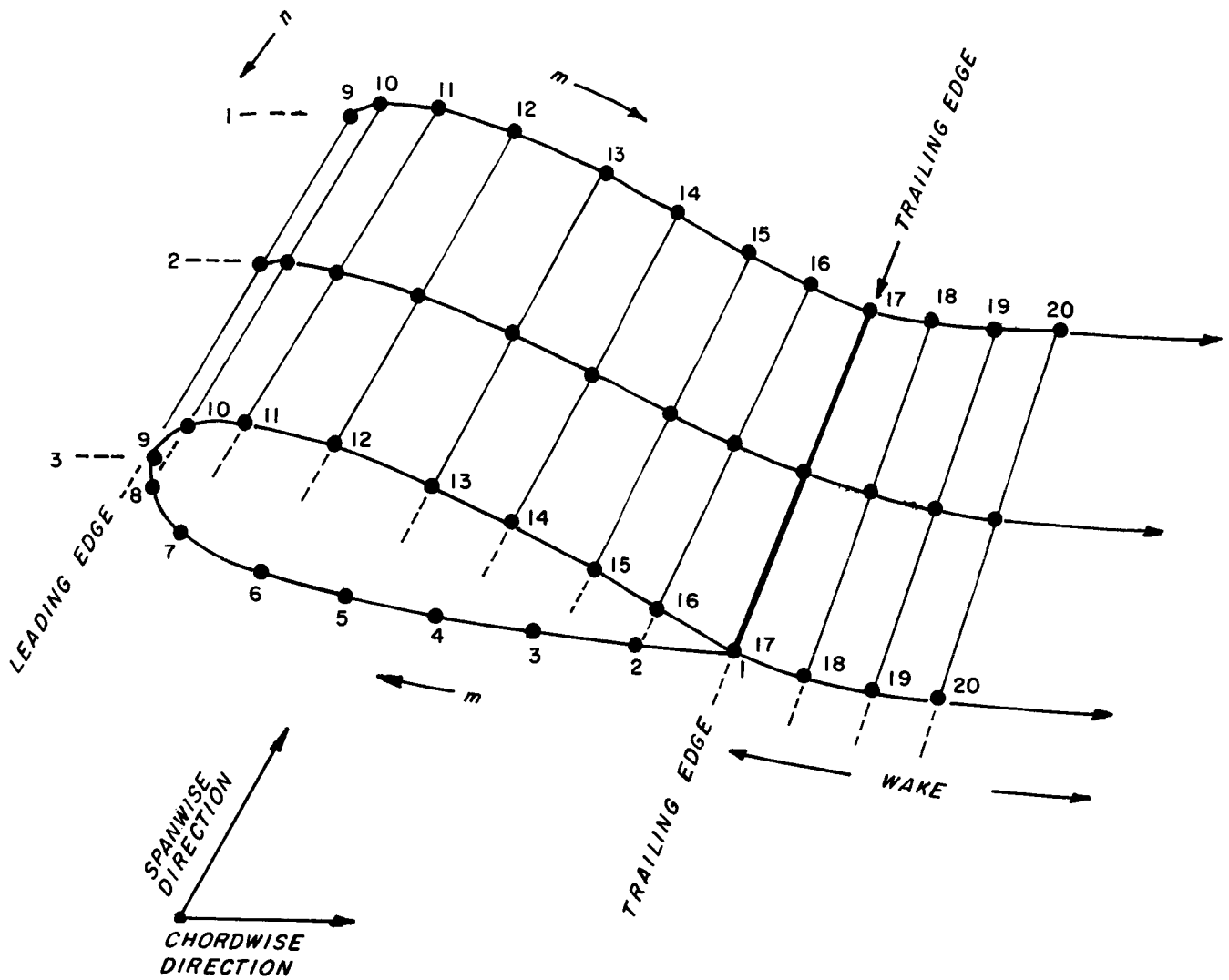


Figure 4. Organization of  $m$  and  $n$  lines in a lifting section. A lifting strip is delineated by sequential  $n$  lines, and extends over the complete circuit from  $m = 1$  at the trailing edge, along the underside to and around the leading edge, back to the trailing edge, and finally to the furthest aftward extent of the wake.

Wake elements may be defined downstream as far as desired. The user has the option, which is recommended, to specify, via election of the semi-infinite last wake element option (see p. 35), that the code extend the trailing edge of the last defined wake element to infinity. Thus, the user should specify enough wake elements to account for whatever curvature is considered necessary, plus one final element, and exercise the semi-infinite wake element option; two or three wake elements should be sufficient.

The considerations above of wake structure and position are mitigated by the following. First it is not known a priori exactly how a wake for a particular case should be configured. Second, it has been found that the flow on a lifting body is insensitive to the position of its own wake, and thus, for ordinary moderate values of: angle of attack, trailing edge angle and degree of camber, any reasonable wake gives a satisfactory solution (ref. 3, sec. 8.5).

When a wing is subdivided into several lifting sections, the organization proceeds in the same directions within each section, and in the typical situation begins with the outermost section and proceeds inboard in orderly succession of sections.

Hess has studied flow calculations around an isolated wing to determine the number of lifting strips and elements per strip that are needed for accurate results (ref. 3, sec. 8.1). He found that thirteen lifting strips per half wing and about thirty elements per strip, equally divided between the upper and lower surfaces, were satisfactory.

#### Surface Description Data for Lifting Sections - Extra Strips And Ignored Elements

Two special situations arise from intersection of nonlifting structures with lifting sections. First there is the case where the end of a lifting section abuts a nonlifting structure along the entire length of both its upper and lower surfaces. An example is the intersection of a wing with a fuselage. The lifting section should not simply terminate at the intersection because the local lift does not fall to zero there, and in addition, termination would result in a concentrated vortex filament on the surface.

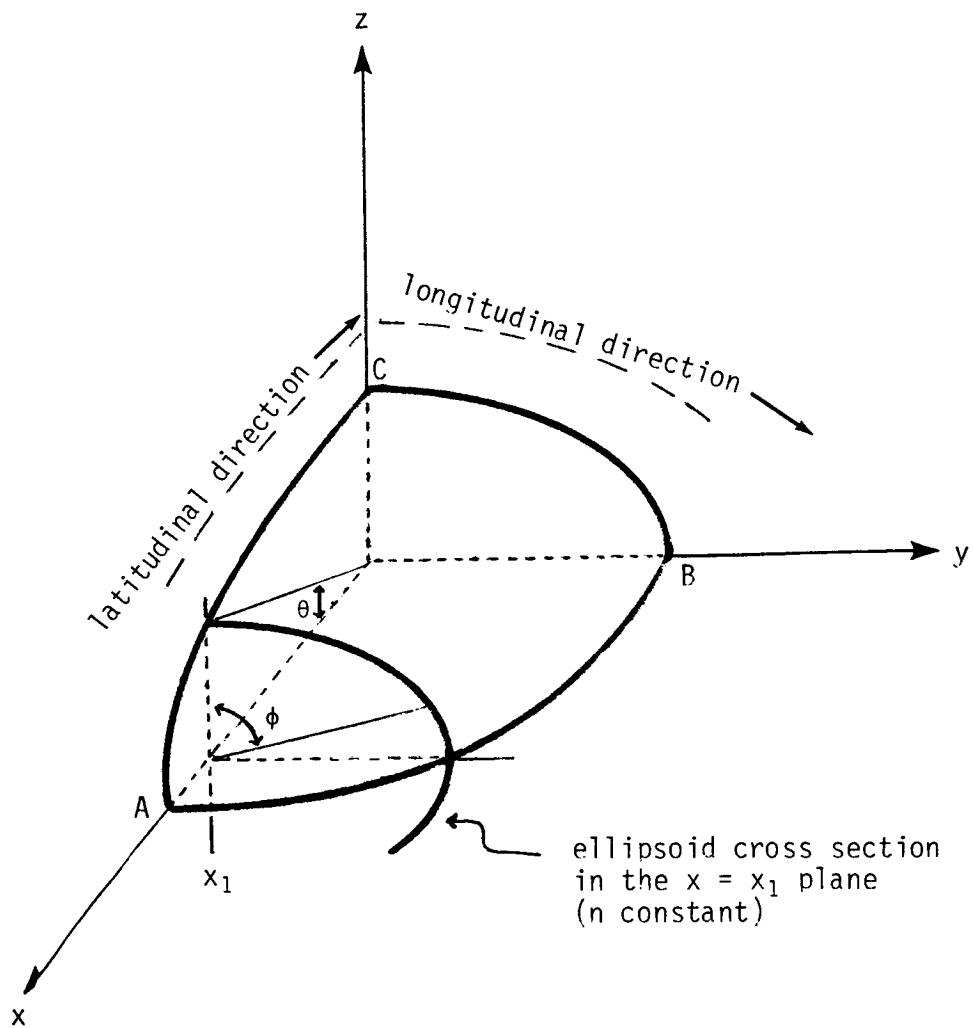
To remedy this, an "extra strip" is added to the end of the lifting section which extends into the nonlifting body. This extra strip is geometrically similar to the others in the section and includes a wake. (Of course, element source densities are not computed for elements in extra strips.) In the case of intersection with a fuselage, the extra strip extends the lifting section to the airplane symmetry plane. These extra strips must be specified by the user in the same way that ordinary strips are specified.

The second situation arises when a nonlifting structure covers part of a lifting section, usually over only a portion of a lifting strip, such as to not break the continuity of the trailing edge. Examples would be engine cowlings and wing pylons. The affected elements are designated as "ignored elements", but the vortex distribution continuity is maintained over them to avoid numerical problems. Thus as regards the vortex distribution, the lifting surface is taken to extend through the nonlifting structure as though the nonlifting structure did not exist. Of course, source densities are not computed for the ignored elements, and they contribute nothing to the nonlifting flow.

Special extra strips are required at junctions of independent, contiguous lifting sections when the piecewise linear option is used to smooth the spanwise vortex distribution. However, these special extra strips are specified by the code on the basis of information supplied via the NLINE1 and NLINEN parameters (pp. 40-42), and the user does not need to otherwise concern himself with them.

#### Surface Description Data for Generated Ellipsoids (IFLAG = 1 or 2)

Ellipsoids are generated by specifying the semi-axis lengths B and C (A = 1 always), and by specifying the numbers of "latitudinal" and "longitudinal" (Fig. 5) element divisions, NLM1 and MMIN respectively.



$\theta$  is in the  $y = 0$  plane  
 $\phi$  is in the  $x = x_1$  plane

m-lines run in the latitudinal direction from  $\theta = 0$  to  $\theta = \pi$   
 n-lines run in the longitudinal direction from  $\phi = 0$  to  $\phi = 2\pi$

Figure 5. Definition of angles  $\theta$  and  $\phi$ , and m and n-line directions used by PBOXC for generation of ellipsoids.

There are two modes for specification:

Mode 1. IFLAG = 1, NSYM = 3

All three symmetry planes are used and NLM1 and MMIN are specified for one octant only. Element increments are computed for NLM1 and MMIN equal increments in angles  $\theta$  and  $\phi$  (Fig. 5).

Mode 2. IFLAG = 2, NSYM = 2

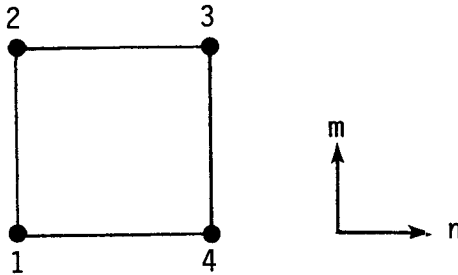
Only two symmetry planes are used, and  $(x, z)$  values in the  $y = 0$  plane must be input for  $-1 \leq x \leq 1$ , beginning at  $(1,0)$  and proceeding to  $(-1,0)$  for either all positive  $z$  or all negative  $z$  (i.e., for  $180^\circ$  in angle  $\theta$ ). (The code automatically ensures that the "underlined" input rule is obeyed.) Thus, NLM1 must be specified for the entire  $x$  axis, but MMIN is for one octant only as for the other option, and element increments in the "longitudinal" direction are created at equal increments of the angle  $\phi$ .

Body surface data for generated ellipsoids cannot be plotted nor can the data be translated, scaled, and rotated by subroutine PATPRS. DUGLFT does not have a capability to generate ellipsoids. This capability is used only by the nonlifting code described in reference 2.

## Printed Output

The printed output is the result of the first stage of surface data processing (ref. 4, sec. 9.4) and is obtained by specifying `IPRNT = .TRUE.` in the input. For each quadrilateral element on the surface it consists of:

1. Coordinates  $(X,Y,Z)$  of the four points on a quadrilateral in the order



around the quadrilateral.

2. Components  $(NX,NY,NZ)$  of the unit normal vector to the plane of the quadrilateral. This vector should point toward the exterior of the body rather than toward its interior. If it points in the wrong direction the data have been input in violation of the "underlined rule" on p. 22 and the data must be reordered.
3. Coordinates  $(NPX,NPY,NPZ)$  of the quadrilateral null point (ref. 4, sec. 9.3).
4. The common projection distance  $(D)$  of the four input points into the plane of the quadrilateral. (The four points from which a plane quadrilateral is formed do not in general, and need not, lie exactly in a plane.)
5. The maximum diagonal length  $(T)$  of the quadrilateral.
6. The area  $(A)$  of the quadrilateral.

Additional output appears for certain abnormal quadrilaterals. If the integer 1 or 2 appears at the far right of the page, they indicate the following conditions:

Integer 1. The null point was found to lie outside of the quadrilateral. The coordinates listed are for the quadrilateral centroid.

Integer 2. The iterative procedure used to determine the null point did not converge and thus the null point is only approximate.

(ref. 4, sec. 9.3).

#### Subroutines Required

PINPUT, PICTUR, PEADER, PATPRS, plotting subroutines.

#### External Storage Units

Units 1, 5 and 6 are the system punch, input and print units respectively.

Unit 8 temporary storage.

Unit 9 storage for surface data to be used later for plotting by PGM STEREO.

PBOXC Card Input

Card No.	Variables and Format	Description
1	HEDR(15), IFLAG, NSYM, KMACH, KASE, (15A4, I1, 10X, I1, 1X, I1, 2X, A4)	<p>HEDR (Cols. 1-60) Hollerith run identification</p> <p>IFLAG (Col. 61) Body surface description input control</p> <p>IFLAG = 0 Input data for a general, three-dimensional body (See pp. 21 ff.)</p> <p>IFLAG = 1 Generate an ellipsoid using the mode 1 option, with three reflection planes. (See p. 29.) Be sure that NSYM = 3.</p> <p>IFLAG = 2 Generate an ellipsoid using the mode 2 option, with two reflection planes, and input x,z coordinates for the ellipsoid via cards no. 5C. (See p. 29.) Be sure that NSYM = 2.</p> <p>Note: The generated ellipsoid capability (IFLAG ≠ 0) applies only to the non-lifting code (ref. 2).</p> <p>NSYM (Col. 72) Number of data reflection planes. Limited to values 0,1,2,3. (See p. 20.)</p> <p>KMACH (Col. 74) Always zero or blank.</p> <p>KASE (Cols. 77-80) Hollerith body identification.</p>
2	MACH, (F10.6)	Mach number This card is input only if KMACH ≠ 0 on card 1.
3	IPROS, IPUNCH, IPRNT, IPICT, ICRT, (5L1)	<p>Logical variables which cause the following if true:</p> <p>IPROS Body surface data for a general body are to be translated, scaled and rotated about the y axis before processing, and card 4 is to be input.</p> <p>IPUNCH Body surface data are copied to the system punch unit. (After translating, scaling and rotating about the y axis.)</p> <p>IPRNT Print of the output described on p. 30.</p> <p>IPICT Body surface data for a general body are plotted.</p> <p>ICRT Plotting is via CRT. If ICRT is false, plotting is via pen and ink.</p>
4.	ANGLE, XSCALE, YSCALE, ZSCALE, XTRANS, YTRANS, ZTRANS, (7F10.0)	<p>This card is input only if IPROS (card 3) is true.</p> <p>ANGLE Angle (degrees) that the body is rotated about the y axis. A positive value causes a counterclockwise rotation from the aspect of a viewer looking down the positive y axis toward the origin. (Note: For a nose-up airplane angle of attack, ANGLE is negative.)</p> <p>XSCALE, YSCALE, ZSCALE Scale factors to be applied to surface point x, y and z coordinates respectively after translation. Default values are unity.</p> <p>XTRANS, YTRANS, ZTRANS Translations to be applied to surface point x, y and z coordinates before scaling.</p>
5A	X,Y,Z,STAT, XX, YY, ZZ, STATT, (3F10.0, I2/3F10.0, I2)	<p>Cards 5A apply to general bodies (IFLAG = 0, see pp. 21 ff).</p> <p>X,Y,Z and XX, YY, ZZ Are coordinates of points used to define the body surface.</p> <p>STAT Are point status integers. Allowed values are 0, 1, 2, 3. The meanings of these values are:</p> <p>(Col. 32)</p> <p>0 This point is on the same n line as the last point</p> <p>1 This point starts a new n line</p> <p>2 This point starts a new section</p> <p>3 This is the last point in the input.</p>
32		

PBOXC Card Input, cont.

Card No.	Variables and Formats	Description
5A cont.		Note: For the last coordinate card STAT or STATT = 3. A blank card should follow this if there is an odd number of body surface point cards.
5B	NLM1, MMIN, B, C, (2I5, 2F10.5)	Card 5B applies to generated ellipsoids (IFLAG > 0) NLM1 Number of "latitudinal" element divisions MMIN Number of "longitudinal" element divisions B y semi-axis of the ellipse C z semi-axis of the ellipse  (See p. 27 Modes 1 and 2, and Fig. 5.)
5C	x <sub>1</sub> , z <sub>1</sub> , x <sub>2</sub> , z <sub>2</sub> , ... . ...x <sub>NLM1+1</sub> , z <sub>NLM1+1</sub> . (8F10.0) . . .	Cards 5C apply to generated ellipsoids for which the x,z coordinates are input (IFLAG = 2, NSYM = 2).  (x <sub>i</sub> , z <sub>i</sub> ) are coordinates in the y = 0 plane, beginning at (1,0) and proceeding to (-1,0), that define the "latitudinal" element subdivisions. (See p. 29 Mode 2, and Fig. 5.)
6,7	LINE1, LINE2, (7A6/7A6)	Cards 6 and 7 are read only if ICRT is true (card 3). These are two lines of 42 columns each of Hollerith labeling for a microfiche film.

DUGLFT

### General Discussion

Program DUGLFT is an extensively modified version of the lifting code developed by Hess (ref. 3) and documented for users by Mack (ref. 6). Modifications were required to accomplish the following:

1. Provide data output (on storage unit 18) for use by SR FLOVEL for calculation of flow velocities at arbitrary space points.
2. Provide capability to treat nonlifting as well as lifting bodies, and combinations of lifting and nonlifting bodies.
3. Provide capability to translate, scale and rotate body surface coordinates.
4. Provide capability to treat flow inlets.
5. Provide approximate correction for compressibility effects at high subsonic free stream speeds.
6. Generalize array capacities in the code such as to make the code open ended with regard to its capacity to handle numbers of: quadrilateral elements, sections, lifting and nonlifting strips, etc.

The discussions to follow are intended to provide guidance to code users. An understanding of the method, its strengths, weaknesses and range of potential applications can only be obtained by thorough study of references 3, 4 and 5.

### Body Surface and Wake Description

Coordinates of corner points of the plane quadrilateral elements which described the body surface and wake are organized and input via cards no. 12 as described above for PGM PBOXC (pp. 19-27).

### Semi-Infinite Last Wake Element Option

By specifying `LASWAK = .TRUE.` on card 7, the user specifies that the semi-infinite last wake option be exercised. In this case, the trailing edge of the last wake element in each lifting strip is automatically extended to  $x = \infty$  by the program. Thus, the wake vorticity also extends aftward to infinity, as is consistent with theory, and the user is encouraged to exercise this option.

All four corner points, including points that define the trailing edge, of each of the semi-infinite last wake elements must be specified by input (cards no. 12) just as is done for all other elements. This is done such that a set of finite geometric quantities, including a control (i.e., centroid) point, can be calculated. For example, Fig. 1b shows three wake elements on each lifting strip of the C130 wing. If the semi-infinite last wake element option is exercised, geometric properties would be calculated for the last (most aftward) of each of these wake elements according to the geometry shown in the figure, but in calculating the contribution of this element to the lift vorticity, the code would take the trailing edge of this last wake element to be at  $x = \infty$ .

### Flow Inlets

We have added a feature to the Hess code to allow simulation of flow into the aperture of an inlet. (The code is not organized to handle internal flows.)

The aperture is represented by quadrilateral panels in the same manner as the body surface. To illustrate this, Fig. 6 shows the paneling of the orifice in the tip of the intake tube of a cloud water meter, the EWER, which is mounted under the wing of a C130 research airplane (ref. 14). Inlet aperture panel coordinates must be the first in the deck of surface point cards (card 12).

Input card no. 2 contains the number of aperture quadrilaterals (LEAK) and also the fraction of the free-stream flow speed that is "leaked" through

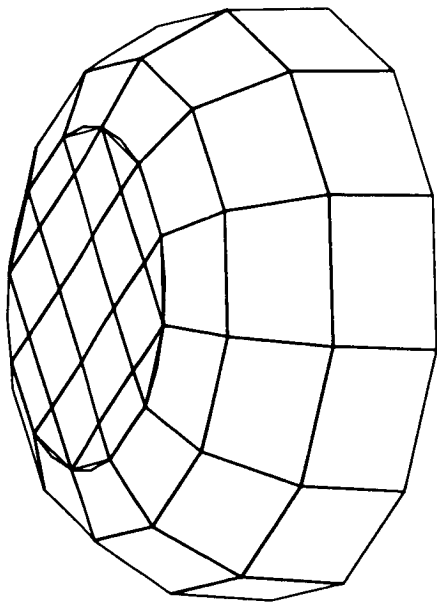


Figure 6. Computer plot of tip and orifice of a EWER cloud water content meter probe (ref. 14).

described above for PGM BPOXC (p. 20) and are applied in the same order. That is, the first symmetry plane, or the single symmetry plane if only one is specified, is the  $y = 0$  plane. The second symmetry plane is the  $z = 0$  plane. When both symmetry planes are specified, surface point coordinates are reflected across the  $y = 0$  plane first, then across the  $z = 0$  plane and finally back across the  $y = 0$  plane. Only the primary surface point data should be input; if reflected as well as primary data are input, and both are reflected, the flow calculation results will be incorrect.

the apertures (FRAC). This leakage is taken to be the same for each aperture quadrilateral. If there is no flow inlet, the LEAK and FRAC fields on card 2 are blank.

#### Off-Body Points

If logical parameter LOFF (card 3) is true, flow velocities are computed at user-specified arbitrary points (cards 15) and printed near the end of the output. The computation and processing of these velocities have no effect on the calculation and storage of data to be used by FLOVEL.

#### Symmetry Planes

Two symmetry planes are allowed by this code. These correspond to the first and second symmetry planes

Each symmetry plane is designated as either "plus" or minus". A plus symmetry plane is an ordinary reflection plane, on which zero normal velocity is defined at all points. Velocity potential is zero at all points on a minus symmetry plane; the minus symmetry plane reflects coordinates normally, but reverses the direction of induced velocities computed from the reflected point. An example of a minus symmetry plane is a free surface for the condition of infinite Froude number.

When symmetry is specified for a body with one or more lifting sections (airfoil), the code assumes that the  $y = 0$  plane is the airfoil symmetry plane, and that the  $y$  direction is the airfoil spanwise direction. This requires reversal of direction of vorticity induced velocities computed from points reflected across the  $y = 0$  plane. (Note that this reversal would be independent of that caused by specification of the  $y = 0$  plane as a minus symmetry plane; indeed the two reversals would cancel.) Vorticity induced velocities computed from points reflected across the  $z = 0$  plane are not reversed in direction (unless, of course, the  $z = 0$  plane is designated a minus symmetry plane).

Read the next section before a decision is made to use symmetry.

#### Uniform Onset Flow (Free Stream Flow)

In the context of the unmodified Hess code, specification of a uniform onset (i.e., free stream) flow is equivalent to specification of airplane angle of attack. Since extra angles of attack add relatively little to the computation burden, the code allows up to ten specifications. However, if symmetry is specified (see above) free stream vectors must be parallel to symmetry planes.

For calculation of particle trajectories certain restrictions are imposed. First, only the first specified of the angles of attack is used for trajectory calculations. Second, since gravity is involved in the trajectory calculations, the  $z$  axis is always directed vertically upward. The  $x$  and  $y$  axes are in the horizontal plane with the positive  $x$  axis directed along, or at least close to the direction of, the uniform onset flow vector. The  $y$  axis is oriented such as to define a right-handed cartesian system of axes. More detail is given above on pp. 19-20.

Uniform onset flows are defined in terms of the direction cosines of their vectors with respect to the above coordinate system. Normally, with the uniform onset flow vector coincident with the x axis vector, the direction cosines are: 1.0, 0.0, 0.0, and airplane attitude angle is adjusted by rotation of coordinates about the y axis as specified by input data on card no. 5. Since uniform onset flow velocities always are taken to have unit magnitude, the direction cosines are equivalent to the free stream velocity components.

### Correction for Compressibility Effects

Since the Hess method computes potential flow it is not capable of directly coping with compressibility effects, so that an auxiliary correction must be used. The Prandtl-Glauert correction (ref. 15) is used here.

The correction is applied by user specification of a nonzero free stream Mach number (MACH) on card 2. While the correction is automatically applied for any free stream Mach number,  $N_M$ , in the range  $0 \leq N_M < 1$ , it is not significant for  $N_M < 0.5$ , so that the MACH field of card 2 may as well be left blank unless  $N_M > 0.5$ .

The small perturbation approximation is basic to the derivation of the correction (ref. 15), with the consequence that only streamwise compressibility effects are accounted for. Thus, compressibility effects that would result from locally high Mach numbers are ignored.

This correction is included in the nonlifting code described in reference 2, but it is not described by Hess and Smith in reference 4, nor is it included in Hess' lifting code (refs. 3 and 6). Since the correction is not described in connection with these codes elsewhere, details are given here in Appendix A.

### The Kutta Condition: Pressure Equality and Flow Tangency Options

Since the air that leaves the trailing edge of a three-dimensional airfoil after passage over its upper surface differs in flow from that which has passed under, there is a flow discontinuity extending aft of the trailing edge which constitutes the wake vortex sheet. Specification of flow at the trailing edge, the so-called Kutta condition, is fundamentally important in

specifying the overall lifting flow. In a method which uses finite elements, such as this one, the discontinuity is not abrupt at the trailing edge, and selection and application of an appropriate Kutta condition is less obvious than for analytical methods. This situation is discussed in depth in sec. 6.5 of reference 3, to which the reader is referred for details.

Two options are available for specification of the Kutta condition:

1. Flow tangency. This option requires specification of the point of application of the Kutta condition for each lifting strip, and for each point must be specified the normal unit vector to the wake. (These data are not required for extra strips.) Results are sensitive to these quantities.
2. Pressure equality. For this option, surface pressures at the centroids of the two on-body elements in each lifting strip which include the trailing edge are constrained to be equal. This constraint is imposed automatically by the code so that no additional information or data are required. Moreover, it turns out that this method is insensitive to the distance of the points of application from the trailing edge.

The user is encouraged to select the pressure equality option (ref. 3, sec. 8.2).

#### Spanwise Variation of Vorticity: Step Function and Piecewise Linear Options

As illustrated in Figures 1 and 4, a lifting surface is partitioned by  $n$ -lines into strips of elements which are called lifting strips. Each lifting strip consists of all of the elements in a complete circuit around the airfoil, including the wake. A dipole distribution, from which vorticity is calculated, varies systematically around the lifting strip circuit such that all individual element contributions in a strip may be summed. This is done such as to yield two vortex strengths,  $B$ , per unit strip length for each strip: one for each edge of each strip. Spanwise variation of these vortex strengths is handled by one of two options:

1. Step function. The vortex strength is constant spanwise across each lifting strip and changes discontinuously at the n-line boundaries between lifting strips.
2. Piecewise linear. Vortex strength varies linearly spanwise across each lifting strip such as to reduce the discontinuities at the n-lines to higher order effects.

The step function option is both simpler and less demanding computationally, and, in practice, seems to yield results which are not significantly inferior to the piecewise linear option (ref. 3, sec. 8.3). Use of the piecewise linear option also requires input of special data, among which are widths of all of the lifting strips. This is required since a particular strip does not necessarily have a constant width along its (chordwise) length, and if not, it may not be obvious how to determine the required nominal width for the strip. Thus, the user must enter a width for each strip, which for the usual case of constant width is the constant width value. Also when the piecewise linear option is used, complications arise at the ends of lifting sections, which complications are handled by specification of input parameters NLINE1 and NLINEN (card 8) as described next.

End Conditions for Lifting Sections When the Piecewise Linear Option is Exercised: Parameters NLINE1 and NLINEN

Parameters NLINE1 and NLINEN must be specified by the user for each lifting section when the piecewise linear option is selected to ensure a reasonable treatment of wing tip and root, and to provide continuity between contiguous, independent lifting sections. NLINE1 specifies the edge condition at the beginning (i.e., at the first lifting strip) of the section, and NLINEN specifies the edge condition at the opposite end of the section. For the Jth lifting section we define:

NLINE1(J) Value	Description
1	For the first lifting section (J=1) this provides the "normal" definition of a wing tip (ref. 3, pp. 92-93). An extra strip with width equal to the first regularly defined strip is created. Used to define the wing tip when the wing is described by strips (and sections) in sequence from tip to root.
2	Never used. Causes an error condition print and job abortion.
3	Used for $J > 1$ when the first lifting strip of the Jth lifting section is contiguous with the last strip of the J-1th lifting section. Creates an extra strip of width equal to the width of the last strip of the J-1th section. In combination with $NLINEN(J-1) = 2$ , it ensures spanwise continuity of vorticity between contiguous lifting sections.
4	The code accepts input to define an extra first strip. The complete extra strip is defined as though it were an ordinary strip, via input of no. 12 cards, and its width is defined via $WIDXTR(1,J)$ of card 11. Used to define the root, inside of the fuselage, of a wing described by strips (and sections) in sequence from root to tip.
5	Same as $NLINE1=4$ , but the input (via $WIDXTR(1,J)$ in card 11) strip width is ignored, and the extra strip is assigned the width value of the first ordinary strip in the section.

NLINEN(J)  
Value

Description

- | NLINEN(J)<br>Value | Description   |
|--------------------|---|
| 1                  | For the last lifting section, this provides the "normal" definition of a wing tip (ref. 3, pp. 92-93). An extra strip with width equal to that of the last regularly defined strip is created. Used to define the wing tip when the wing is described by strips (and sections) in the sequence from root to tip.                                |
| 2                  | Used when the end of the Jth lifting section is contiguous with the start of the J+1th lifting section. Creates an extra strip of width equal to that of the first strip of the J+1 section. In combination with NLINE1(J+1) = 3, it ensures spanwise continuity of vorticity between contiguous lifting sections.                              |
| 3                  | Never used. Causes an error condition print and job abortion.   |
| 4                  | The code accepts input to define an extra strip. The complete extra strip is defined as though it were an ordinary strip, via input of no. 12 cards, and its width is defined via WIDXTR(2,J) of card 11. Used to define the root, inside of a fuselage, of a wing that is described by strips (and sections) in the sequence from tip to root. |
| 5                  | Same as NLINEN=4, but the input (via WIDXTR(2,J) on card 11) strip width is ignored, and the extra strip is assigned the width of the last ordinary strip of the section.   |

## Forces and Moments

As explained in detail in sec. 7.14 of reference 3, pressure force is calculated on each element, and the moment of this element is computed about an origin that is specified by the user (card no. 6). Total forces and moments, for strips, sections and the whole body, are calculated by simply adding the individual vectors.

## Variable Array Dimensioning

To render the code open ended with respect to its capacity to handle numbers of quadrilateral elements, and numbers and types (lifting or non-lifting) of sections and strips, we have incorporated the variable dimension FORTRAN feature into the DUGLFT code. Thus, in all but the main program, DUGLFT, array dimensions are represented by symbolic parameters that are discussed below and in the COMMENT statements found in the FORTRAN listing of DUGLFT. These parameters are assigned numerical values in DUGLFT (cards 131 and 132). Also in DUGLFT, all of the arrays are dimensioned numerically, rather than symbolically, with values that are identical to those assigned to the symbolic parameters. Therefore, to adjust array dimensions to fit requirements of a particular problem, it is necessary to change them only in program DUGLFT (and in COMMON/BASDAT/of SR SETFLO and SR FLOVEL if flow velocities are to be calculated using the data output from DUGLFT).

Minimum values for the variable dimension parameters are as follows. They never include quantities that are generated by symmetry.

LFSX	Number of lifting sections
NL2X	NSLX + 2
NOBX	Total number of lifting strips, not counting extra strips
NONX	Number of on-body elements in the flow (not counting ignored, wake and extra strip elements) plus Kutta points defined by input (flow tangency option only) plus off body points (cards 15)

NSEX	Total Number of sections (lifting plus nonlifting)
NSLX	Maximum number of lifting strips in any lifting section (including extra strips if input)
NSTX	Total number of strips (i.e., n-lines) (lifting plus nonlifting including extra strips if input)
NWAX	Similar to $3 \times$ (number of on-body quadrilateral elements in the flow (see NONX) plus the number of onset flows*)

and

Cube of the number of lifting strips (not counting extra strips) (i.e.  $NOBX^3$ ) if the pressure equality Kutta condition option is selected.

N2BX	$2 \times NOBX$
------	-----------------

The DUGLFT codes are the only ones in the package described here that use the variable dimension FORTRAN feature. The trajectory codes and program FLOPNT are not explicitly affected by the DUGLFT dimensioning, but since they all call subroutines SETFLO and FLOVEL, they are implicitly affected.

Subroutine SETFLO recovers data from external unit 18 for use by FLOVEL that was previously stored there by the DUGLFT codes. Therefore, the dimensions of the arrays in COMMON/BASDAT/ in subroutines SETFLO and FLOVEL must be consistent with those defined in DUGLFT; and if the DUGLFT array dimensions are changed, the user must be careful to also change corresponding dimensions in COMMON/BASDAT/, or at least to be sure that the COMMON/BASDAT/ array dimensions are sufficient to contain the data on unit 18.

---

\*The number of onset flows is the number of lifting strips (not counting extra strips) plus the number of uniform onset flows.

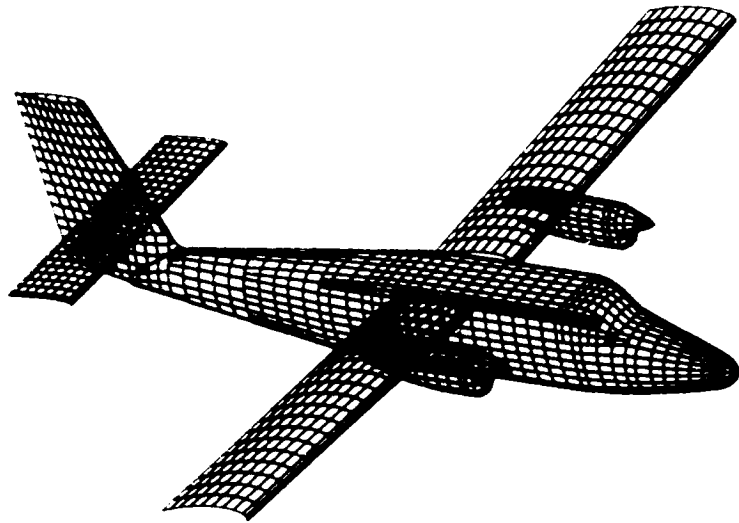
A warning is in order regarding expansion of the arrays to handle very large problems. The user should remember that flow velocity computation time increases directly with the number of quadrilateral elements used. Moreover, a large number of calls to subroutine FLOVEL is required for each trajectory calculation, and FLOVEL may use all of its subroutines on each call, some of them repeatedly. Therefore, it is not practical to use segmentation or overlays with FLOVEL so that all of the data and all of the code must be carried in rapid access memory all of the time.

Obviously, large problems can be costly in terms of both computing time and storage, and accordingly, detail in a surface description that is not required for a particular problem should be ignored or be replaced by paneling that is as coarsely resolved as is practicable. This may require that more than one digital description of a body surface be prepared. An example is shown in Figure 7, which shows digital descriptions of the De Havilland Twin Otter airplane at two levels of resolution. They have been prepared in mutually compatible sectional form such that various sections can be interchanged. For example, if attention is focused on the forward fuselage, the detailed nose and cabin sections from Figure 7a can be combined with the coarsely resolved cylindrical fuselage of Figure 7b, and the wings and tail assemblies can be ignored completely.

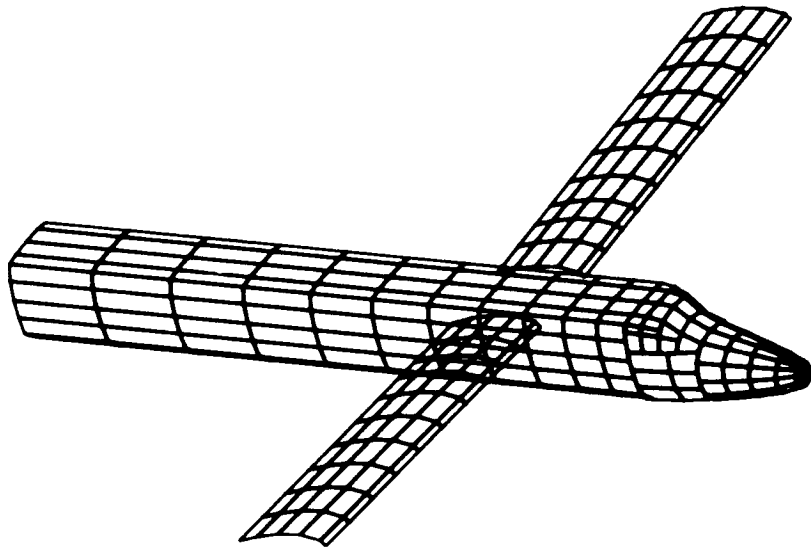
### Printed Output

Printed output consists of two main parts, plus a summary of input control data, various error condition messages, and optional outputs of data that are used for debugging. An example printout, which is for the test problem, is included in the Example Problem section below.

1. The first printout is a summary of input control data, and is self-explanatory.
2. Next, which is the first main part, is a printout (from NOLIFT and LIFT) of element data which is almost the same as the printout for PGM PBOXC discussed above on pp. 30-31. The major differences reflect the fact that DUGLFT code uses element centroids as



a. Finely resolved version



Coarsely resolved version

Figure 7. Digital description of the DeHavilland Twin Otter.

control points rather than null points, which eliminates need for the print of the integers 1 or 2 to label abnormal null points, and the control point coordinates are indicated as X0, Y0, Z0 rather than NPX, NPY, NPZ. Also elements are labeled as nonlifting, lifting or wake. For lifting sections, D is the denominator of equation (7.2.3) of reference 3.

A short table follows (from INPUTL) titled TABLE OF INPUT INFORMATION, which summaries the data in terms of section type, number of elements per section, number of strips, etc.

3. In the course of computing velocities induced by each element on all others, additional summary information is printed (from VIJMX) for each section. For lifting strips, this includes information on ignored elements which does not appear elsewhere.
4. If the piecewise linear option for determination of spanwise variation of vortex strength is used, strip widths,  $W_k$ , and parameters  $D_k$ ,  $E_k$ ,  $F_k$  (ref. 3, sec. 7.11) are printed for each strip for each section, along with a summary of edge conditions (NLINEL and NLINEN, card 8 and pp. 40-42).
5. A short statement is printed (from COLSOL) regarding the dimensions of the matrix that is solved to determine element source strengths, and the number of right-hand-sides (i.e., number of uniform onset flows plus number of lifting strips) for which the solutions are obtained.
6. The second main printout (from PRINTL) contains the final results of the calculations. A printout for each on-body element is labeled as follows:

X0, Y0, Z0	Control point coordinates
VX, VY, VZ	Flow velocity components at the control point
VT	Velocity magnitude
VTSQ	Square of velocity magnitude
CP	Pressure coefficient = $1.0 - VTSQ$
DCX, DCY, DCZ	Direction cosines of the velocity components
NX, NY, NZ	Components of the unit normal to the plane of the element
SIG	Source density
VN	Velocity component in the direction of the unit normal
AREA	Area of the element.

Printouts for off-body and Kutta points are similarly labeled.

Also printed are vector components for pressure force and moment for each strip, each section and for the entire body, as well as a table of vortex strengths per unit length,  $B^{(k)}$ , for each lifting strip.

## 7. Error Messages (ref. 6)

- (a) Message: MISMATCH OF ELEMENTS IN A LIFTING STRIP IS DETECTED.  
ELEMENTS FORMED = xxx, ELEMENTS INPUT = xxx, COMPUTATION TERMINATED. (SR INPUTL)

Cause of error: Inconsistent input data. The program sums the number of on-body elements plus the wake elements specified on card 8. This sum does not match with the elements formed from the input coordinates.

Action: Check the lifting body information card (card 8) and the quadrilateral corner point coordinate cards (cards 12). The number of points on an n-line should equal the number of elements plus 1.

For example. If in a lifting section each lifting strip consists of 10 on-body elements and 1 wake element, the total number of elements is 11, and there should be 12 points on each n-line input via cards no. 12.

- (b) Message: ERROR IN IGNORED ELEMENT COUNT xxx, SHOULD BE xxx.  
(SR LIFT)

Cause of error: Erroneous specification of the ignored element information.

Action: Check card 10 to make sure the ignored element information is properly specified.

- (c) Message: LABEL ERROR IN NONLIFTING VFORM. (SR VFMLF)  
LABEL ERROR IN LIFTING VFORM. (SR VFMLFT)

Cause of error: Geometric data for each element strip, preceded by a lifting or nonlifting label, are stored on unit 4. The error occurs when a labeling mixup is detected during input of the data from unit 4 for calculation of velocities. That is, data for a strip labeled lifting are encountered during computation for a nonlifting section, or vice versa.

Action: Check that the number of lifting strips specified on card no. 8 for each lifting section corresponds with the cards no. 12 input.

(d) The following messages pertain to errors in specification of variable dimensions (SR CKARRY):

ELEMENT CAPACITY, NONX = xxxxxx IS LESS THAN TOTAL ELEMENTS,  
NON = xxxxxx

STRIP CAPACITY, NSTX = xxxx IS LESS THAN TOTAL STRIPS, NSTRP  
= xxxxx

SECTION CAPACITY, NSEX = xxxx IS LESS THAN TOTAL SECTIONS,  
ISECT = xxxx

LIFTING SECTION CAPACITY, LFSX = xxx IS LESS THAN NUMBER OF  
LIFTING SECTIONS, LIFSEC = xxxx

LIFTING STRIP CAPACITY, NOBX = xxx IS LESS THAN TOTAL LIFTING  
STRIPS, LSTRP = xxxx

N2BX = xxx IS NOT .GE. TWICE NOBX AS REQUIRED, NOBX = xxx

NSLX = xxxx IS LESS THAN THE MAX. NO. OF STRIPS IN A LIFTING  
SECTION, WHICH IS xxxx

CAPACITY OF ARRAY WKAREA, NWAX = xxxxxx, USED BY COLSOL TO  
DETERMINE SOURCE STRENGTHS, IS INSUFFICIENT. IT MUST BE  
.GE. xxxxxxxx

NWAX = xxx IS NOT .GE. NO. OF LIFTING STRIPS = xxx CUBED, AS  
REQUIRED FOR THE PRESSURE EQUALITY KUTTA OPTION

Cause of error: Array dimensions are inadequate to accommodate the input data.

Action: Check array dimensions and variable array parameter (see pp. 43-45 and PGM DUGLFT FORTRAN listing) against the storage demands of the element data input via cards no. 12. Also check input parameter LIFSEC, NSORCE, NWAKE, NSTRIP, and IXFLAG.

(e) Messages: xxx ANGLES OF ATTACK HAVE BEEN SPECIFIED, ONLY ONE IS ALLOWED SINCE COMPRESSION EFFECTS ARE CONSIDERED.

ANGLE OF ATTACK,  $\pm x.xxxxxE\pm xx$ ,  $\pm x.xxxxxE\pm xx$ ,  $\pm x.xxxxxE\pm xx$  IS INAPPROPRIATE FOR A CASE WITH COMPRESSION CORRECTION. (SR CKARRY)

Cause of error: Only one uniform onset flow (i.e., free stream) is allowed if the compressibility correction is applied (MACH > 0.0 on card no. 2). Moreover, the direction cosines (ALPHAX, ALPHAY, ALPHAZ) of this onset flow must be (1.0, 0.0, 0.0)(card no. 4).

Action: Set IATAACK = 1 on card 2, and/or specify direction cosines on card 4 as stated above.

(f) Message: THE NUMBER OF KUTTA POINTS SPECIFIED = xxx IS INCORRECT AND SHOULD BE xxx (SR CKARRY)

Cause of error: The flow tangency Kutta option has been specified, and the number of Kutta points specified by input (cards no. 9, 13 and 14) does not equal the number of lifting strips.

Action: Check parameter KUTTA on card 9, and the number of KUTTA data points on cards 13 and 14, against the number of lifting strips input via cards no. 12. (Do not count extra strips.)

(g) Message: ERROR IN VFORM. THE ELEMENTS FORMED DO NOT CORRESPOND TO THE NO. OF BODY ELEMENTS. (SRS VFMNLF AND VFMLFT)

Cause of error: Element tally recorded by SR INPUTL does not match with tally recorded from input of data from unit 4 during velocity calculation.

Action: Check lifting strip specification data on card 8 for consistency with cards no. 12 input data.

(h) Message: AFTER xxx ITERATIONS, DELTA B STILL DID NOT CONVERGE TO THE GIVEN CRITERION / LARGEST DELTA B =  $\pm x.xxxxxxE+xx$  / PROGRAM PROCEEDS WITH THE MOST CURRENT VORTEX STRENGTH. (SR PKUTTA)

Cause of error: Nonconvergence of vortex strengths, B, calculation via the pressure equality Kutta condition method (ref. 3, sec. 7.13.2).

Action: Check the cards no. 12 input data.

(i) Message: THIS CODE SHOULD BE APPLIED TO FIRST STRIP.  
or  
THIS CODE SHOULD BE APPLIED TO LAST STRIP. (SR DKEKFK or PSONST)

Cause of error: Improper specification of NLINE1 or NLINEN for piecewise linear option. Specifically, either

NLINE1 = 2 or NLINEN = 3 is specified, both of which are forbidden. (see pp. 40-42)

Action: Check card 8 specifications.

- (j) Message: xxx ON-BODY POINTS MISSED. EXECUTION TERMINATED.  
(SR PRINTL)

Cause of error: The number of on-body source elements tallied during final printout does not agree with the count tallied during input.

Action: Check input data.

- (k) Message: xxx KUTTA POINTS MISSED. EXECUTION TERMINATED.  
(SR PRINTL)

Cause of error: The number of Kutta points tallied during final print out does not agree with the number specified by parameter KUTTA on card 9.

Action: Check the number of Kutta points input via cards 13 and 14 against parameter KUTTA.

- (l) Message: xxx OFF-BODY POINTS MISSED. EXECUTION TERMINATED.  
(SR PRINTL)

Cause of error: The number of off-body points tallied during final printout does not agree with the number tallied during input.

Action: Check input data.

8. Optional Printouts for Use In Debugging

(a) Geometrical data for each element. (IOUT = .TRUE., card 3)  
(SR INPUTL) For each nonlifting element is printed the element sequence number and twenty-nine geometric quantities (ref. 4, sec. 9.51), and for each lifting element is printed the element sequence number and forty-five geometric quantities (ref. 3, sec. 7.2).

(b) Source induced velocity matrix,  $\vec{V}_{ij}$ . (MPR = 1, card 2) (SR PNTVIJ)

COLUMN                      Matrix column number (j)  
CNTRL PT                     Control point number (i)  
VXS, VYS, VZS               Velocity components

If LIFSEC.GT.0 (card 2), dipole induced velocity matrices,  $\vec{V}_{ik}^{(F)}$ ,  $\vec{V}_{ik}^{(S)}$ , also are printed.

STRIP                        Lifting strip number  
CONTRL PT                    Control point number  
VXF, VYF, VZF               First and second velocity components  
VXS, VYS, VZS

(c) Onset flow matrices,  $\vec{V}_i^{(k)}$  and  $\vec{V}_i^{(\infty)}$ . (MPR = 3) (SR UNIFLO)

ONSET FLOW NO.  
CONTROL POINTS              Control point numbers  
X - FLOW  
Y - FLOW                      Onset flow velocity components  
Z - FLOW

(d) Dot product matrices,  $A_{ij}$ ,  $N_i^{(k)}$  and  $N_i^{(\infty)}$ . (MPR  $\geq 2$ , card 2)  
 (SR AIJMX and NIKMX) (See ref. 3, eq. (7.12.5))

COLUMN	Matrix column number (j)
AIJ	Elements of $A_{ij}$
FLOW NO.	Onset flow number (k)
RIJ	Right side of eq. (7.12.5), ref. 3

(e) Source density matrix (MPR  $\geq 2$ , card 2) (PGM SIGMAL) SOLUTION OBTAINED AFTER COLSOL FLOW NO. Onset flow number. Element source densities,  $\sigma_i^{(k)}$  and  $\sigma_i^{(\infty)}$ , are printed eight to a line.

### Unit 18 Output

The following data are stored on peripheral storage unit 18 (in binary format) for use later by SR FLOVEL in calculating flow velocities at arbitrary space points. Actual record structures are most easily determined by examining the SR SETFLO FORTRAN listing.

#### SR STOR18:

CASE	Body identifier (input card 2)
ISECT	Number of sections (lifting plus nonlifting)
LIFSEC	Number of lifting sections (input card 2)
ALPHAX(1) ALPHAY(1) ALPHAZ(1)	Uniform onset flow direction cosines (card 4)
SYM1 SYM2	Floating point equivalents of input parameters NSYM1 and NSYM2 (card 2)
NSYM	Total number of symmetry planes
NSTRP	Total number of strips, including extra lifting strips if input.

BETAM  $\sqrt{1 - N_M^2}$  where  $N_M$  is free stream Mach number  
 BETSQ  $1 - N_M^2$   
 NLT(NSTRP) Number of elements on each strip, including extra strips, and ignored and wake elements are counted. It is negative for the last strip of each section.  
 NTYPE(ISECT) Section type indicator:  
     0 for nonlifting  
     1 for lifting  
 NLINE(ISECT) Number of strips in a section, not including extra strips  
 If LIFSEC.GT.0:  
 IGW If true, there are ignored elements  
 LASWAK If true, the semi-infinite final wake element option is exercised  
 PESWIS If true, the piecewise linear method for computing spanwise variation of lift vorticity is used.  
 NSTRIP(LIFSEC)  
 NLINE1(LIFSEC)  
 NLINEN(LIFSEC) See input card 8  
 NSORCE(LIFSEC)  
 IXFLAG(LIFSEC)  
 IG1(I,J)  
 IGN(I,J) Only if IGW = .TRUE. See input card 10

For each nonlifting element, the twenty-nine geometric quantities written on unit 4 by SR NOLIFT.

For each lifting element, the forty-five geometric quantities written on unit 4 by SR LIFT.

SR DKEKFK:

Only if the piecewise linear method is used for calculation of spanwise variation of vorticity. For each of K strips in J = LIFSEC lifting sections,

$$K, (D(I,J), E(I,J), F(I,J)), I=1, K$$

where D, E, F are  $D_k, E_k, F_k$  of eq. (7.11.5) of reference 3.

SR SUMSIG:

KFLOW            Number of lifting strips  
 KONTRL           Number of on-body source elements (not including ignored, wake and extra strip elements)  
 COMSIG(KONTRL) Combined source densities (ref. 3, eq. (7.13.1))  
 B(KFLOW)        Vortex strength per unit length

Segmentation Structure

The DUGLFT code may consume a large amount of storage, and it is best to use overlays or segmentation to reduce this. Figure 8 shows a segmentation tree structure that can be used, and Table 3 shows the corresponding tree directions required by the Control Data Corporation CYBER loader. The exact tree structure can be derived from these displays.

TABLE 3

CDC CYBER LOADER TREE DIRECTIVES REQUIRED FOR THE SEGMENTATION STRUCTURE OF FIGURE 8

Directive Number	Label	Verb	Specification
1	INPUT	TREE	INPUTL - (NOLIFT,LIFT)
2	VFLIFT	TREE	VFMLFT - (NEAR,WNEAR)
3	VMATX2	TREE	VIJMX - (VMNLF,VFLIFT)
4	PIECE	TREE	PISWIS - (DKEKFK,PERSONST)
5	VMATX1	TREE	VMATRX - (VMATX2,PNTVIJ,STEPFN,PIECE,UNIFLO)
6	BVORXX	TREE	BVORTX - (PKUTTA,FKUTTA)
7	DUGROT	TREE	DUGLFT - CONTRL - (INPUT,CKARRY,VMATX1, SIGMAL,BVORXX,SUMSIG,VELOCITY)

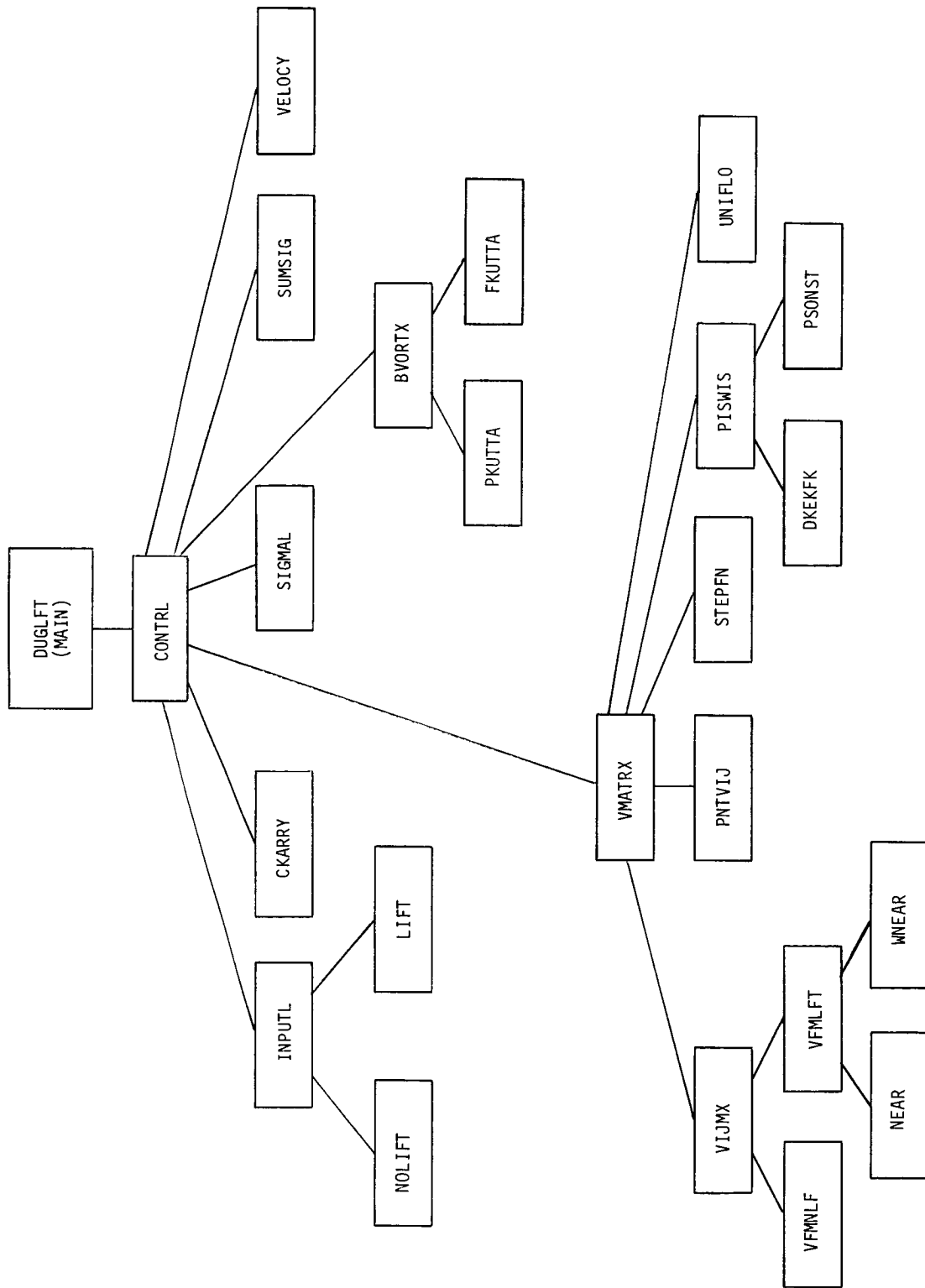


Figure 8. DUGLFT segmentation tree structure.

## Peripheral Storage

In addition to the system input and print units (5 and 6), and unit 18 which is used for output of data required by subroutines SETFLO and FLOVEL (see pp. 55-57), DUGLFT uses eleven units for scratch storage. All data stored on these units are in binary format. In the following, use of each unit is considered only in terms of the maximum number of data words (numbers) and record lengths that would be stored on it. The following variables are defined to aid in this:

KONTRL	Number of quadrilateral elements, not including those: generated by symmetry, ignored, in the wake and in extra strips.
KUTTA	Points defined by input cards no. 13 and 14 at which the Kutta condition is to be applied. (KUTTA > 0 only if the flow tangency option is exercised.)
NOFF	Number of off-body points at which velocity is to be calculated as defined by input cards no. 15.
NON	$KONTRL + KUTTA + NOFF$
IATAACK	Number of uniform onset flows
KFLOW	Number of lifting strips, not counting extra strips, nor those generated by symmetry
NFLOW	$KFLOW + IATAACK$

Unit 3: NFLOW records each consisting of 3 x NON numbers

Unit 4: There is a record of 29 numbers for each nonlifting quadrilateral element

plus

There is a record of 45 numbers for each lifting quadrilateral element (including ignored, wake and extra strip elements)

plus

A one-word record for each section of elements

Unit 8: The larger of

Two records each of length  $3 \times \text{NON}$  numbers

or

NFLOW records each of length  $6 \times \text{KFLOW}$  numbers

or

KONTRL records each of length KUTTA numbers

Units 9 and 10: KONTRL records of maximum length  $\text{KONTRL} + 1$  numbers

Units 11 and 12:  $\frac{1}{2}$  KONTRL records each of length  $3 \times \text{NON}$  numbers

Unit 13: The larger of

$2 \times \text{KONTRL}$  records each of length  $3 \times \text{NON}$  numbers

or

KONTRL records of maximum length  $\text{KONTRL} + \text{NFLOW} + 1$  numbers

Unit 14: The larger of

KFLOW records each of length  $3 \times \text{NON}$  numbers

or

KONTRL records of maximum length  $\text{KONTRL} + 1$  numbers

Unit 15: The larger of

KFLOW records each of length  $3 \times \text{NON}$  numbers

or

KONTRL records of maximum length  $\text{KONTRL} + \text{NFLOW} + 1$  numbers

DUGLFT Card Input

Card No.	Variables and Format	Description
1	(TITLE(I),I=1,18), (18A4)	Run identification
2	CASE,LIFSEC,IATAACK, NSYMI,NSYM2,MPR, LEAK,FRAC,MACH (A4,6I4,2X,2F10.0)	<p>Run control data:</p> <p>CASE (Col.1-4) Four character body identification.</p> <p>LIFSEC (Col.5-8) Total number of lifting sections.</p> <p>IATAACK (Col.9-12) Number of angles of attack (i.e., uniform free stream flows) to be specified via cards no. 4. Maximum value is 10. If the compression correction is to be applied (MACH &gt; 0.0), it is necessary that IATAACK = 1.</p> <p>NSYMI (Col.13-16) One of the three values 0, 1 or -1 is entered. NSYMI specifies the 1st symmetry plane, and NSYM2 (Col.17-20) NSYM2 specifies the second symmetry plane according to:</p> <ul style="list-style-type: none"> <li>0 nonexistent</li> <li>+1 a plus (ordinary) symmetry plane</li> <li>-1 a minus (anti) symmetry plane</li> </ul> <p>See pp. 36-37.</p> <p>MPR (Col.21-24) Print flag used for program debugging only (See pp. 54-55.)</p> <ul style="list-style-type: none"> <li>0 No debug print. This is the normal value for this parameter.</li> <li>1 Print the source induced velocity matrix, <math>\vec{V}_{ij}</math>, and, if LIFSEC &gt; 0, print the dipole induced velocity matrices, <math>\vec{V}_{ik}^{(F)}</math> and <math>\vec{V}_{ij}^{(S)}</math>.</li> <li>&gt;2 Print the dot product matrices <math>A_{ij}</math>, <math>N_i^{(k)}</math> and <math>N_i^{(\infty)}</math>, and the element source densities <math>\sigma_i^{(k)}</math> and <math>\sigma_i^{(\infty)}</math>.</li> <li>3 Print the onset flow matrices, <math>\vec{V}_i^{(k)}</math> and <math>\vec{V}_i^{(\infty)}</math></li> </ul> <p>LEAK (Col.25-28) Number of inlet quadrilateral elements. These must be the first elements in the digital description set (cards no. 12). See pp. 35-36.</p> <p>FRAC (Col.31-40) Fraction of the unit free stream flow that passes through each of the LEAK inlet elements. If LEAK = 0, leave this field blank.</p> <p>MACH (Col.41-50) Mach number of the free stream flow. (Note that this is a floating point number.) If <math>M_\infty \leq 0.5</math>, leave this field blank. See p. 38.</p>
3	IROS,LOFF,MOMENT,LIST, IOUT(5L1)	<p>Logical control flags:</p> <p>IROS (Col.1) If true, the card 12, 13 and 15 coordinates are to be translated, scaled, and rotated about the y axis before processing, and card no. 5 is to be input. If false, no translation, scaling or rotation is done, and card no. 5 is not input.</p>

DUGLFT Card Input, con't.

Card No.	Variables and Format	Description
		<p>LOFF (Col.2) If true, velocities at off-body points are to be calculated. The off-body points are specified by the user via input of the no. 15 cards. If false, off-body velocities are not calculated and there is no input of the no. 15 cards.</p> <p>MOMENT (Col.3) If true, the moment origin is specified by input of card no. 6. If false, card 6 is not input and moments are computed about point (0,0,0).</p> <p>LIST (Col.4) If false, specifies complete execution. If true, execution is terminated after the first main part of the printed output (i.e., after completion of printed output item 2 as described on pp. 45 and 47).</p> <p>IOUT (Col.5) If true, the 29 geometric quantities for each nonlifting element and 45 geometric quantities for each lifting element are printed. The normal value for this parameter is false.</p>
4	(ALPHAX(I),ALPHAY(I), ALPHAZ(I),I=1,IATAACK) (3E10.0)	Direction cosines of uniform onset (i.e., free stream) flow vectors. IATAACK is the number of uniform onset flows specified in card no. 2. One set of direction cosines per card. If the compression correction is applied (MACH > 0.0), only one uniform onset flow vector can be specified. If more than one vector is specified, only the first is passed along via unit 18 for use by SR SETFLO and FLOVEL. The direction cosines are with reference to the airplane coordinate system (after rotation by angle ANGLE (card 5)). These vectors are equivalent to unit free stream velocities. Ordinarily, free stream unit velocity components are (1.0,0.0,0.0). See pp. 37-38.
5	ANGLE,XSCALE,YSCALE, ZSCALE,XTRANS,YTRANS, ZTRANS,(7F10.0)	Input only if IPROS = .TRUE. on card 3. Same as card no. 4 of program PBOXC.
6	ORIGNX,ORIGNY,ORIGNZ, (3E10.0)	Coordinates of the moment origin. This card is input only if MOMENT = .TRUE. on card 3.
----- Cards 7 through 11 are input only if LIFSEC > 0 on card 2. -----		
7	LKUTT,LASWAK,PESWIS, IGW(5L1)	<p>Logical control flags for lifting section data:</p> <p>LKUTT (Col.1) If true, the flow tangency method for application of the Kutta condition is selected. This means that one point in or near the wake of each lifting strip (not counting extra strips) must be specified via input of the no. 13 and 14 cards, and the number of these points must be specified via input of card no. 9. If false, the pressure equality method is selected, and cards no. 9, 13 and 14 are not input.</p> <p>LASWAK (Col.2) If true, the trailing edge of the last wake element is automatically extended by the code to <math>x = \infty</math>. This is the semi-infinite last wake element option. (See p. 35.)</p>

DUGLFT Card Input, Con't.

Card No.	Variables and Format	Description
		<p>PESWIS (Col.3) If true, the piecewise linear method for calculating spanwise variation of lift vorticity is selected, and lifting strip widths must be input via cards no. 11. If false, the step function option is selected, and cards no. 11 are not input. See pp. 39-40.</p>
		<p>IGW (Col.4) If true, there are ignored lifting elements which must be defined via input of the no. 10 cards. If false, there are no ignored elements, and cards no. 10 are not input. See p. 27.</p>
8	(NSORCE(J),NWAKE(J),NSTRIP(J),NLINE1(J),NLINEN(J),IXFLAG(J),J=1,LIFSEC),(6I4)	<p>NSORCE(J) (Col.1-4) Number of on-body elements (including ignored) in each lifting strip of the Jth lifting section.</p> <p>NWAKE(J) (Col.5-8) Number of wake elements in each lifting strip of the Jth lifting section, including a semi-infinite final element if this option is selected. (See pp. 26 and 35.)</p> <p>NSTRIP(J) (Col.9-12) Number of lifting strips in the Jth lifting section. Include extra strips only if they are defined via input of cards no. 12.</p> <p>NLINE1(J) (Col.13-16) If the piecewise linear option is selected; (PESWIS=.TRUE. on card 7), NLINE1(J) specifies the edge condition of the first strip on the Jth lifting section (pp. 41-42). If the step function option is specified, ignore this field.</p> <p>NLINEN(J) (Col.17-20) Same as NLINE1(J) but for the last strip of the Jth lifting section.</p> <p>IXFLAG(J) (Col.21-24) IXFLAG(J)=0 means that no extra strips are defined via input for the Jth lifting section. For extra strips defined via input (i.e., via cards no. 12), we have:</p> <p style="padding-left: 2em;">IXFLAG(J)=1 means the first strip is an extra strip. If the piecewise linear option is selected, (PESWIS=.TRUE. on card 7), this also requires NLINE1(J) = 4 or 5.</p> <p style="padding-left: 2em;">IXFLAG(J)=3 means the last strip is an extra strip. If the piecewise linear option is selected, this also requires NLINEN(J) = 4 or 5.</p> <p style="padding-left: 2em;">IXFLAG(J)=2 means that both first and last strips are extra strips. If the piecewise linear option is specified, this requires that both NLINE1(J) and NLINEN(J) = 4 or 5.</p>
		<p>LIFSEC is specified on card 2. A separate card is required for each lifting section, and the cards are input in the same order as is input of the quadrilateral data via cards no. 12.</p>
9	KUTTA(I4)	<p>Input only if LKUTT=.TRUE. on card 7. Number of points at which the flow tangency method for application of the Kutta condition is to be applied. It is required that KUTTA equal the total number of lifting strips, not counting extra strips. KUTTA is used to read the point coordinates, and the unit vectors normal to the wake or airfoil surface at these points, via cards no. 13 and 14.</p>

DUGLFT Card Input

Card No.	Variables and Format	Description
10	((IG1(I,J),IGN(I,J), I=1,NSTRIP(J)),J=1, LIFSEC),(12I4)	<p>Input only if IGW=.TRUE. on card 7. I=lifting strip index; J=lifting section index. If on the Ith strip of the Jth lifting section there is a substrip of ignored elements, the substrip is defined by specifying its beginning and ending element indices (see footnote below) via:</p> <p>IG1(I,J) = index of the first ignored element on the lifting strip</p> <p>IGN(I,J) = index of the last ignored element on the lifting strip</p> <p>If there are no ignored elements on a strip, leave both fields blank; but IG1 and IGN must be specified for every lifting strip if IGW = .TRUE. on card 7. Six strips per card. Each lifting section begins a new card.</p> <p>LIFSEC is specified on card 2, and NSTRIP(J) on card 8.</p>
11	(WIDXTR(I,J),(WIDTH(I,J), I=2,NSTRIP(J)-K), WIDXTR(2,J),J=1,LIFSEC), (7E10.0) K = 0 if IXFLAG(J)=0 K = 1 if IXFLAG(J)=1 or 3 K = 2 if IXFLAG(J)=2	<p>Input only if PESWIS=.TRUE. on card 7. These quantities are the widths of each lifting strip for use in calculating spanwise variation of vorticity via the piecewise linear method.</p> <p>WIDXTR(1,J) specifies the width of the first extra strip of the Jth lifting section. If NLINEL(J)≠4, leave this field blank.</p> <p>WIDTH(I,J) specifies the width of the Ith lifting strip of the Jth lifting section.</p> <p>WIDXTR(2,J) specifies the width of the last extra strip of the Jth lifting section. If NLINEN(J)≠4, leave this field blank.</p> <p>LIFSEC is specified on card 2, and NSTRIP(J), NLINEL(J), NLINEN(J) and IXFLAG(J) are specified on card 8.</p>
12	X,Y,Z,STAT,LAB,XX,YY,ZZ, STATT,LABL, (3E10.0,2I2/3E10.0,2I2)	<p>On-body and wake quadrilateral element corner point coordinates are specified by these cards for both lifting and nonlifting sections, one point per card. The body and wake surface panels are constructed from these data.</p> <p>X,Y,Z            Quadrilateral corner point coordinates. XX,YY,ZZ (Col.1-30)</p> <p>STAT            Status parameter: Allowed values are 0,1,2,3: STATT (Col.32) 0 This point is on the same n-line as the last point. 1 This point starts a new n-line. 2 This point starts a new section. 3 This is the last point in the card 12 input.</p> <p>LAB            Specifies a lifting or nonlifting section: LABL (Col.34) 0 nonlifting 1 lifting</p> <p>This field is relevant only when STAT or STATT = 2; that is, only on the first card of a new section.</p> <p>Note: There must be an even number of no. 12 cards; add a blank card to the end of the card 12 deck if necessary.</p>

DUGLFT Card Input

<u>Card No.</u>	<u>Variables and Format</u>	<u>Description</u>
13	(XC(I),YC(I),ZC(I), I=1,KUTTA)(3E10.0)	Input only if LKUTT=.TRUE. on card 7. KUTTA is specified via the card 9 input. Coordinates of points (one point per card) at which the Kutta condition is to be applied via use of the flow tangency method. If IPROS=.TRUE. (card 3), the code automatically translates, scales and rotates these coordinates according to the card 5 input data.
14	(XN(I),YN(I),ZN(I), I=1,KUTTA)(3E10.0)	Input only if LKUTT = .TRUE. on card 7. KUTTA is specified via the card 9 input. Components of the unit vectors (one vector per card) normal to the wake or airfoil surface at the points specified by the no. 13 cards at which the Kutta condition is to be applied via use of the flow tangency method. The order of input must be consistent with that of the no. 13 cards. If IPROS = .TRUE. (card 3), a transformation is automatically applied by the code to adjust for rotation of coordinates by angle ANGLE (card 5).
15	XOF,YOF,ZOF,STAT,XOFF, YOFF,ZOFF,STATT, (3E10,0,I2/3E10.0,I2)	<p>XOF,YOF,ZOF      Coordinates of off-body points at which flow velocities are to be calculated, one point per card. (Col.1-30)</p> <p>STAT              Status parameter. A value of 3 signifies the end of the off-body points. Otherwise, leave this field blank. STATT (Col.32)</p> <p>If IPROS=.TRUE. (card 3), the code automatically translates, scales and rotates these coordinates according to the card 5 input data.</p>

Footnote: Element indices on a lifting strip are simply the sequence numbers of the elements, beginning with one at the trailing edge and proceeding along the n-lines in the order with which the elements are defined by input. For example, if the 3rd through 7th elements of a strip are ignored then IGI = 3 and IGN = 7.

## SUBROUTINE FLOVEL

### General Discussion

Given the coordinates of a point in space (X, Y, Z), the current time step interval, H, used in the integration of the particle equations of motion, and the particle coordinates at the previous time step, PPR(3), SR FLOVEL returns the flow velocity components (VX, VY, VZ) at point (X, Y, Z), and an indicator, INBODY, of whether the body surface has been penetrated. INBODY = 0 if the point is exterior to the body, but INBODY = 1 if penetration has occurred during the current time step.

The discussion to follow assumes that a Hess flow field (ref. 3) is being considered. However, if the user wishes to compute flow by use of some other method, for example, flow about a two-dimensional airfoil, he may replace FLOVEL by a subroutine of his own design.\* Implicit in the coding is the assumption that flow velocities are being calculated in the course of a particle trajectory calculation. When this is not the case, for example when called by FLOPNT, the time step, H, can be set to zero in the calling program. This avoids body penetration print-outs that may be meaningless or misleading.

SR FLOVEL is based mainly on the Hess subroutines VFMLNF, VFMLFT, NEAR, WNEAR and PSWISE, with modifications and additions required for application of combined source densities, vortex strengths, body penetration tests and special calculations required for points very close to element surfaces, element edges or extensions of element edges. The combined source densities and vortex strengths are used straightforwardly as indicated by eqs. (7.13.1) through (7.13.3) of reference 3.

---

\*In the trajectory codes a call of SR SETFLO precedes the first call of FLOVEL. SETFLO reads the data stored on unit 18 by PGM DUGLFT (see p. 55), which data are required by FLOVEL for calculation of a Hess flow velocity, and puts these data into COMMON storage. If a user-designed version of FLOVEL is used, SETFLO must be replaced by a dummy subroutine.

## Body Penetration Tests

FLOVEL calculates and sums velocities induced at the calculation point by each element. Three modes of calculation are used (ref. 3, sec. 7.4): (1) for large distances between the calculation point and the element centroid, point singularity methods are used, (2) for intermediate distances, multipole methods are used, and (3) for short distances exact calculations are used. For each on-body element for which exact calculations are required, a sequence of three sets of body penetration tests are applied. The sequence is arranged to save computation time by application first of simple, nonexhaustive tests that can determine that penetration cannot have occurred; as soon as the possibility of penetration is eliminated, further testing is bypassed. In the descriptions of the tests below, we assume that a particle trajectory is being computed.

Sequence 1. If any of the following tests is satisfied, penetration is taken not to have occurred:

1. The vector of separation between the centroid of the element and the particle position is projected onto the unit normal vector to the plane of the element, and the sign of the projection is checked to see if the point is on the exterior side of the element.
2. The square of the distance of the particle position to the element centroid is greater than one-fourth the square of the maximum element diagonal plus the square of the time step.
3. The magnitude of the projection calculated in test 1 is greater than the time step,  $H$ .

For tests 2 and 3 we assume that the maximum particle speed is of order unity, so that the maximum distance a particle can travel in one time step is of order  $H$ .

Sequence 2. The vector of separation between the element centroid and the particle position at the previous time step is projected onto the unit normal vector to the plane of the element. If the sign of this projection is the same as that determined in test 1 of the first sequence for the current position, or if both previous and current positions are exactly in the plane of the element, penetration is taken not to have occurred.

Sequence 3. The line connecting the current particle position with its position at the previous time step is determined, and the point of intersection of this line with the element plane is calculated. If this intersection point lies inside the element or on its boundaries, penetration is taken to have occurred. Details of this sequence of tests are given in Appendix B.

When penetration is detected, the coordinates of the point on the body at which penetration has occurred are printed along with the following information:

REFLECTION LOOP INDEX (I2)	This tells whether the primary element (I2 = 1) or a reflected element (I2 > 1) is involved. (See pp. 20 and 36.)
ZNP (nonlifting element)	Projection of the centroid-to-particle position separation vector onto the unit normal vector to the plane of the element. For a point on the exterior side of the element, we have the following signs on ZNP or Z for the primary and reflected elements:
Z (lifting element)	

<u>I2</u>	<u>Sign of ZNP or Z</u>
1,3	+
2,4	-

ROSQ	Square of the distance of the particle position from the element centroid.
TSQ	Square of the maximum diagonal of the element.
H	Time step.
ELEMENT NUMBER	This is the sequence number of the element in the primary (i.e., unreflected) surface description data set as input via the no. 12 cards.

Calculation of the velocity continues, but return to the calling program is done with parameter INBODY set to unity instead of zero.

If the calling program is SR TRAJEC, SR TRAJEC prints (in addition to and following the above): the particle coordinates inside the body at the end of the current time step, the initial y and z coordinates of the trajectory and the count, JT, of sequential trajectories that have resulted in impact. SR TRAJEC then calls SR IMPACT which may, at the discretion of the user, adjust initial trajectory coordinates,\* and, if  $JT < JLIM$  (JLIM is set in a program above TRAJEC in the calling hierarchy), another trajectory is begun with the adjusted initial coordinates.

### Special Calculations

Special calculation procedures must be used for points that are very close to element surfaces, to element edges, and for lifting elements, very close to extensions of element edges. Details are given in Appendix C. For nonlifting elements and for calculation of source contributions from lifting elements the special procedures have been found to work satisfactorily, and we expect no problems to be encountered by users. On the other hand, completely satisfactory and trouble-free procedures do not seem to be available for some dipole contribution calculations. For example, as a lifting element edge is approached during a particle trajectory

---

\*When used with PGM TANTRA, SR IMPACT must always be a dummy subroutine.

calculation, anomalously large flow velocities may be returned by SR FLOVEL, which may cause the integration time step to fall to such a low value as to indicate a stall or stagnation condition. This usually can be taken to be tantamount to body penetration, however, the user would be well advised to examine the situation closely. In any case, when the integration time step falls below a threshold value set by SR TRAJEC, a comment is printed and the trajectory is terminated. (See the discussion of SR TRAJEC, p. 74.)

### Array Dimensions

The dimensions of arrays in COMMON/BASDAT/ must be adequate to accommodate the data stored on unit 18 previously by program DUGLFT, and must be identical to those in the SR SETFLO COMMON/BASDAT/. Details are included in the discussion of SR SETFLO below. COMMON/BASDAT/ appears in FLOVEL and SETFLO but nowhere else; neither subsidiary subroutines required for the FLOVEL calculations (VFNLFT, VFLIFT, NEARF AND WNEARF) nor the trajectory codes contain this labeled COMMON.

### SUBROUTINE SETFLO

Subroutine SETFLO is called by programs FLOPNT, ARYTRJ, CONFAC and TANTRA prior to any calculation to recover data previously stored by DUGLFT on unit 18 (see pp. 55-57) that are needed by SR FLOVEL to calculate flow velocities about a three-dimensional body. To ensure that the proper set of data is recovered, SETFLO reads a four-character Hollerith body identifier, and checks to see if this is identical to the identifier obtained from the DUGLFT output (parameter CASE on DUGLFT input card no. 2). If not, a comment is printed and the calculation is stopped.

COMMON/BASDAT/ contains all of the arrays that are recovered from the DUGLFT unit 18 output file. These arrays have variable dimensions in DUGLFT, and if dimensions are changed there, care must be taken to ensure that COMMON/BASDAT/ dimensions are adequate to contain the data.

Array dimensions in terms of the symbolic parameters used in DUGLFT are given in COMMENT statements at the beginning of the SR SETFLO FORTRAN listing. Definitions of the symbolic parameters are given above on pp. 43-44, and the contents of the unit 18 output file are described on pp. 55-57.

COMMON/BASDAT/ appears only in subroutines SETFLO and FLOVEL, but it must be identical in these subroutines. Therefore, if dimensions are changed in the SETFLO COMMON/BASDAT/ they must be changed identically in FLOVEL.

If flow around the body is calculated by means other than the Hess method, SETFLO must be replaced by a dummy subroutine.

PROGRAM FLOPNT

### General Description

This program computes flow velocities at an array of points in three-dimensional space. The array is oriented parallel with the three coordinate axes discussed above on pp. 19-20. Flow velocities are computed by SR FLOVEL, which uses data that, for example, are prepared by program DUGLFT for flow about an arbitrary three-dimensional lifting body.

Initial coordinates, array increment values along the three coordinate directions and the number of increments desired along each direction (including the initial point) are input. Also input are integers M(3) which control the order of incrementing along three axes. For example, suppose  $M(1) = 3$ ,  $M(2) = 1$ ,  $M(3) = 2$ :

1. The x and z coordinates are held fixed while y is incremented over its range.
2. y is returned to its initial value, z is incremented once, and y is incremented over its range.
3. This is repeated until z covers its complete range.

4. z is returned to its initial value, x is incremented once, and y is incremented over its complete range.

5. etc.

The printed output is self-explanatory and consists of point coordinates, velocity components and speed.

If data prepared by DUGLFT are used, SR SETFLO reads these data from unit 18; units 5 and 6 are used for input and printing, respectively.

Subroutines called are: SETFLO, FLOVEL.

FLOPNT Card Input

<u>Card No.</u>	<u>Variables and Format</u>	<u>Description</u>							
1	KASE, (A4)	Body identification. Read by SR SETFLO and must be identical to identifier on card 2 of DUGLFT.							
2	HOLL(18), (18A4)	Run identification.							
3	M(3), (3I2)	Coordinate incrementation sequence control. (See discussion above.)							
4	X(I), D(I), N(I): I = 1 (2E10.0, I4)	<table border="0"> <tr> <td>X(1) (Col.1-10)</td> <td>initial x coordinate</td> <td rowspan="3">} (dimensionless)</td> </tr> <tr> <td>D(1) (Col.11-20)</td> <td>x coordinate increment</td> </tr> <tr> <td>N(1) (Col.21-24)</td> <td>number of increments desired in the x direction (including initial value).</td> </tr> </table>	X(1) (Col.1-10)	initial x coordinate	} (dimensionless)	D(1) (Col.11-20)	x coordinate increment	N(1) (Col.21-24)	number of increments desired in the x direction (including initial value).
X(1) (Col.1-10)	initial x coordinate	} (dimensionless)							
D(1) (Col.11-20)	x coordinate increment								
N(1) (Col.21-24)	number of increments desired in the x direction (including initial value).								
5	X(I), D(I), N(I): I = 2	Same as card 4 but for the y axis.							
6	X(I), D(I), N(I): I = 3	Same as card 4 but for the z axis.							
3'	Cards 3 - 6 are repeated for another array.								
.	.								
.	.								
.	.								
.	.								
3	Blank card	A blank card 3 terminates the run.							

## TRAJECTORY CODE DESCRIPTIONS

### GENERAL UTILITY CODES

#### Subroutine PARTCL

Subroutine PARTCL is called by all three of the executive trajectory codes (Table 1B) to input particle specification data and compute still-air, terminal particle settling speed and other data that depend on particle type. This is a particle type - specific code, the version used here being for water drops. It calls SR FALWAT.

#### Subroutine TRAJEC

Trajectories are calculated by SR TRAJEC with the assistance of: SR DVDQ, the numerical integrator code, SR FLOVEL and the functions PRFUN and IMPACT. It also stores trajectory point coordinates at user-specified (normalized) time intervals (TPRINT) in arrays XPLOT(60), YPLOT(60), ZPLOT(60), providing logical parameter IPLOT is specified as true.

SR DVDQ uses a variable time step in integrating the particle equations of motion. An initial minimum time step, HMINI, is input by the user or set to 0.005 on default of input. (See program ARYTRJ input card 4.) During the calculations, the current value of the minimum time step is called HMIN and the time step is H. When DVDQ finds that  $H < HMIN$ , HMIN is set to H, a comment to this effect is printed, and the calculation is continued unless HMIN is found to have fallen to or below a threshold, HEPS, where  $HEPS = 2 \times 10^{-5} HMINI$ . In this case, a comment,

```
HMIN .LT. X.XXXXXE-XX THIS INDICATES STAGNATION
```

is printed, the trajectory is terminated and control is returned to the calling program.

## Function PRFUN

Function PRFUN is a particle type - specific code which is called by TRAJEC to provide the  $N_D - N_R$  relation used in calculating the particle equations of motion (eq. (1)). Actually, through use of the pre-calculated quantity COF ( $= N_{D,S} v_s N_F / N_{R,S}$ ), PRFUN returns the factor on the first term on the right side of eq. (1) which when multiplied by  $\vec{v}_a - \vec{v}_p$  yields the particle equation of motion. The version of PRFUN used here is for water drops, and it calls functions CDRR and WCDRR.

## Subroutine IMPACT

Subroutine IMPACT is called by TRAJEC following penetration of a particle into the body. When used with CONFAC, IMPACT is programmed by the user to adjust trajectory initial y and z coordinates such as to avoid impaction by the next trajectory; accordingly IMPACT is a problem-specific code. No such adjustment is required for cases run under control of ARYTRJ and TANTRA\*, so that a dummy version of IMPACT is used. Examples of IMPACT use are as follows, in which we assume the coordinate system shown in Figure 2 and described on pp. 19-20.

Suppose we wish to compute a trajectory to a target point on the starboard side of an airplane fuselage. Since all initial points of our trajectories will lie in the constant plane  $x = x_i$  (which is far ahead of the airplane in the unperturbed free stream), we need be concerned only with the initial y and z coordinates,  $y_i$  and  $z_i$ . If impaction on the body occurs, the most straightforward way to avoid impaction during the next trajectory is to adjust its  $y_i$  value to be further outboard in the starboard direction (see Fig. 2). Thus, to initiate the next trajectory we use  $y_i = y_i + \epsilon$ , where  $\epsilon$  is a (normalized) positive increment of our choice. For example if  $\epsilon = 0.01$ , SR IMPACT would be:

---

\*Be very sure that IMPACT does not adjust initial trajectory coordinates during tangent trajectory determination under control of TANTRA.

```

SUBROUTINE IMPACT(YI,ZI)
  YI = YI + .01
  RETURN
END

```

If our target point were to be near the underside of a wing, adjustment of initial coordinates would most likely be  $z_j = z_j - \epsilon$ , and if we choose  $\epsilon = 0.05$ , then SR IMPACT would be:

```

SUBROUTINE IMPACT(YI,ZI)
  ZI = ZI - .05
  RETURN
END

```

### Subroutine DVDQ

This is the variable order, ordinary differential equation integrator of Krogh (ref. 7). Operating instructions, which have proven to be quite adequate, are found in the glossary of the DVDQ FORTRAN listing. This version automatically adapts to the word size of the computer used.

A trajectory termination flag is set in SR DVDQ when the particle reaches a user-set x coordinate limit. This condition is found by interpolation (NGE = 0) or extrapolation (NGE = 1). Interpolation is specified in the code as supplied, and is the more efficient and more accurate procedure. However, when termination is desired immediately upstream of the body surface, for example at a "leaking" aperture orifice (which would be paneled), it is necessary to use extrapolation to avoid overshoot and penetration of the body. Parameter NGE is specified in a DATA statement in SR TRAJEC.

PROGRAM ARYTRJ

### General Description

SR ARYTRJ is called to compute particle trajectories initiated at an array of points in three-dimensional space. Particle properties are computed by SR PARTCL and SR PRFUN. Flow velocities are computed by SR FLOVEL, which uses data that, for example, are prepared by program DUGLFT for flow around an arbitrary three-dimensional body. SR DVDQ integrates the particle equations of motion.

Initial coordinates, in the coordinate system defined above on pp. 19-20, of the initial point array, array increment values for the three coordinate directions and the number of increments desired along each direction (including the initial point) are input. Also input are integers M(3) which control the order of incrementing along the three axes and a skip parameter NSKIP. For example, suppose  $M(1) = 3$ ,  $M(2) = 1$ ,  $M(3) = 2$ :

1. The x and z coordinates are held fixed while y is incremented over its range.
2. y is returned to its initial value, z is incremented once, and y is incremented over its range.
3. This is repeated until z covers its complete range.
4. z is returned to its initial value, x is incremented once, and y is incremented over its complete range.
5. etc.

Trajectories are computed to the limiting x coordinate value XLIMIT or until penetration of the body is sensed.

If not every trajectory is desired, the parameter NSKIP is set greater than zero. Then, after the first trajectory, only every NSKIP + 1 th trajectory is computed.

#### Subroutines Required

FLOVEL, SETFLO, PARTCL, FALWAT, TRAJEC, IMPACT (dummy), PRFUN, DVDQ, WCDRR, CDRR

#### External Storage Units

Units 5 and 6 are the system input and print units, respectively.

Unit 9 is used for temporary storage.

Unit 10 is used to store trajectory data for plotting by PGM STEREO.

Unit 18 is used by SR SETFLO for input of data prepared by PGM DUGLFT.

### Printed Output

The printed output is largely self-explanatory. For each trajectory are printed at time interval TPRINT: time, point coordinates (X, Y, Z), particle velocity components (VPX, VPY, VPZ), flow velocity components (VX, VY, VZ), time step (H), Reynolds number (R), acceleration modulus (AC) and cumulative number of flow velocity computations (NEVAL). (All dimensionless)

Other quantities are: angle between the projection of the initial flow velocity vector on the  $z = 0$  plane and the x axis (ALPHA0), angle between the initial flow velocity vector and its projection on the  $z = 0$  plane (BETA0), angle between the projection of the final particle velocity vector on the  $z = 0$  plane and the x axis (ALPHAR), angle between the final particle velocity vector and its projection on the  $z = 0$  plane (BETAR), direction cosines of the drag vector at the final point, and the angle between the projection of the drag vector on the  $z = 0$  plane and the x axis (A), and the angle between the drag vector and the z axis (GAMMA). (All angles are in degrees.)

ARYTRJ Card Input

Card No.	Variables and Format	Description
1	KASE, (A4)	Body identification. Read by SR SETFLO. Must be identical to parameter CASE on card 2 of the DUGLFT input.
2	HOLL (18), IPLOT, (18A4, 7X, L1)	HOLL 72 columns of Hollerith run identification. IPLOT Logical variable: if true, trajectory data are written on unit 10 for plotting by PGM STEREO. (col.80)
3	V, ELL, RHO, TEMP, XFINAL, (8F10.5)	V Free stream airspeed ( $m s^{-1}$ ) (col.1-10) ELL Characteristic dimension of the body (m). Corresponds to L as defined for eq. (1). (col.11-20) RHO Ambient air density ( $kg m^{-3}$ ) (col.21-30) TEMP Ambient temperature ( $^{\circ}K$ ) (col.31-40) XFINAL x coordinate for trajectory cut off (i.e., maximum x coordinate)(normalized, dimensionless) (col.41-50)
4	TPRINT, HI, HMINI, EPSI(3), (8F10.5)	TPRINT Time interval for trajectory point print. Default value = 0.1. (col.1-10) HI Initial numerical integration time step. (See SR DVDQ.) Default value = 0.1 (col.11-20) HMINI Initial numerical integration minimum time step. (See SR DVDQ.) Default value = .005. (col.21-30) EPSI(3) Parameters used to control numerical integration local error. (See SR DVDQ.) Default values = 1.0E-5. (col.31-60) All normalized dimensionless.
5	DIAM, (F10.0)	Water drop diameter ( $\mu m$ ). This card is read by SR PARTCL.
6	M(3), NSKIP, (4I4)	M(3) Array incrementation control. (col.1-12) NSKIP Array skip parameter. (See discussion above.) (col.13-16)
7	X(I), D(I), N(I); I = 1 (2F10.0, I4)	X(1) Initial x coordinate (dimensionless) (col.1-10) D(1) x coordinate increment (col.11-20) N(1) Number of increments desired in the x direction (including the initial value). (col.21-24)
8	X(I), D(I), N(I); I = 2	Same as card 7, but for the y direction.
9	X(I), D(I), N(I); I = 3.	Same as card 7, but for the z direction
5'	Cards 5 - 9 are repeated for another particle and another array	
.	.	
.	.	
.	.	
.	.	
5	Blank card	A blank card 5 terminates the run.

## PROGRAM CONFAC

### General Discussion

Program CONFAC computes trajectories to user-specified target points. It operates in two modes:

1. Single trajectories are calculated to each target point (NW = 0).
2. A central trajectory is computed to the target point, and NW trajectories, evenly spaced about a circle in the target plane of radius RW about the central trajectory, are calculated such as to define a particle flux tube.

Mode 2 is used to calculate concentration factor,  $C_F$ , which is the ratio of particle flux at the target point to the free-stream particle flux. It is easy to show that

$$C_F \approx \frac{\text{area of flux tube cross section in the free stream}}{\text{area of flux tube cross section at the target point}}$$

The areas are those of plane polygons of NW vertices as calculated by SR POLYGO. Concentration ratio,  $C_M$ , the ratio of particle concentration at the target point to free stream concentration, is obtained via the relation

$$C_M = C_F / |\vec{v}_p| \quad .$$

The desired trajectories are calculated by an iterative method which finds a trajectory that passes within a user-specified distance-tolerance (RW\*TOL) of the desired target point. To initialize, the user may input four sets of coordinate guesses: two sets of y and z coordinates for the initial and target planes. These two sets of data are required by the iterative trajectory method since it always must have at least two sets of initial and final y and z coordinates in storage. No special care need be taken in making these guesses since convergence should be rapid as long as the coordinates are in the correct general neighborhood. On default of input, these coordinate guesses are supplied by the code, and these default

values should be adequate. However, should the user wish to restart a trajectory iteration, he can initialize with data sets from the output of the previous calculation or any values of his choice, such as to avoid an initiation that is identical to the previous one.

The trajectory iteration procedure is described in detail in reference 16. (See pp. 13-16 and Appendix A of ref. 16.) SR MAP controls the iteration and calls SR TRAJEC to calculate trajectories. If convergence is not achieved after calculating twenty-five trajectories, the calculation proceeds to the next particle or stops. The limiting number of trajectories can be changed by changing the value of ILIM in a DATA statement in SR MAP.

SR IMPACT is a problem-specific code whose purpose is to adjust trajectory initial y and z coordinates when penetration of the body occurs such that penetration will be avoided on the next attempt. After twenty-five penetrations, the calculation proceeds to the next particle or stops. The limiting number of penetrations can be changed by changing the value of JLIM in PGM CONFAC.

#### Subroutines Required

FLOVEL, MAP, PARTCL, POLYGO, DVDQ, SETFLO, FALWAT, PRFUN, IMPACT, TRAJEC, TRANSF, MATINV, WCDRR, CDRR.

#### External Storage Units

Same as for ARYTRJ.

#### Printed Output

The printed output is largely self-explanatory, and contains all of the data described for PGM ARYTRJ.

Detailed trajectory data are printed only for final trajectories which result from successful convergence to desired target points. All coordinates and velocities in this printout are defined in terms of the "flow coordinate system", which is as described above on pp. 19-20.

For trial trajectories, only initial and final y and z coordinates are printed. Except for the initial coordinate guesses, these coordinates are given in the "flux tube coordinate system", and are so labeled in the printout. The flux tube coordinate system is different from the flow system only for flux tube peripheral trajectories. Then at every point along the flux tube, the y-z plane of the flux system is normal to the central trajectory, and its origin in the y-z plane is at the central trajectory. In cases where a flux tube central trajectory is not defined (i.e., for single trajectories ( $NW = 0$ ) and during calculation of a central trajectory) the flux tube and flow coordinate systems are identical.

When flux tubes are calculated, a summary of results is printed. This includes:

1. Initial and final coordinates of the central trajectory, defined in the flow system.
2. Coordinates of the polygon vertices (i.e., peripheral trajectory intersections) in the initial and target planes, defined in the flux tube system.
3. Polygon areas in the initial and target planes.
4. Concentration factor and concentration ratio.

Also printed are angles  $\alpha_i, \beta_i$  (ALPHA0, BETA0) at the initial plane and  $\alpha_t, \beta_t$  (ALPHAR, BETAR) at the target plane, which can be used to transform coordinates between the flow and flux tube systems. Given coordinates  $x, y, z$  in the flow system along with central trajectory initial (or final) coordinates  $x_i, y_i, z_i$  (or  $x_t, y_t, z_t$ ) also in the flow system, we define

$\Delta x = x - x_i$  (or  $\Delta x = x - x_t$ ),  $\Delta y = y - y_i$  (or  $\Delta y = y - y_t$ ) and  $\Delta z = z - z_i$  (or  $\Delta z = z - z_t$ ), and designate  $x_f$ ,  $y_f$ ,  $z_f$  to be the corresponding coordinates in the flux tube system. Then

$$x_f = \Delta x \cos\alpha \cos\beta + \Delta y \sin\alpha \cos\beta + \Delta z \sin\beta$$

$$y_f = -\Delta x \sin\alpha + \Delta y \cos\alpha$$

$$z_f = -\Delta x \cos\alpha \sin\beta - \Delta y \sin\alpha \sin\beta + \Delta z \cos\beta$$

and

$$\Delta x = x_f \cos\alpha \cos\beta - y_f \sin\alpha - z_f \cos\alpha \sin\beta$$

$$\Delta y = x_f \sin\alpha \cos\beta + y_f \cos\alpha - z_f \sin\alpha \sin\beta$$

$$\Delta z = x_f \sin\beta + z_f \cos\beta$$

Here  $\alpha$  is the angle between the projection of the velocity vector in the x-y plane and the x axis, and  $\beta$  is the angle between the velocity vector and its projection in the x-y plane, where the x-y plane is defined in the flow coordinate system.

CONFAC Card Input

Card No.	Variables and Format	Description
1	KASE, (A4)	Body identification. Read by SR SETFLO. Must be identical to parameter CASE on card 2 of the DUGLFT input.
2	HOLL(18), IPLOT, (18A4, 7X, L1)	HOLL 72 columns of Hollerith run identification. IPLOT Logical variable: if true, trajectory data (col. 80) are written on unit 10 for plotting by PGM STEREO.
3	V, ELL, RHO, TEMP, XSTART, (8F10.5)	V (Col.1-10) Free stream airspeed ( $m s^{-1}$ ) ELL (Col.11-20) Characteristic dimension of the body (m). Corresponds to L as defined in eq. (1). It is used to normalize all lengths. RHO (Col.21-30) Ambient air density ( $kg m^{-3}$ ). TEMP (Col.31-40) Ambient temperature ( $^{\circ}K$ ). XSTART (Col.41-50) Initial x coordinate of trajectory. (normalized, dimensionless)
4	TPRINT, HI, HMINI, EPSI(3), (8F10.5)	Same as for ARYTRJ.
5	NW, RW, TOL, (I10, 7F10.5)	NW (Col.1-10) Number of trajectories used to define flux tube peripheries for concentration factor calculation. If NW = 0, single trajectories are calculated to target points defined by cards 9.* Right justify in the field. RW (Col.11-20) Flux tube radius (normalized). TOL (Col.21-30) Tolerance factor for trajectory iteration convergence. Convergence occurs when a trajectory passes within a distance of RW*TOL of the target point.
6	YE, ZE, YI, ZI (8F10.5)	YE, ZE Initial guesses of trajectory y and z coordinates in the target plane
7	YE, ZE, YI, ZI, (8F10.5)	YI, ZI Initial guesses of trajectory coordinates in the initial plane  These coordinates are in the coordinate system used to define the body and the flow field (normalized, dimensionless). The data in the two cards can be very approximate, but if not blank, the two cards should not be identical. On input of two blank cards, the code supplies default estimates based on the first target coordinates.
8	DIAM, (7F10.0)	Water drop diameter ( $\mu m$ ). This card is input by SR PARTCL.

\*Parameters RW and TOL must be given non-zero values even when NW = 0.

CONFAC Card Input (cont.)

<u>Card No.</u>	<u>Variables and Format</u>	<u>Description</u>
9	XW, YW, ZW, (8F10.5)	x,y,z coordinates of the target point (normalized, dimensionless).
8'	Cards 8 and 9 are repeated for as many particles as desired.*	
9'	.	
.	.	
.	.	
.	.	
8	Blank card	A blank card 8 terminates the run.

\*Previous trajectory y and z coordinates are used as trajectory iteration initialization estimates for each new target point. Thus, if target points are widely spaced, separate runs should be made for each.

## PROGRAM TANTRA

### General Discussion

The purpose of this code is to compute tangent particle trajectories to a three-dimensional body. The code is designed to be as general and as automatic as practical, but owing to the unlimited number of geometrical possibilities in three dimensions, some compromise is necessary. Since we cannot know a priori what parts of a body the tangents will touch, we do not, in general, have the option of specifying target points on the body or even target planes through the body. Therefore, we specify curves in the free stream well ahead of the body on which all trajectories are initiated for a particular tangent determination.

Given the equation of the starting-point curve and an initial point on the curve, the code computes the trajectory from this point toward the body until penetration of the body occurs or until a specified x-coordinate stop point is reached. If penetration occurs, a specified coarse step is taken along the starting-point curve such that the resulting trajectory will pass further from the body, and another trajectory is computed. If penetration does not occur, the coarse step is taken along the starting-point curve in direction such that the resulting trajectory will pass closer to the body, and another trajectory is calculated. Once penetration occurs for trajectories that initially miss the body, or the reverse for trajectories that initially impact, the initial point is backed up one step along the starting-point curve, and the process of stepping toward or away from the body is resumed with a fine step size until the tangent trajectory is found. Thus, the tangent trajectory misses the body by no greater than the tolerance implied by the fine step size. Note that this does not imply that the tolerance is the fine step size. Separation of trajectories in the free stream will not be the same as separation of the same trajectories near the body, nor even approximately the same except for very large, heavy particles which have sufficient inertia to essentially ignore the flow around the body. In general, trajectory separations near the body will be less than in the free stream.

Specification of the starting-point curve is done via SR STRPNT, which in the version supplied uses straight line curves. The user provides the coordinates of two points on the line:

Point 1. Initial coordinates of the initial trajectory.

Point 2. Coordinates of any other point on the line chosen such that a small step taken along the line from point 1 toward point 2 will initiate a trajectory that will pass closer to the body surface, or intersect it at a point that will project closer to the body center, than the trajectory initiated at point 1.

This definition of Point 2 relative to Point 1 is such as to ensure that stepping along the starting-point curve will proceed in the proper direction. Point 2 need not be, and in general will not be, the initial point of an actual trajectory. Note that both of these points must be sufficiently far upstream to be essentially in the free stream. Also specified are the coarse and fine stepping distances. All coordinates and distances are normalized. (See eq. (1).)

If so specified (IPLLOT = true), tangent trajectory data are stored on unit 10 for plotting later by PGM STEREO.

#### Subroutines Required

FLOVEL, SETFLO, PARTCL, FALWAT, STRPNT, TRAJEC, IMPACT\*, PRFUN, DVDQ, WCDRR, CDRR.

#### External Storage Units

Same as for ARYTRJ.

---

\*Be sure that IMPACT is a dummy subroutine. Resetting of initial trajectory coordinates by SR IMPACT will ruin a tangent trajectory determination.

## Printed Output

Trajectory data are as described for PGM ARYTRJ and are printed for every trajectory computed regardless of whether or not the trajectory is accepted as the tangent trajectory. Beyond that, the output is fully labeled and self-explanatory. All input data are printed: including the points used to define the starting-point line, coarse and fine increments, and starting point coordinates. The switching from coarse to fine step size is clearly identified, as are the tangent trajectory data.

TANTRA Card Input

<u>Card No.</u>	<u>Variables and Format</u>	<u>Data Description</u>
1-4		Cards 1 through 4 are the same as for ARYTRJ.
5	DIAM, (7F10.0)	Water drop diameter ( $\mu\text{m}$ ). This card is read by SR PARTCL.
6	DCORS, DFINE, (8F10.0)	Respectively, the coarse and fine step sizes to be used in stepping along the starting-point line (normalized, dimensionless). Card 6 is read by SR STRPNT.
7	X,Y,Z,X1,Y1,Z1, (8F10.0)	X,Y,Z Coordinates of Point 1, which specifies the initial trajectory coordinates on the starting-point line (normalized, dimensionless).  X1,Y1,Z1 Coordinates of Point 2, which is any point on the line that will initiate a trajectory that will pass closer to the body than the trajectory initiated by Point 1. (normalized, dimensionless).
<p>Note that the starting-point line should be far enough upstream of the body to be essentially in the free stream. Card 7 is read by SR STRPNT.</p>		
-----		
6'		Cards 6 and 7 are repeated for as many trajectories as desired.
7'		
.		
.		
6	Blank card	A blank card 6 signals end of calculation for this water drop, and another card 5 is read.
-----		
5'		
6"		

Tantra Card Input (cont.)

<u>Card No.</u>	<u>Variables and Format</u>	<u>Data Description</u>
7"		
.		
.		
.		
6	Blank card	
-----		
5	Blank card	A blank card 5 terminates the run.

## PROGRAM STEREO

### General Discussion

Program STEREO is used to plot results of the trajectory calculations. Both body and trajectories are plotted. The body data are obtained from unit 9, on which the data were stored by SR PINPUT under control of PGM PBOXC, and the trajectory data are obtained from unit 10, on which the data were stored under control of either ARYTRJ, CONFAC or TANTRA.

Plots are prepared in pairs, members of a pair being separated by a specified angle on each side of a specified viewing direction. Proper specification of the angles, which usually requires some trial-and-error-experimentation, may provide plots which can be used for stereo viewing as illustrated by Figure 9.

The viewing direction is defined by specifying two angles, THETA and PSI. The operation of these angles is as follows: We assume a right-handed coordinate system with its positive z axis directed upward and the free-stream flow in the direction of the positive x axis. First rotate the coordinate system about the y axis by angle THETA such that positive THETA tilts the positive x axis upward. Then rotate about the new z axis by angle PSI such that for positive PSI the rotation is clockwise when viewed from above. The view direction separation angle, DELTA is applied to angle PSI such that the members of a stereo pair are actually viewed from angles THETA, PSI-DELTA and THETA, PSI + DELTA, and are plotted in that order.

For a particular case (i.e., body and set of trajectories), the user must specify the number of trajectories and the (upstream) x coordinate at which plotting of the trajectory data is to be begun. This need not have the same value as the initial x coordinates of the data stored on unit 10.

Translating and scaling of the data such that it will properly fit into the plot area is handled automatically by the program.

Only system and plot subroutines are required.

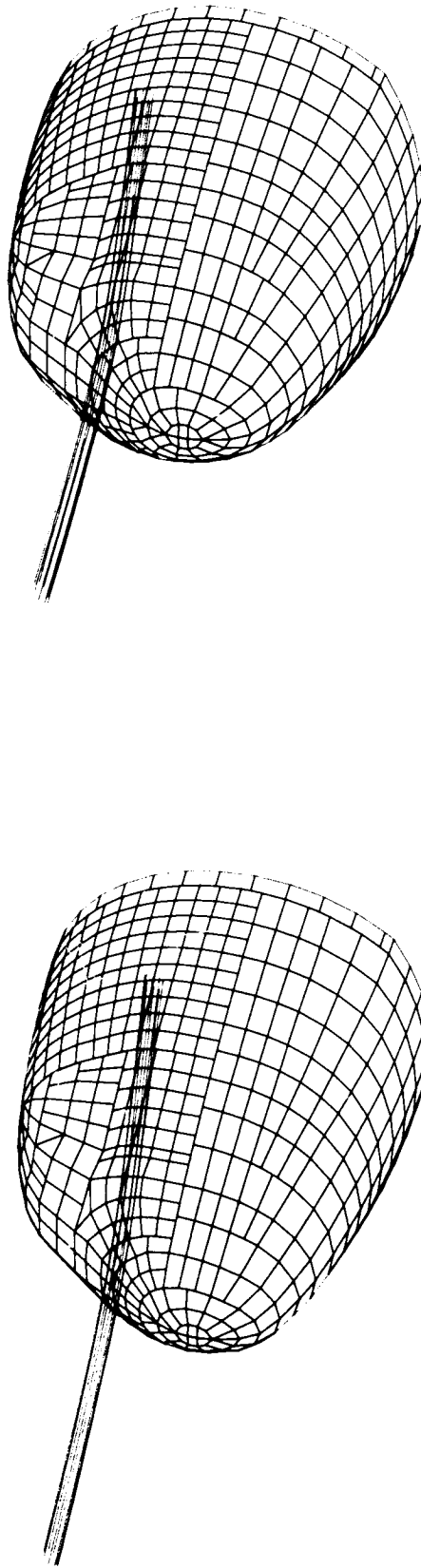


Figure 9. Stereographic plot of an eight-trajectory, 20  $\mu\text{m}$ -diameter water drop flux tube to a particle replicator mounted on the forward fuselage of a Lockheed C130A airplane. The central trajectory is also shown.  $C_F = 1.15$ . (Ref. 16) Three-dimensional perspective can be attained by staring at the center of the figure and then crossing the eyes such that the two images merge.

### External Storage Units

Units 5 and 6 are the system input and print units.

Unit 9 contains the three-dimensional body surface data, plus some scaling information, as stored by SR PINPUT.

Unit 10 contains the trajectory data as stored under control of PGMS ARYTRJ, CONFAC or TANTRA.

### Printed Output

The printed output is simple. It consists of a run identification, the input data and some scaling information. For each trajectory is printed:

1. the coordinates (XTRAJ, YTRAJ, ZTRAJ) of each point before translation, scaling and projection onto the plot plane, and
2. the translated, scaled and projected coordinates (XPLOT, YPLOT) of each point plotted.

~~CS~~

## STEREO Card Input

<u>Card No.</u>	<u>Variables and Format</u>	<u>Description</u>
1	HOLL(18), (18A4)	72 columns of Hollerith run identification.
2	ICRT, NTRJS, XSTART, (L1, I9, F10.0)	ICRT (Col.1) A logical variable which when true causes plotting to be via CRT. Otherwise, plotting is via pen and ink.  NTRJS (Col.2-10) Number of trajectories to be plotted.  XSTART (Col.11-20) x coordinate at which trajectory plotting is to begin. Need not correspond to the initial x coordinates of trajectories stored on unit 10.
3,4	LINE1, LINE2, (7A6/7A6)	Cards 3 and 4 are read only if ICRT is true (card 2). Two lines of 42 columns each of Hollerith labeling for a microfiche film.
5,6	THETA, PSI, DELTA, HLABEL(18), (3F10.2/ 18A4)	THETA Viewing angles and viewing angle PSI separation (degrees). (See DELTA definitions above.)  HLABEL 72 columns of Hollerith labeling for the plots.
-----		
5',6'	Cards 5 and 6 are repeated for as many additional plot pairs as desired.	
-----		
5,6	Blank cards	Blank cards 5 and 6 terminate the run.

## VALIDATION

### PRIOR WORK

Hess and Smith report a large number of validation studies for non-lifting flow (refs. 4 and 5). These studies include flow about bodies of simple geometries for which analytical solutions are known, and comparison of calculated results with wind tunnel data for complex aircraft bodies. Excellent agreement is obtained in almost all cases.

Hess (ref. 3) presents the results of a variety of studies on airfoils and combinations of airfoils with nonlifting bodies using his lifting code. Pressure distributions, both chordwise and spanwise, are generally in good agreement with measured data. Local lift coefficient, however, is always overpredicted, though there is usually good agreement in shape of the calculated and observed distribution curves. Overprediction of lift coefficient is substantial, being typically in the range of 10-20%. Results of one study in which boundary layer effects were approximately accounted for indicate that most, if not all, of this calculation error is caused by neglect of viscosity (ref. 3). In some cases, neglect of local compressibility also substantially affects the lift calculations, but Hess concludes that a simple correction suitable for lifting flow is not available (ref. 3).

Studies of trajectory calculations using the nonlifting code are discussed in references 2 and 16, and those results are merely summarized here: (1) Very small particles were calculated to follow flow streamlines around an ellipsoid with negligible deviation, and from this we conclude that our numerical integration procedure is highly accurate. (2) Trajectory results for water drops over a range of sizes in flow about an analytical ellipsoid were compared with results from an ellipsoid defined by quadrilateral elements. Small differences were found except for a drop on the edge of a shaded zone, where numerical difficulties are inevitable in any case. (3) Tangent trajectory results calculated for flow about ellipsoids

were compared with prior calculated results, and acceptable agreement was found. (4) Tangent trajectory results were compared with observed data and prior calculations for four wind tunnel tests of flow about an ellipsoidal forebody. Maximum impact distance along the surface from the nose point was consistently overpredicted by about 60%, but this is an improvement over the prior calculations which overpredicted in the range from 60% to 160%. Moreover, overprediction by the prior study consistently increases as droplet size decreases, whereas this trend is not particularly evident in our calculations. Since the trajectory calculations become more demanding as particle size decreases, this improvement is suggestive of improved capability.

#### ADDITIONAL VERIFICATION

NACA TN 3839 (ref. 17) reports wind tunnel data for impact of water drops on several airfoils. Calculated results also are given for the NACA 65<sub>1</sub>-212 airfoil at 4° angle of attack, so that we have selected this case for verification study, plus the same airfoil at 0° angle of attack. Airfoil coordinate points (Table 4a) were taken from Table 1 of NACA TN 3047 (ref. 18), and plots of the digital representation of the airfoil are given in Figure 10. Also in TN 3839 are wind tunnel data for the NACA 65<sub>1</sub>-212 airfoil that was yawed at an angle of 35° to the onset flow such as to represent an airfoil with a 35° sweep angle. The airfoil crosssection in the plane normal to its leading edge is the same as for the unswept airfoil. To determine the crosssection coordinates in the plane parallel with the onset flow, simply multiply the z coordinates in Table 3a by  $\cos(35^\circ)$ , and these coordinates are listed in Table 4b. Figure 11 shows a plot of the swept wing digital description.

TABLE 4

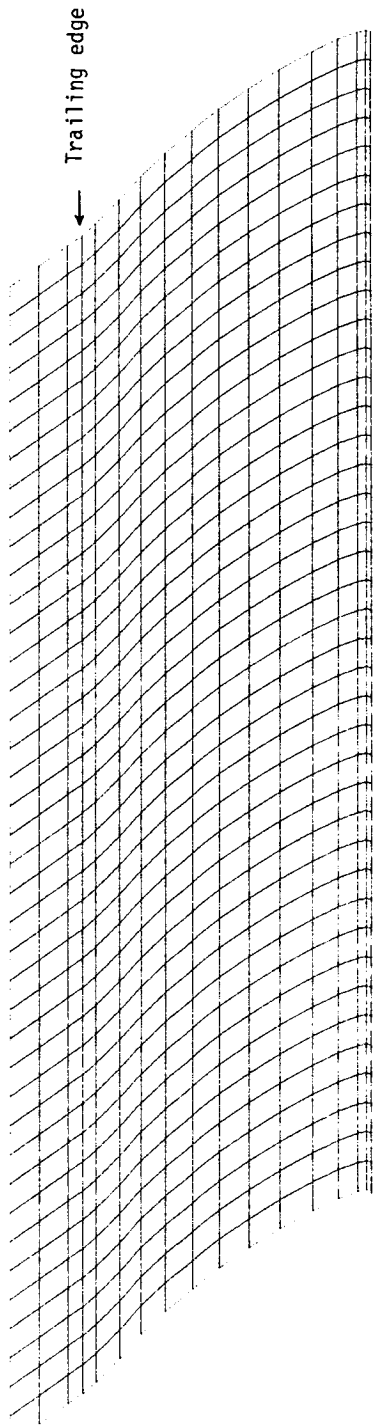
a. NACA 65<sub>1</sub>-212 AIRFOIL CROSSSECTION COORDINATE POINTS (Ref. 18)

Lower Surface			Upper Surface		
x	z	s*	x	z	s*
0	0	0	0	0	0
.00577	-.00870	.0100	.00423	.00970	-.0100
.02609	-.01686	.0325	.02391	.02058	-.0325
.07627	-.02745	.0830	.07373	.03593	-.0840
.15121	-.03727	.1600	.14879	.05073	-.1610
.25094	-.04510	.2590	.24906	.06300	-.2620
.35058	-.04882	.3590	.34942	.06942	-.3630
.45019	-.04854	.4605	.44981	.07044	-.4640
.54983	-.04317	.5610	.55017	.06507	-.5705
.64957	-.03351	.6625	.65043	.05411	-.6720
.74947	-.02164	.7640	.75053	.03954	-.7730
.84955	-.00956	.8640	.85045	.02302	-.8750
.94983	-.00039	.9650	.95017	.00671	-.9775
1.00000	0	1.0150	1.00000	0	-1.0275

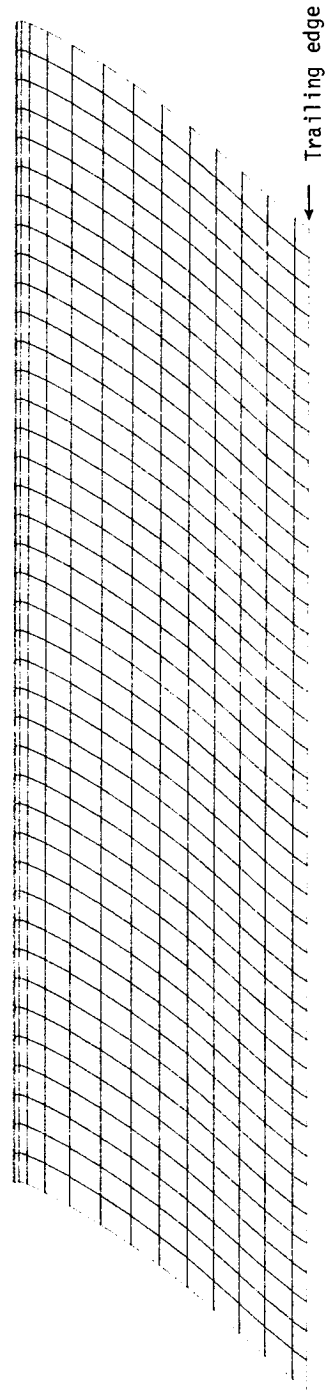
\*s is the distance from the leading edge along the airfoil surface.

b. CROSSSECTION COORDINATE POINTS FOR NACA 65<sub>1</sub>-212 AIRFOIL WITH 35° SWEEP

Lower Surface		Upper Surface	
x	z	x	z
0	0	0	0
.00577	-.00713	.00423	.00795
.02609	-.01381	.02391	.01686
.07627	-.02249	.07373	.02943
.15121	-.03053	.14879	.04156
.25094	-.03694	.24906	.05161
.35058	-.03999	.34942	.05687
.45019	-.03976	.44981	.05770
.54983	-.03536	.55017	.05330
.64957	-.02745	.65043	.04432
.74947	-.01773	.75053	.03239
.84955	-.00783	.85045	.01886
.94983	-.00032	.95017	.00550
1.00000	0	1.00000	0



a. Upper surface



b. Lower surface

Figure 10. Computer drawn plots of the digital description of the NACA 65-212 airfoil.

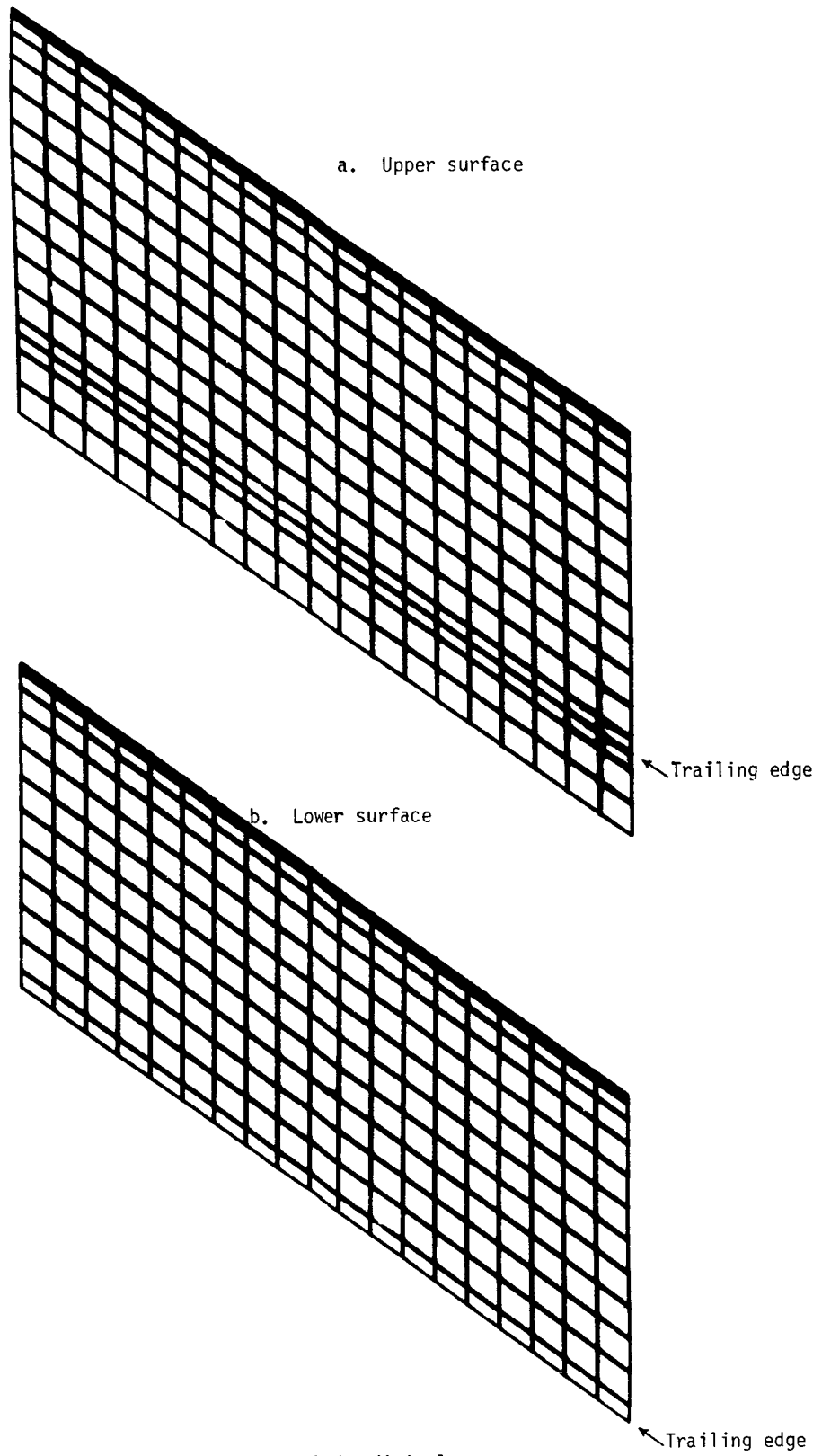


Figure 11. Computer-drawn plots of the digital description of the NACA 65<sub>1</sub>-212 airfoil with 35° sweep angle.

Data were collected in the Lewis Laboratory Icing Research Tunnel for the following atmospheric conditions (ref. 17):

Airspeed	152 kts (78.195 m s <sup>-1</sup> )
Temperature	50°F (283.16°K)
Pressure	28.1"Hg (94985 Pa)

Air density and viscosity are calculated to be 1.1686 kg m<sup>-3</sup> and 1.76520X10<sup>-5</sup> kg m<sup>-1</sup> s<sup>-1</sup>.

As shown in Figure 10, the unswept airfoil is represented by twenty lifting strips, each with twenty-six on-body elements and three wake elements, including the semi-infinite final wake element. A (plus) y=0 symmetry plane was defined which has the effect of doubling the airfoil to forty lifting strips. The swept airfoil (Figure 11) is represented by nineteen lifting strips, each with twenty-six on-body elements and three wake elements, including the semi-infinite final wake element. No symmetry is used. The pressure equality Kutta condition and the step function spanwise vorticity variation options were exercised for both airfoils. Chord lengths were taken to be 13 and 87.5 inches respectively for the unswept and swept airfoils.

Data were collected in the wind tunnel using water sprays with three different distributions of water droplet sizes (ref. 17). To compare with tangent trajectory calculation results, we are interested in the maximum distance aftward from the leading edge, on both the upper and lower surfaces, at which droplet impact was observed. Such distances measured along the surface of the airfoil,  $s_u$  and  $s_l$ , correspond approximately to impact points of barely subtangent trajectories of droplets of maximum diameter,  $\delta_{max}$ , in the sprays. For the unswept airfoil, we calculated  $s_u$  and  $s_l$  for each of the three sprays for 0° and 4° angles of attack. For the swept airfoil, we calculated  $s_u$  and  $s_l$  for the spray of intermediate droplet size for angles of attack of 0° and 4.3°.

Results are listed in Table 5 and displayed graphically in Figure 12 for the unswept airfoil. Table 6 lists results for the swept airfoil.

TABLE 5  
TANGENT TRAJECTORY RESULTS FOR THE UNSWEPT AIRFOIL

a. 0° Angle of Attack

$\delta_{\max}$ ( $\mu\text{m}$ )	$s_u/s_\ell$		% Error
	Observed	New Calculation	
59	.250/.202	.230/.260	-8/29
48	.199/.170	.240/.185	21/9
29	.121/.081	.144/.096	19/19

b. 4° Angle of Attack

$\delta_{\max}$ ( $\mu\text{m}$ )	$s_u/s_\ell$			% Error	
	Observed	New Calculation	NACA Calculation	New Calculation	NACA Calculation
59	.109/.460	.160/.456	.20/.45	47/-0.9	83/-2
48	.085/.394	.082/.452	.17/.42	-4/15	100/7
29	.041/.248	.036/.359	.10/.33	-12/45	144/33

Note: All s values are normalized by dividing by the chord length, 13".

TABLE 6  
TANGENT TRAJECTORY RESULTS FOR THE AIRFOIL WITH 35° SWEEP

$$\delta_{\max} = 48 \mu\text{m}$$

Angle of Attack	$s_u/s_\ell$		% Error
	Observed	Calculated	
0°	.05/.04	.073/.030	46/-25
4.3°	.01/.14	.009*/.156	-10/11

Note: All s values are normalized by dividing by the chord length, 87.9".

\*The particle stalled at a distance of about .012" from an element edge.  
See the discussion of special calculations (pp. 69-70), p. 74 and Appendix C.

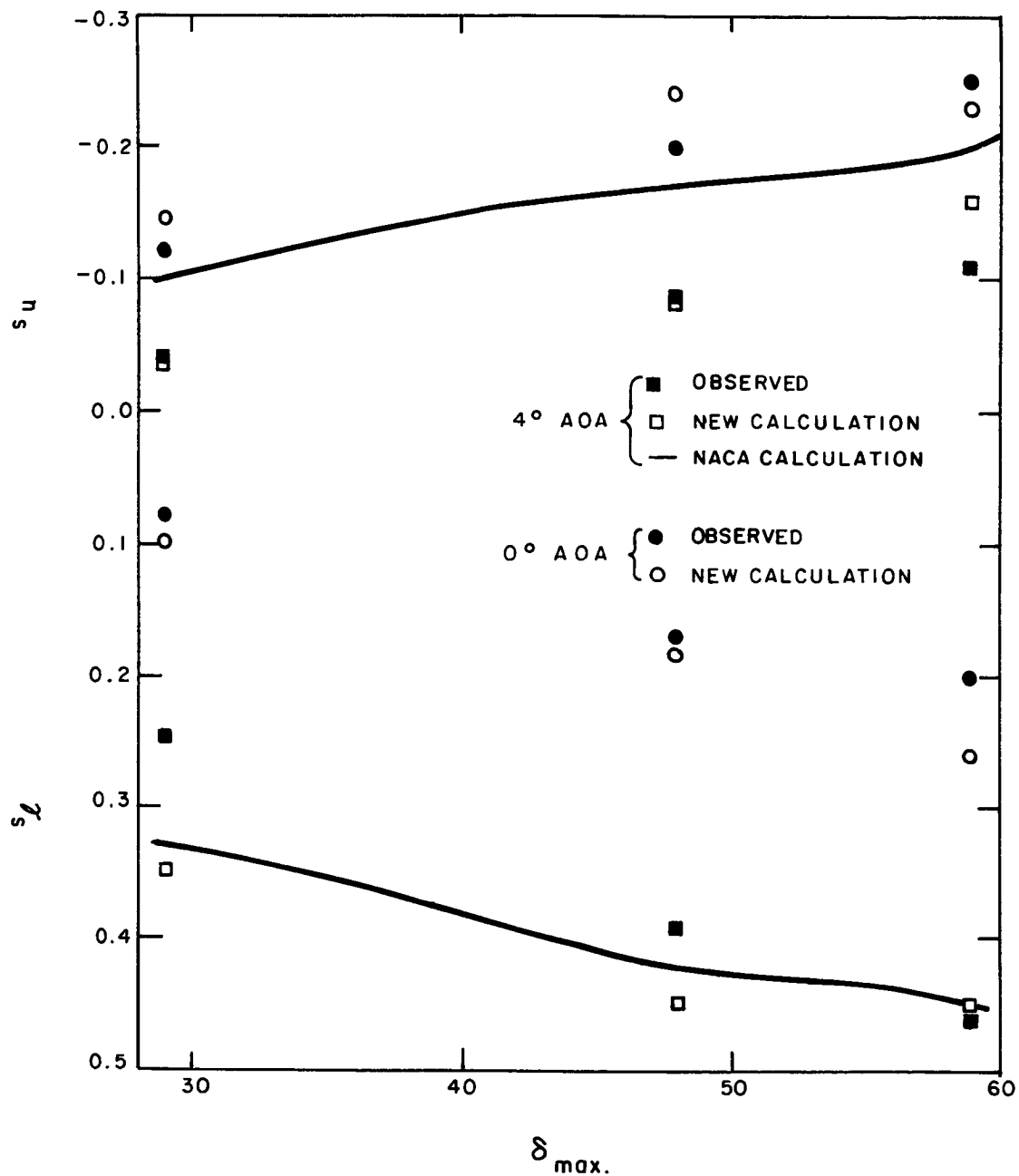


Figure 12. Calculated and observed results for water drop impaction on an unswept NACA 65<sub>1</sub>-212 airfoil.  $s_u$  and  $s_l$  are maximum impact distances from the leading edge, measured along the airfoil surface, on the upper and lower sides of the airfoil respectively.  $\delta_{max}$  is the diameter of the largest drop in the water spray.

As might be expected, agreement with the observed data is not outstanding. However, when experimental problems which must have influenced the observed results are considered (speculatively), and also we consider that the use of rather coarsely resolved flat elements to represent the slightly curved airfoil surface will at least occasionally cause substantial error in determining impact points of nearly tangent trajectories, we conclude that the comparisons are satisfactory. Moreover, for the unswept airfoil at 4° angle of attack, we can compare the new calculation results with the calculated results reported in reference 17. The average absolute percent error for the new calculation is 21% while it is 47% for the NACA calculations. Thus, the new code appears to provide substantial improvement over the previous calculations.

#### CALCULATION TIMES

##### IBM 370/3033 Computer

Element processing (program DUGLFT) and tangent trajectory (subroutine TANTRA) calculations for the unswept NACA 65<sub>1</sub>-212 airfoil were performed on the IBM 370/3033 computer at the NASA Lewis Research Center. The DUGLFT run to process the 1200 elements at 0° angle of attack required 197 seconds of CPU time. Again for the 0° angle of attack case, tangent trajectories were computed in two runs: one for all three particles to the upper airfoil surface, and the other for the three particles to the lower surface. Results are as follows:

##### a. Upper Surface

$\delta_{\max}$ ( $\mu\text{m}$ )	<u>Number of Trajectories</u>	<u>Number of Velocity Calculations</u>
59	10	3411
48	13	4123
29	13	4722

Total CPU time = 2892 seconds.

b. Lower Surface

$\delta_{\max}$ ( $\mu\text{m}$ )	<u>Number of Trajectories</u>	<u>Number of Velocity Calculations</u>
59	9	2422
48	10	3249
29	13	5039

Total CPU time = 2492 seconds.

Each trajectory calculation is initiated at  $x = -5$  and stopped at  $x = 1$  unless impaction occurs. (Distances are normalized by dividing by the chord length.)

Since most of the computing time is used for velocity calculation, we have included the number of velocity calculations in the tabulation above, and a rough value of the computing time per velocity calculated from these data are (for 1200 lifting elements):

upper surface      0.236 second/velocity  
lower surface      0.233 second/velocity.

CDC 6600 Computer

Calculations similar to those described above were done for the NACA 65<sub>1</sub>-212 airfoil with 35° sweep on the CDC 6600 computer at the Air Force Geophysics Laboratory, Hanscom AFB, Massachusetts.

PBOXC calculations required to prepare plots of the digital description of the airfoil, which is comprised of 551 elements, required 22 seconds of CPU time. (PBOXC processing of the 1200 elements of the unswept wing required 21 seconds of CPU time on the CDC 6600 computer.)

Trajectory calculations, for the water drop of diameter 48  $\mu\text{m}$ , required the following:

<u>Angle of Attack (deg.)</u>	<u>Upper or Lower Surface</u>	<u>Number of Trajectories</u>	<u>Number of Velocity Calculations</u>	<u>CPU Time (sec.)</u>
0	Upper	5	2824	1039
4.3	Upper	7	3058	1102
0	Lower	7	3514	1273
4.3	Lower	6	4245	1588

From these data we compute the following rough estimates of computing time per velocity (for 551 elements):

upper surface	0.364 second/velocity
lower surface	0.369 second/velocity

### Discussion

As discussed on p. 13 above, the complexity of, and hence the time required for, calculation of a velocity contribution from a particular element increases as separation between the calculation point and the element decreases, according to which of three classifications, far field, intermediate field or near field, the separation distance falls into. Since in the tangent trajectory calculations described above the distance of each element from each calculation point changes with each time step during integration of the particle equations of motion, we have a changing mixture of far field, intermediate field and near field velocity contribution calculations, so that it would be difficult to extract from the results generally meaningful information on calculation time required per element per velocity. The reader should be aware that the calculation time is sensitive to the mixture of far, intermediate and near field elements (as well as total number of elements), and this mixture and its change with time during trajectory calculation will be determined by the geometry of the particular problem.

Calculation time is also sensitive to particle size, particularly in curved flow fields. For large (i.e., massive) particles, which possess sufficient inertia to substantially ignore complexities in the flow field, trajectory calculations require few velocity calculations and hence little computer time. On the other hand, very small particles closely follow the flow streamlines, which requires small time steps and much more computer time.

## EXAMPLE PROBLEM

### GENERAL DISCUSSION

Example card input data and printouts are given below for programs DUGLFT and FLOPNT. Example problem input data, printouts and computation times for the other codes are given in reference 2 for the nonlifting code.

### THE TEST BODY

The test body is a simple, hollow, box fuselage with airfoils attached (Fig. 13). The body is constructed of two nonlifting sections (fuselage), and one lifting section (airfoil), with one symmetry plane. The airfoil consists of four lifting strips, including an extra strip that extends through the fuselage to the symmetry plane, each with ten on-body elements plus three wake elements. This is the same test body described by Mack for the McDonnell Douglas lifting code (ref. 6).

### EXAMPLE PROBLEM CALCULATION

The example calculations are for the test body with a ten-degree nose-up angle of attack. The step function and pressure equality options are selected, and semi-infinite final wake elements are used. Flow velocities at six off-body points are calculated by PGM DUGLFT, and calculations for these same points are repeated by PGM FLOPNT.

The data set stored on unit 18 by DUGLFT may be saved (catalogued) such as to be available to FLOPNT during a separate run.

### CALCULATION TIMES

CPU times for the test problem are (seconds):

	<u>CYBER 750</u>
PBOXC	1.27
DUGLFT	4.48
FLOPNT	0.23

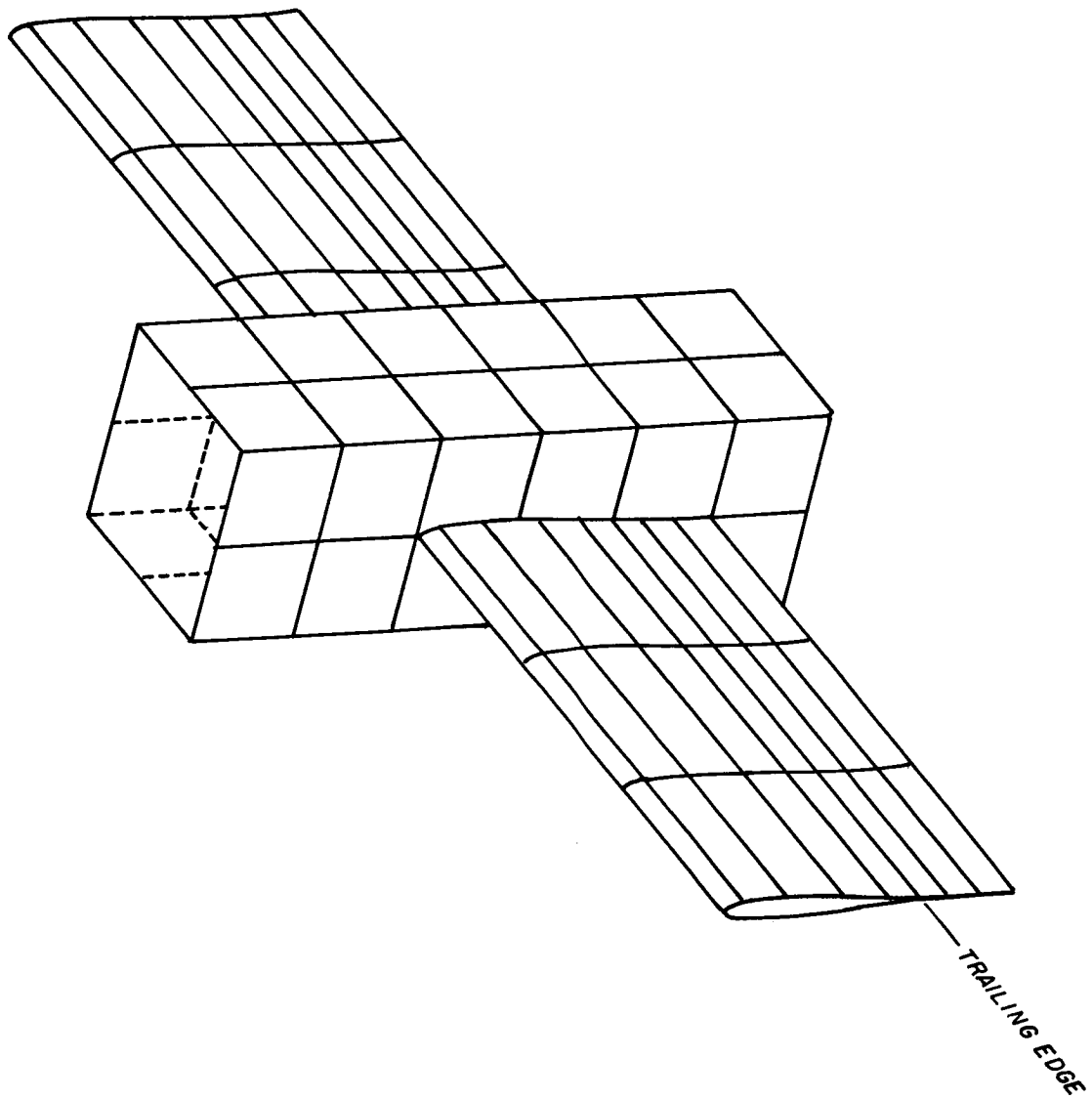


Figure 13. Test problem body for the Hess lifting code (ref. 6).

STORAGE

High-speed access storage required for the test problem are (decimal):

	<u>CYBER 750</u> <u>(kilo words)</u>
PROXC	27
DUGLFT	29
FLOPNT	18



Listing of No. 12 Data Cards for the DUGLFT Test Problem

Columns:	11	21	32	34		
	↓	↓	↓	↓		
		0.5	2		WSQF	7
	0.5	0.5			WSQF	8
	0.5				WSQF	9
0.5		0.5	1		WSQF	10
0.5	0.5	0.5			WSQF	11
0.5	0.5				WSQF	12
1.0		0.5	1		WSQF	13
1.0	0.5	0.5			WSQF	14
1.0	0.5				WSQF	15
1.5		0.5	1		WSQF	16
1.5	0.5	0.5			WSQF	17
1.5	0.5	0.0427			WSQF	18
2.0		0.5	1		WSQF	19
2.0	0.5	0.5			WSQF	20
2.0	0.5				WSQF	21
2.5		0.5	1		WSQF	22
2.5	0.5	0.5			WSQF	23
2.5	0.5				WSQF	24
3.0		0.5	1		WSQF	25
3.0	0.5	0.5			WSQF	26
3.0	0.5				WSQF	27
	0.5		2		WSQF	28
	0.5	-0.5			WSQF	29
		-0.5			WSQF	30
0.5	0.5		1		WSQF	31
0.5	0.5	-0.5			WSQF	32
0.5		-0.5			WSQF	33
1.0	0.5		1		WSQF	34
1.0	0.5	-0.5			WSQF	35
1.0		-0.5			WSQF	36
1.5	0.5	-0.0427	1		WSQF	37
1.5	0.5	-0.5			WSQF	38
1.5		-0.5			WSQF	39
2.0	0.5		1		WSQF	40
2.0	0.5	-0.5			WSQF	41
2.0		-0.5			WSQF	42
2.5	0.5		1		WSQF	43
2.5	0.5	-0.5			WSQF	44
2.5		-0.5			WSQF	45
3.0	0.5		1		WSQF	46
3.0	0.5	-0.5			WSQF	47
3.0		-0.5			WSQF	48
2.	3.5		2 1		WSQF	49
1.85	3.5	-.0134			WSQF	50
1.6	3.5	-.0353			WSQF	51
1.3	3.5	-.05			WSQF	52
1.1	3.5	-.0361			WSQF	53
1.	3.5				WSQF	54
1.1	3.5	.0361			WSQF	55
1.3	3.5	.05			WSQF	56
1.6	3.5	.0353			WSQF	57
1.85	3.5	.0134			WSQF	58
2.0	3.5				WSQF	59
2.15	3.5				WSQF	60
2.3	3.5				WSQF	61
2.5	3.5				WSQF	62
2.	2.5		1		WSQF	63
1.85	2.5	-.0134			WSQF	64
1.6	2.5	-.0353			WSQF	65
1.3	2.5	-.05			WSQF	66

1.1	2.5	-.0361		WSQF	67
1.0	2.5			WSQF	68
1.1	2.5	.0361		WSQF	69
1.3	2.5	.05		WSQF	70
1.6	2.5	.0353		WSQF	71
1.85	2.5	.0134		WSQF	72
2.	2.5			WSQF	73
2.15	2.5			WSQF	74
2.3	2.5			WSQF	75
2.5	2.5			WSQF	76
2.0	1.5		1	WSQF	77
1.85	1.5	-.0134		WSQF	78
1.6	1.5	-.0353		WSQF	79
1.3	1.5	-.05		WSQF	80
1.1	1.5	-.0361		WSQF	81
1.0	1.5			WSQF	82
1.1	1.5	.0361		WSQF	83
1.3	1.5	.05		WSQF	84
1.6	1.5	.0353		WSQF	85
1.85	1.5	.0134		WSQF	86
2.0	1.5			WSQF	87
2.15	1.5			WSQF	88
2.3	1.5			WSQF	89
2.5	1.5			WSQF	90
2.0	.5		1	WSQF	91
1.85	.5	-.0134		WSQF	92
1.6	.5	-.0353		WSQF	93
1.3	.5	-.05		WSQF	94
1.1	.5	-.0361		WSQF	95
1.0	.5			WSQF	96
1.1	.5	.0361		WSQF	97
1.3	.5	.05		WSQF	98
1.6	.5	.0353		WSQF	99
1.85	.5	.0134		WSQF	100
2.0	.5			WSQF	101
2.15	.5			WSQF	102
2.3	.5			WSQF	103
2.5	.5			WSQF	104
2.0			1	WSQF	105
1.85		-.0134		WSQF	106
1.6		-.0353		WSQF	107
1.3		-.05		WSQF	108
1.1		-.0361		WSQF	109
1.0				WSQF	110
1.1		.0361		WSQF	111
1.3		.05		WSQF	112
1.6		.0353		WSQF	113
1.85		.0134		WSQF	114
2.0				WSQF	115
2.15				WSQF	116
2.3				WSQF	117
2.5			3	WSQF	118



EXAMPLE PROBLEM PRINTOUTS

DUGLFT

PROGRAM DUGLFT  
CASE WSQF

DOUGLAS AIRCRAFT COMPANY  
MODIFIED BY H.G. NORMENT, ATMOSPHERIC SCIENCE ASSOCIATES, BEDFORD, MASS.

PAGE 1.

WSQF TEST PROBLEM FOR THE DUGLFT CODE

----- \* -----  
CASE ID --- WSQF  
NO. OF LIFTING SECTIONS --- 1  
NO. OF KUTTA POINTS --- 0  
NO. OF SYMMETRY PLANES --- 1  
NO. OF LEAKY ELEMENTS --- 0  
OFF-BODY POINTS (LLOFF) --- T  
TRANSLATE, SCALE AND ROTATE DATA (IPROS) --- F  
IGNORED ELEMENTS (IGW) --- F  
INFINITE LAST WAKE ELEMENT (LASTWK) --- T  
PRELIMINARY PROCESSING AND LISTING ONLY (LIST) --- F  
PIECEWISE LINEAR OPTION (PESWIS) --- F  
ACCOUNT FOR COMPRESSION EFFECTS (LMACH) --- F  
FLOW TANGENCY KUTTA OPTION (LKUTT) --- F

COMPONENTS OF THE UNIFORM ONSET FLOWS  
( 1) .984R10. 0.000000, .173650

----- \* -----  
OTHER INPUT INFORMATION WILL BE WRITTEN ELSEWHERE IN THE OUTPUT.

DOUGLAS AIRCRAFT COMPANY  
MODIFIED BY H.G. NORMENT, ATMOSPHERIC SCIENCE ASSOCIATES, BEDFORD, MASS.

PROGRAM DUGLFT  
CASE WSQF

WSQF TEST PROBLEM FOR THE DUGLFT CODE

-----\*

BEGIN THE SUBROUTINE INPUT.

BEGIN THE FORMATION OF ELEMENTS.





WSQF TEST PROBLEM FOR THE DUGLFT CODE

N	M	X			Y			Z			NX			NY			NZ			XO	YO	ZO	D	T	A	TYPE OF ELEMENT
		X	Y	Z	X	Y	Z	X	Y	Z	X	Y	Z	X	Y	Z	X	Y	Z							
1	1	2.00000	1.85000	1.85000	1.85000	2.00000	2.00000	2.00000	2.00000	2.00000	2.00000	2.00000	2.00000	2.00000	2.00000	2.00000	2.00000	2.00000	2.00000	1.92500	3.00000	3.00000	3.0119E-01	1.0113E+00	1.5060E-01	LIFT
2	1	1.85000	1.60000	1.60000	1.60000	1.85000	1.85000	1.85000	1.85000	1.85000	1.85000	1.85000	1.85000	1.85000	1.85000	1.85000	1.85000	1.85000	1.85000	1.72500	3.00000	3.00000	5.0191E-01	1.0310E+00	2.5096E-01	
3	1	1.60000	1.30000	1.30000	1.30000	1.60000	1.60000	1.60000	1.60000	1.60000	1.60000	1.60000	1.60000	1.60000	1.60000	1.60000	1.60000	1.60000	1.60000	1.45000	3.00000	3.00000	6.0072E-01	1.0441E+00	3.0036E-01	
4	1	1.30000	1.10000	1.10000	1.10000	1.30000	1.30000	1.30000	1.30000	1.30000	1.30000	1.30000	1.30000	1.30000	1.30000	1.30000	1.30000	1.30000	1.20000	3.00000	3.00000	4.0096E-01	1.0199E+00	2.0048E-01		
5	1	1.10000	1.00000	1.00000	1.00000	1.10000	1.10000	1.10000	1.10000	1.10000	1.10000	1.10000	1.10000	1.10000	1.10000	1.10000	1.10000	1.10000	1.05000	3.00000	3.00000	2.1263E-01	1.0056E+00	1.0632E-01		
6	1	1.00000	1.00000	1.00000	1.00000	1.00000	1.00000	1.00000	1.00000	1.00000	1.00000	1.00000	1.00000	1.00000	1.00000	1.00000	1.00000	1.00000	1.05000	3.00000	3.00000	2.1263E-01	1.0056E+00	1.0632E-01		
7	1	1.00000	1.00000	1.00000	1.00000	1.00000	1.00000	1.00000	1.00000	1.00000	1.00000	1.00000	1.00000	1.00000	1.00000	1.00000	1.00000	1.00000	1.05000	3.00000	3.00000	2.1263E-01	1.0056E+00	1.0632E-01		
8	1	1.00000	1.00000	1.00000	1.00000	1.00000	1.00000	1.00000	1.00000	1.00000	1.00000	1.00000	1.00000	1.00000	1.00000	1.00000	1.00000	1.00000	1.20000	3.00000	3.00000	4.0096E-01	1.0199E+00	2.0048E-01		
9	1	1.00000	1.00000	1.00000	1.00000	1.00000	1.00000	1.00000	1.00000	1.00000	1.00000	1.00000	1.00000	1.00000	1.00000	1.00000	1.00000	1.00000	1.20000	3.00000	3.00000	4.0096E-01	1.0199E+00	2.0048E-01		
10	1	1.00000	1.00000	1.00000	1.00000	1.00000	1.00000	1.00000	1.00000	1.00000	1.00000	1.00000	1.00000	1.00000	1.00000	1.00000	1.00000	1.00000	1.20000	3.00000	3.00000	4.0096E-01	1.0199E+00	2.0048E-01		
11	2	2.00000	2.15000	2.15000	2.15000	2.00000	2.00000	2.00000	2.00000	2.00000	2.00000	2.00000	2.00000	2.00000	2.00000	2.00000	2.00000	2.00000	2.07500	3.00000	3.00000	3.0000E-01	1.0112E+00	1.5000E-01	WAKE	
12	2	2.15000	2.30000	2.30000	2.30000	2.15000	2.15000	2.15000	2.15000	2.15000	2.15000	2.15000	2.15000	2.15000	2.15000	2.15000	2.15000	2.15000	2.22500	3.00000	3.00000	3.0000E-01	1.0112E+00	1.5000E-01	WAKE	



PROGRAM DUGLFT  
 CASE WSQF  
 MODIFIED BY H.G.NCRMENT, AIRCRAFT COMPANY  
 DOUGLAS AIRCRAFT COMPANY  
 ATMOSPHERIC SCIENCE ASSOCIATES, BEDFORD, MASS.

WSQF TEST PROBLEM FOR THE DUGLFT CODE

N	M	X	Y	Z	X	Y	Z	X	Y	Z	X	Y	Z	NX	NY	NZ	X0	Y0	Z0	D	T	A	TYPE OF ELEMENT
2	12	2.150000	2.300000	2.500000	2.300000	2.500000	2.700000	2.300000	2.500000	2.700000	2.150000	2.300000	2.500000	0.000000	0.000000	0.000000	2.225000	2.000000	2.000000	3.0000E-01	0.000000	0.000000	WAKE
		0.500000	0.500000	0.500000	0.500000	0.500000	0.500000	0.500000	0.500000	0.500000	0.500000	0.500000	0.500000	1.000000	1.000000	1.000000	0.000000	0.000000	0.000000	1.0112E+00	1.5000E-01	1.5000E-01	
13		2.300000	2.500000	2.700000	2.500000	2.700000	2.900000	2.300000	2.500000	2.700000	2.300000	2.500000	2.700000	0.000000	0.000000	0.000000	2.400000	2.000000	2.000000	4.0000E-01	0.000000	0.000000	WAKE
		0.000000	0.000000	0.000000	0.000000	0.000000	0.000000	0.000000	0.000000	0.000000	0.000000	0.000000	0.000000	1.000000	1.000000	1.000000	0.000000	0.000000	0.000000	2.0000E-01	2.0000E-01	2.0000E-01	
3	1	2.000000	1.850000	1.500000	1.850000	1.500000	1.150000	2.000000	1.850000	1.500000	2.000000	1.850000	1.500000	0.88879	0.000000	0.000000	1.925000	1.000000	1.000000	3.0119E-01	1.0113E+00	1.5060E-01	LIFT
		0.000000	0.000000	0.000000	0.000000	0.000000	0.000000	0.000000	0.000000	0.000000	0.000000	0.000000	0.000000	-0.996034	-0.996034	-0.996034	-0.066700	-0.066700	-0.066700	1.5060E-01	1.5060E-01	1.5060E-01	
2		1.850000	1.600000	1.500000	1.600000	1.500000	1.400000	1.850000	1.600000	1.500000	1.850000	1.600000	1.500000	0.87266	0.000000	0.000000	1.725000	1.000000	1.000000	5.0191E-01	1.0310E+00	2.5096E-01	
		0.000000	0.000000	0.000000	0.000000	0.000000	0.000000	0.000000	0.000000	0.000000	0.000000	0.000000	0.000000	-0.996185	-0.996185	-0.996185	-0.024350	-0.024350	-0.024350	2.5096E-01	2.5096E-01	2.5096E-01	
3		1.600000	1.300000	1.500000	1.300000	1.500000	1.600000	1.300000	1.500000	1.600000	1.300000	1.500000	1.600000	0.48941	0.000000	0.000000	1.450000	1.000000	1.000000	6.0072E-01	1.0441E+00	3.0036E-01	
		0.000000	0.000000	0.000000	0.000000	0.000000	0.000000	0.000000	0.000000	0.000000	0.000000	0.000000	0.000000	-0.998802	-0.998802	-0.998802	-0.042650	-0.042650	-0.042650	3.0036E-01	3.0036E-01	3.0036E-01	
4		1.300000	1.100000	1.500000	1.100000	1.500000	1.300000	1.100000	1.500000	1.300000	1.100000	1.500000	1.300000	-0.69333	0.000000	0.000000	1.200000	1.000000	1.000000	4.0096E-01	1.0199E+00	2.0048E-01	
		0.000000	0.000000	0.000000	0.000000	0.000000	0.000000	0.000000	0.000000	0.000000	0.000000	0.000000	0.000000	-0.997594	-0.997594	-0.997594	-0.043050	-0.043050	-0.043050	2.0048E-01	2.0048E-01	2.0048E-01	
5		1.100000	1.000000	1.500000	1.000000	1.500000	1.100000	1.000000	1.500000	1.100000	1.000000	1.500000	1.100000	-0.33952	0.000000	0.000000	1.050000	1.000000	1.000000	2.1263E-01	1.0056E+00	1.0632E-01	
		0.000000	0.000000	0.000000	0.000000	0.000000	0.000000	0.000000	0.000000	0.000000	0.000000	0.000000	0.000000	-0.940587	-0.940587	-0.940587	-0.018050	-0.018050	-0.018050	1.0632E-01	1.0632E-01	1.0632E-01	
6		1.000000	1.000000	1.500000	1.000000	1.500000	1.000000	1.000000	1.500000	1.000000	1.000000	1.500000	1.000000	-0.33952	0.000000	0.000000	1.050000	1.000000	1.000000	2.1263E-01	1.0056E+00	1.0632E-01	
		0.000000	0.000000	0.000000	0.000000	0.000000	0.000000	0.000000	0.000000	0.000000	0.000000	0.000000	0.000000	-0.940587	-0.940587	-0.940587	-0.018050	-0.018050	-0.018050	1.0632E-01	1.0632E-01	1.0632E-01	
7		1.100000	1.300000	1.500000	1.300000	1.500000	1.100000	1.300000	1.500000	1.300000	1.100000	1.300000	1.500000	-0.69333	0.000000	0.000000	1.200000	1.000000	1.000000	4.0096E-01	1.0199E+00	2.0048E-01	
		0.000000	0.000000	0.000000	0.000000	0.000000	0.000000	0.000000	0.000000	0.000000	0.000000	0.000000	0.000000	-0.997594	-0.997594	-0.997594	-0.043050	-0.043050	-0.043050	2.0048E-01	2.0048E-01	2.0048E-01	
8		1.300000	1.500000	1.600000	1.500000	1.600000	1.300000	1.500000	1.600000	1.500000	1.300000	1.500000	1.600000	0.48941	0.000000	0.000000	1.450000	1.000000	1.000000	6.0072E-01	1.0441E+00	3.0036E-01	
		0.000000	0.000000	0.000000	0.000000	0.000000	0.000000	0.000000	0.000000	0.000000	0.000000	0.000000	0.000000	-0.998802	-0.998802	-0.998802	-0.042650	-0.042650	-0.042650	3.0036E-01	3.0036E-01	3.0036E-01	
9		1.600000	1.850000	1.500000	1.850000	1.500000	1.600000	1.850000	1.500000	1.600000	1.850000	1.500000	1.600000	0.87266	0.000000	0.000000	1.725000	1.000000	1.000000	5.0191E-01	1.0310E+00	2.5096E-01	
		0.000000	0.000000	0.000000	0.000000	0.000000	0.000000	0.000000	0.000000	0.000000	0.000000	0.000000	0.000000	-0.996185	-0.996185	-0.996185	-0.024350	-0.024350	-0.024350	2.5096E-01	2.5096E-01	2.5096E-01	
10		1.850000	2.000000	2.000000	2.000000	2.000000	1.850000	2.000000	2.000000	2.000000	1.850000	2.000000	2.000000	0.88879	0.000000	0.000000	1.925000	1.000000	1.000000	3.0119E-01	1.0113E+00	1.5060E-01	
		0.000000	0.000000	0.000000	0.000000	0.000000	0.000000	0.000000	0.000000	0.000000	0.000000	0.000000	0.000000	-0.996034	-0.996034	-0.996034	-0.066700	-0.066700	-0.066700	1.5060E-01	1.5060E-01	1.5060E-01	

ORIGINAL DATA IS  
 OF POOR QUALITY

WSQF TEST PROBLEM FOR THE DUGLFT CODE

N	M	X			Y			Z			NX			YO			TYPE OF ELEMENT
		X	Y	Z	X	Y	Z	X	Y	Z	NX	NY	NZ	YO	ZO	D	
3	11	2.000000	2.150000	2.150000	2.000000	2.000000	2.000000	0.000000	0.000000	0.000000	0.000000	0.000000	2.075000	3.0000E-01	WAKE		
		1.500000	1.500000	.500000	.500000	.500000	.500000	0.000000	0.000000	0.000000	0.000000	0.000000	1.000000	1.0112E+00			
		0.000000	0.000000	0.000000	0.000000	0.000000	0.000000	0.000000	0.000000	0.000000	0.000000	0.000000	0.000000	1.5000E-01			
12		2.150000	2.300000	2.300000	2.150000	2.150000	2.150000	0.000000	0.000000	0.000000	0.000000	0.000000	2.225000	3.0000E-01	WAKE		
		1.500000	1.500000	.500000	.500000	.500000	.500000	0.000000	0.000000	0.000000	0.000000	0.000000	1.000000	1.0112E+00			
		0.000000	0.000000	0.000000	0.000000	0.000000	0.000000	0.000000	0.000000	0.000000	0.000000	0.000000	0.000000	1.5000E-01			
13		2.300000	2.500000	2.500000	2.300000	2.300000	2.300000	0.000000	0.000000	0.000000	0.000000	0.000000	2.400000	4.0000E-01	WAKE		
		1.500000	1.500000	.500000	.500000	.500000	.500000	0.000000	0.000000	0.000000	0.000000	0.000000	1.000000	1.0198E+00			
		0.000000	0.000000	0.000000	0.000000	0.000000	0.000000	0.000000	0.000000	0.000000	0.000000	0.000000	0.000000	2.0000E-01			
4	1	2.000000	1.850000	1.850000	2.000000	2.000000	2.000000	.088879	1.925000	3.0119E-01	.088879	1.925000	3.0119E-01	3.0119E-01	XTRA		
		.500000	.500000	0.000000	0.000000	0.000000	0.000000	0.000000	0.000000	0.000000	0.000000	0.000000	.250000	5.2219E-01			
		0.000000	-0.134000	-0.134000	0.000000	0.000000	0.000000	-0.996034	-0.006700	7.5299E-02	-0.996034	-0.006700	-0.006700	7.5299E-02			
2		1.850000	1.600000	1.600000	1.850000	1.850000	1.850000	.087266	1.725000	5.0191E-01	.087266	1.725000	5.0191E-01	5.0191E-01			
		.500000	.500000	0.000000	0.000000	0.000000	0.000000	0.000000	0.000000	0.000000	0.000000	0.000000	.250000	5.5945E-01			
		-0.134000	-0.035300	-0.035300	-0.134000	-0.134000	-0.134000	-0.996185	-0.024350	1.2548E-01	-0.996185	-0.024350	-0.024350	1.2548E-01			
3		1.600000	1.300000	1.300000	1.600000	1.600000	1.600000	.048941	1.450000	6.0072E-01	.048941	1.450000	6.0072E-01	6.0072E-01			
		.500000	.500000	0.000000	0.000000	0.000000	0.000000	0.000000	0.000000	0.000000	0.000000	0.000000	.250000	5.8328E-01			
		-0.035300	-0.050000	-0.050000	-0.035300	-0.035300	-0.035300	-0.998802	-0.042650	1.5018E-01	-0.998802	-0.042650	-0.042650	1.5018E-01			
4		1.300000	1.100000	1.100000	1.300000	1.300000	1.300000	-0.693333	1.200000	4.0096E-01	-0.693333	1.200000	4.0096E-01	4.0096E-01			
		.500000	.500000	0.000000	0.000000	0.000000	0.000000	0.000000	0.000000	0.000000	0.000000	0.000000	.250000	5.3870E-01			
		-0.050000	-0.036100	-0.036100	-0.050000	-0.050000	-0.050000	-0.997594	-0.043050	1.0024E-01	-0.997594	-0.043050	-0.043050	1.0024E-01			
5		1.100000	1.000000	1.000000	1.100000	1.100000	1.100000	-0.39552	1.050000	2.1263E-01	-0.39552	1.050000	2.1263E-01	2.1263E-01			
		.500000	.500000	0.000000	0.000000	0.000000	0.000000	0.000000	0.000000	0.000000	0.000000	0.000000	.250000	5.1118E-01			
		-0.036100	0.000000	0.000000	-0.036100	-0.036100	-0.036100	-0.940587	-0.018050	5.3158E-02	-0.940587	-0.018050	-0.018050	5.3158E-02			
6		1.000000	1.100000	1.100000	1.000000	1.000000	1.000000	-0.339552	1.050000	2.1263E-01	-0.339552	1.050000	2.1263E-01	2.1263E-01			
		.500000	.500000	0.000000	0.000000	0.000000	0.000000	0.000000	0.000000	0.000000	0.000000	0.000000	.250000	5.1118E-01			
		0.000000	0.036100	0.036100	0.000000	0.000000	0.000000	.940587	.018050	5.3158E-02	.940587	.018050	.018050	5.3158E-02			
7		1.100000	1.300000	1.300000	1.100000	1.100000	1.100000	-0.693333	1.200000	4.0096E-01	-0.693333	1.200000	4.0096E-01	4.0096E-01			
		.500000	.500000	0.000000	0.000000	0.000000	0.000000	0.000000	0.000000	0.000000	0.000000	0.000000	.250000	5.3870E-01			
		0.036100	.050000	.050000	.036100	.036100	.036100	.997594	.043050	1.0024E-01	.997594	.043050	.043050	1.0024E-01			
8		1.300000	1.600000	1.600000	1.300000	1.300000	1.300000	.048941	1.450000	6.0072E-01	.048941	1.450000	6.0072E-01	6.0072E-01			
		.500000	.500000	0.000000	0.000000	0.000000	0.000000	0.000000	0.000000	0.000000	0.000000	0.000000	.250000	5.8328E-01			
		.050000	.035300	.035300	.050000	.050000	.050000	.998802	.042650	1.5018E-01	.998802	.042650	.042650	1.5018E-01			
9		1.600000	1.850000	1.850000	1.600000	1.600000	1.600000	.087266	1.725000	5.0191E-01	.087266	1.725000	5.0191E-01	5.0191E-01			
		.500000	.500000	0.000000	0.000000	0.000000	0.000000	0.000000	0.000000	0.000000	0.000000	0.000000	.250000	5.5945E-01			
		.035300	.013400	.013400	.035300	.035300	.035300	.996185	.024350	1.2548E-01	.996185	.024350	.024350	1.2548E-01			

WSQF TEST PROBLEM FOR THE DUGLFT CODE

N	M	X Y Z	X Y Z	X Y Z	X Y Z	X Y Z	NX NY NZ	X0 Y0 Z0	D T A	TYPE OF ELEMENT
4	10	1.850000 .500000 .013400	2.000000 0.000000 0.000000	2.000000 0.000000 0.000000	1.850000 0.000000 -0.13400	.088979 0.000000 .996034	1.925000 .250000 -0.06700	3.0119E-01 5.2219E-01 7.5299E-02	XTRA	
	11	2.000000 .500000 0.000000	2.150000 0.000000 0.000000	2.150000 0.000000 0.000000	2.000000 0.000000 0.000000	0.000000 0.000000 1.000000	2.075000 .250000 0.000000	3.0000E-01 5.2202E-01 7.5000E-02	WAKE	
	12	2.150000 .500000 0.000000	2.300000 0.000000 0.000000	2.300000 0.000000 0.000000	2.150000 0.000000 0.000000	0.000000 0.000000 1.000000	2.225000 .250000 0.000000	3.0000E-01 5.2202E-01 7.5000E-02	WAKE	
	13	2.300000 .500000 0.000000	2.500000 0.000000 0.000000	2.500000 0.000000 0.000000	2.300000 0.000000 0.000000	0.000000 0.000000 1.000000	2.400000 .250000 0.000000	4.0000E-01 5.3852E-01 1.0000E-01	WAKE	

\*\*\*\*\*

\*\*\*\*\*

FINISH THE FORMATION OF ELEMENTS.

PROGRAM DUGLFT DOUGLAS AIRCRAFT COMPANY  
 CASE WSQF MODIFIED BY H.G.NORMENT, ATMOSPHERIC SCIENCE ASSOCIATES, BEDFORD, MASS.

WSQF TEST PROBLEM FOR THE DUGLFT CODE

TABLE OF INPUT INFORMATION

INPUT SECTION NO.	SECTION TYPE	TOTAL NO. OF ELEMENTS IN EACH SECTION	IXFLAG	STRIP NO.	SOURCE ELEMENTS IN THE STRIP	WAKE ELEMENTS IN THE STRIP
1	NL	12	0	1	2	0
				2	2	0
				3	2	0
				4	2	0
				5	2	0
				6	2	0
2	NL	12	0	7	2	0
				8	2	0
				9	2	0
				10	2	0
				11	2	0
				12	2	0
3	L	39	3	13	10	3
				14	10	3
				15	10	3
				16	10	3

TOTAL NO. OF ELEMENTS INPUT = 63 (NOT COUNTING EXTRA STRIP ELEMENTS)

TOTAL NO. OF OFF BODY POINTS = 6

END OF THE SUBROUTINE INPUTL.

END OF THE STOR18 ROUTINE

END OF THE CKARRY ROUTINE

DOUGLAS AIRCRAFT COMPANY  
MODIFIED BY H.G. NORMENT, ATMOSPHERIC SCIENCE ASSOCIATES, BEDFORD, MASS.

PROGRAM DUGLFT  
CASE WSQF

WSQF TEST PROBLEM FOR THE DUGLFT CODE

-----\*

BEGINNING THE VIJMX ROUTINE

-----\*

BODY SECTION NO. = 1    TYPE = NL    TOTAL NO. OF POINTS = 12    NO. OF STRIPS = 6  
TOTAL NO. OF CONTROL POINTS ( INCL. OFF BODY POINTS ) = 60  
TOTAL NO. OF ELEMENTS IN THE NON-LIFTING SECTION = 12

PROGRAM DUGLFT  
CASE WSQF

DOUGLAS AIRCRAFT COMPANY  
MODIFIED BY H.G.NORMENT, ATMOSPHERIC SCIENCE ASSOCIATES, BEDFORD, MASS.

WSQF TEST PROBLEM FOR THE DUGLFT CODE

----- \* -----  
BODY SECTION NO. = 2      TYPE = NL      TOTAL NO. OF POINTS = 12      NO. OF STRIPS = 6  
TOTAL NO. OF CONTROL POINTS ( INCL. OFF BODY POINTS ) = 60  
TOTAL NO. OF ELEMENTS IN THE NON-LIFTING SECTION = 12

PROGRAM DUGLFT  
CASE WSQF

MODIFIED BY H.G.NORMENT, ATMOSPHERIC SCIENCE ASSOCIATES, BEDFORD, MASS.

PAGE 13.

DUGLAS AIRCRAFT COMPANY

WSQF TEST PROBLEM FOR THE DUGLFT CODE

----- \* -----  
BODY SECTION NO. = 3      TYPE = L      TOTAL NO. OF POINTS = 39      NO. OF STRIPS = 3

THE FINAL STRIP OF THIS SECTION IS AN EXTRA STRIP

----- \* -----  
LIFTING SECTION NO. 1      NO. OF SOURCE ELEMENTS PER STRIP 10  
NO. OF WAKE ELEMENTS 3      TOTAL NO. OF ELEMENTS PER STRIP 13  
TOTAL NO. OF CONTROL POINTS ( INCL. OFF BODY POINTS ) = 60  
LIFTING STRIP NO. 1, NO. OF IGNORE ELEMENTS 0  
LIFTING STRIP NO. 2, NO. OF IGNORE ELEMENTS 0  
LIFTING STRIP NO. 3, NO. OF IGNORE ELEMENTS 0  
TOTAL NO. OF ELEMENTS IN THE LIFTING SECTION = 39

PROGRAM DUGLFT DOUGLAS AIRCRAFT COMPANY  
MODIFIED BY H.G.NORMENT, ATMOSPHERIC SCIENCE ASSOCIATES, BEDFORD, MASS.

CASE WSQF

WSQF TEST PROBLEM FOR THE DUGLFT CODE  
NO. OF FAR ELEMENTS = 1752 NO. OF INTERMEDIATE ELEMENTS = 2665 NO. OF NEAR ELEMENTS = 4703

END OF THE VIJMX ROUTINE  
END OF THE STEPFN ROUTINE

TOTAL NO. OF GENERATED ONSET FLOWS PLUS INPUT FLOWS IS 4

----- \* ----- \* -----

END OF THE UNIFLO ROUTINE  
END OF THE VMATRX ROUTINE  
END OF THE AIJMX ROUTINE  
END OF THE NIKMX ROUTINE

THE 54 X 54 MATRIX WITH 4 RIGHT SIDES WAS SOLVED DIRECTLY IN COLSOL  
END OF THE SIGNAL ROUTINE  
END OF THE PKUTTA ROUTINE  
END OF THE SUMSIG ROUTINE

DOUGLAS AIRCRAFT COMPANY  
MODIFIED BY H.G.NORMENT, ATMOSPHERIC SCIENCE ASSOCIATES, BEDFORD, MASS.

. PROGRAM DUGLFT  
CASE WSQF

WSQF TEST PROBLEM FOR THE DUGLFT CODE  
UNIFORM ONSET FLOW = ( .984810E+00, 0. , .173650E+00 )

FINAL OUTPUT FOR THE FOLLOWING ANGLE OF ATTACK

( .984810, 0.000000, .173650 )

PROGRAM DUGLFT DOUGLAS AIRCRAFT COMPANY  
MODIFIED BY H.G.NORMENT, ATMOSPHERIC SCIENCE ASSOCIATES, BEDFORD, MASS.

CASE WSQF

WSQF TEST PROBLEM FOR THE DUGLFT CODE

UNIFORM ONSET FLOW = ( .984810E+00, 0. , .173650E+00 )

ON - BODY POINTS FINAL OUTPUT

N	M	XO	YO	ZO	VX	VY	VZ	VT	VTSQ	CP	DCX	DCY	DCZ	NX	NY	NZ	SIG	VN	AREA
1	1	.250000	.250000	.500000	1.082733	-.072804	.000000	1.085178	1.177610	-.177610	.997747	-.057090	.000000	0.000000	0.000000	0.000000	-.042314		
2		.250000	.500000	.250000	1.018595	-.000000	.349642	1.076933	1.159785	-.159785	.945829	-.000000	.324665	0.000000	1.000000	0.000000	.009766		

\*\*\*\*\*

THE FORCE COMPONENTS OF THIS STRIP ARE 0. .399462E-01 .444026E-01

THE MOMENT COMPONENTS OF THIS STRIP ARE .111409E-02 -.111006E-01 .998655E-02

\*\*\*\*\*

2	1	.750000	.250000	.500000	1.064650	-.084917	.000000	1.068031	1.140691	-.140691	.996834	-.079508	.000000	0.000000	0.000000	0.000000	-.046423		
2		.750000	.500000	.250000	1.061187	.000000	.437973	1.148015	1.317940	-.317940	.924367	.000000	.381505	0.000000	1.000000	0.000000	.011598		

\*\*\*\*\*

THE FORCE COMPONENTS OF THIS STRIP ARE 0. .794849E-01 .351726E-01

THE MOMENT COMPONENTS OF THIS STRIP ARE -.110781E-01 -.263795E-01 .596137E-01

\*\*\*\*\*

3	1	1.250000	.250000	.500000	1.091786	-.044078	.000000	1.092675	1.193939	-.193939	.999186	-.040340	.000000	0.000000	0.000000	0.000000	-.037236		
2		1.246263	.500000	.260516	1.211096	.000000	.312937	1.250873	1.584684	-.584684	.958201	.000000	.250174	0.000000	1.000000	0.000000	-.003100		

\*\*\*\*\*

THE FORCE COMPONENTS OF THIS STRIP ARE 0. .135143E+00 .464848E-01

THE MOMENT COMPONENTS OF THIS STRIP ARE -.230857E-01 -.606060E-01 .168426E+00



PROGRAM DUGLFT \*\*\*\*\*  
 MODIFIED BY H.G.NORMENT, ATMOSPHERIC SCIENCE ASSOCIATES, BEDFORD, MASS.  
 CASE WSQF

WSQF TEST PROBLEM FOR THE DUGLFT CODE

UNIFORM ONSET FLOW = ( .984810E+00, 0. , .173650E+00 )

ON - BODY POINTS FINAL OUTPUT

N	M	XO	YO	ZO	VX	VY	VZ	VT	VTSQ	CP	DCX	DCY	DCZ	NX	NY	NZ	SIG	AREA	
7	1	.250000	.500000	-.250000	.937565	.000000	.339867	.997265	.994537	.005463	.940136	.000000	.340799	0.000000	1.000000	0.000000	-.008576	.000000	.250000
7	2	.250000	.250000	-.500000	.883769	.066041	.000000	.886233	.785410	.214590	.997220	.074518	.000000	0.000000	0.000000	-1.000000	.040853	.000000	.250000

\*\*\*\*\*  
 THE FORCE COMPONENTS OF THE SECTION ARE 0. .303430E+00 .148083E+00  
 THE MOMENT COMPONENTS OF THE SECTION ARE -.408203E-01 -.120656E+00 .318535E+00

\*\*\*\*\*  
 THE FORCE COMPONENTS OF THIS STRIP ARE 0.  
 THE MOMENT COMPONENTS OF THIS STRIP ARE .130705E-01 -.134119E-01 -.341411E-03

\*\*\*\*\*  
 THE FORCE COMPONENTS OF THIS STRIP ARE 0.  
 THE MOMENT COMPONENTS OF THIS STRIP ARE .807000E-02 -.324127E-01 -.820268E-02

\*\*\*\*\*  
 THE FORCE COMPONENTS OF THIS STRIP ARE 0.  
 THE MOMENT COMPONENTS OF THIS STRIP ARE .807000E-02 -.324127E-01 -.820268E-02

\*\*\*\*\*  
 THE FORCE COMPONENTS OF THIS STRIP ARE 0.  
 THE MOMENT COMPONENTS OF THIS STRIP ARE .807000E-02 -.324127E-01 -.820268E-02

\*\*\*\*\*

WSQF TEST PROBLEM FOR THE DUGLFT CODE

UNIFORM ONSET FLOW = ( .984810E+00, 0. , .173650E+00 )

ON - BODY POINTS FINAL OUTPUT

N	M	X0	Y0	Z0	VX	VY	VZ	VT	VTSQ	CP	DCX	DCY	DCZ	NX	NY	NZ	SIG	VN	AREA
9	1	1.246283	.500000	-.260516	.829766	-.000000	-.278171	.875151	.765890	.234110	.948140	-.000000	.317854	0.000000	1.000000	0.000000	.006754	-.000000	.239325
2	1	-.250000	.250000	-.500000	.899020	.034098	.809399	.899666	.803790	.190601	.999282	.000000	.000000	0.000000	0.000000	-1.000000	.035490	-.000000	.250000

\*\*\*\*\*

THE FORCE COMPONENTS OF THIS STRIP ARE 0. -.560284E-01 .476501E-01

THE MOMENT COMPONENTS OF THIS STRIP ARE -.268377E-02 -.595627E-01 -.698272E-01

\*\*\*\*\*

10	1	1.753717	.500000	-.260516	.900002	.000000	.183517	.918522	.843682	.156318	.979837	.000000	.199796	0.000000	1.000000	0.000000	-.000494	.000000	.239325
2	1	-.250000	.250000	-.500000	.925406	.034958	.800000	.926066	.857599	.142401	.999287	.000000	.000000	0.000000	0.000000	-1.000000	.023839	-.000000	.250000

\*\*\*\*\*

THE FORCE COMPONENTS OF THIS STRIP ARE 0. -.374108E-01 .356003E-01

THE MOMENT COMPONENTS OF THIS STRIP ARE -.846055E-03 -.623005E-01 -.656080E-01

\*\*\*\*\*

11	1	2.250000	.500000	-.250000	.959292	.000000	.131396	.968249	.937507	.062493	.990749	.000000	.135705	0.000000	1.000000	0.000000	-.005768	.000000	.250000
2	2	2.250000	.250000	-.500000	.961893	.041419	.000000	.962785	.926954	.073046	.999074	.000000	.043020	0.000000	0.000000	-1.000000	.018147	-.000000	.250000

\*\*\*\*\*

THE FORCE COMPONENTS OF THIS STRIP ARE 0. -.156233E-01 .182614E-01

THE MOMENT COMPONENTS OF THIS STRIP ARE .659530E-03 -.410881E-01 -.351524E-01

\*\*\*\*\*  
 PROGRAM DUGLFT DOUGLAS AEROCRAFT COMPANY  
 MODIFIED BY H.G.NORMENT, ATMOSPHERIC SCIENCE ASSOCIATES, BEDFORD, MASS.

CASE WSQF

WSQF TEST PROBLEM FOR THE DUGLFT CODE

UNIFORM ONSET FLOW = ( .984810E+00, 0. , .173650E+00 )

ON - BODY POINTS FINAL OUTPUT

N	M	XO	YO	ZO	VX	VY	VZ	VT	VTSQ	CP	DCX	DCY	DCZ	NX	NY	NZ	SIG	VN	AREA
12	1	2.750000	.981114	.990212	.990212	.990212	.990212	.990212	.990212	.990212	.990212	.990212	.990212	0.000000	0.000000	0.000000	-.004612		
		.500000	.000000	.980519	.980519	.980519	.980519	.980519	.980519	.980519	.980519	.980519	.980519	1.000000	1.000000	1.000000	.000000		
		-.250000	.133920	.019481	.019481	.019481	.019481	.019481	.019481	.019481	.135243	.135243	.135243	0.000000	0.000000	0.000000	.250000		
2	2	2.750000	.997689	.998261	.998261	.998261	.998261	.998261	.998261	.998261	.998261	.998261	.998261	0.000000	0.000000	0.000000	.017967		
		.250000	.033777	.996524	.996524	.996524	.996524	.996524	.996524	.996524	.033836	.033836	.033836	0.000000	0.000000	0.000000	-.000000		
		-.500000	.000000	.003476	.003476	.003476	.003476	.003476	.003476	.003476	.000000	.000000	.000000	-1.000000	-1.000000	-1.000000	.250000		

\*\*\*\*\*  
 THE FORCE COMPONENTS OF THIS STRIP ARE 0. - .487029E-02 .868983E-03  
 THE MOMENT COMPONENTS OF THIS STRIP ARE -.100039E-02 -.238970E-02 -.133933E-01

\*\*\*\*\*  
 THE FORCE COMPONENTS OF THE SECTION ARE 0.  
 THE MOMENT COMPONENTS OF THE SECTION ARE .172699E-01 -.211166E+00 -.19245E+00

\*\*\*\*\*  
 THE FORCE COMPONENTS OF THE SECTION ARE 0.  
 THE MOMENT COMPONENTS OF THE SECTION ARE .172699E-01 -.211166E+00 -.19245E+00

N	M	XO	YO	ZO	VX	VY	VZ	VT	VTSQ	CP	DCX	DCY	DCZ	NX	NY	NZ	SIG	VN	AREA
13	1	1.925000	.944511	.948272	.948272	.948272	.948272	.948272	.948272	.948272	.996033	.996033	.996033	0.000000	0.000000	0.000000	.160013		
		3.000000	-.000358	.893220	.893220	.893220	.893220	.893220	.893220	.893220	-.000377	-.000377	-.000377	0.000000	0.000000	0.000000	-.000000		
		-.006700	.084375	.100780	.100780	.100780	.100780	.100780	.100780	.100780	.080979	.080979	.080979	-.996034	-.996034	-.996034	.150597		
2	2	1.725000	.973884	.977654	.977654	.977654	.977654	.977654	.977654	.977654	.996145	.996145	.996145	.087266	.087266	.087266	.139484		
		3.000000	.06907	.955806	.955806	.955806	.955806	.955806	.955806	.955806	.080009	.080009	.080009	0.000000	0.000000	0.000000	-.000000		
		-.024350	.095312	.044194	.044194	.044194	.044194	.044194	.044194	.044194	.087262	.087262	.087262	-.996185	-.996185	-.996185	.250957		
3	3	1.450000	.964833	.966201	.966201	.966201	.966201	.966201	.966201	.966201	.998583	.998583	.998583	.048941	.048941	.048941	.135484		
		3.000000	.020196	.933545	.933545	.933545	.933545	.933545	.933545	.933545	.020903	.020903	.020903	0.000000	0.000000	0.000000	-.000000		
		-.042650	.047277	.066455	.066455	.066455	.066455	.066455	.066455	.066455	.048931	.048931	.048931	-.998802	-.998802	-.998802	.300360		
4	4	1.200000	.831769	.834063	.834063	.834063	.834063	.834063	.834063	.834063	.997249	.997249	.997249	-.069333	-.069333	-.069333	.152146		
		3.000000	.021928	.695661	.695661	.695661	.695661	.695661	.695661	.695661	.026290	.026290	.026290	0.000000	0.000000	0.000000	-.000000		
		-.043050	-.057808	.304339	.304339	.304339	.304339	.304339	.304339	.304339	-.069309	-.069309	-.069309	-.997594	-.997594	-.997594	.200482		
5	5	1.050000	.138854	.148514	.148514	.148514	.148514	.148514	.148514	.148514	.934953	.934953	.934953	-.339552	-.339552	-.339552	.222189		
		3.000000	.016231	.022056	.022056	.022056	.022056	.022056	.022056	.022056	.109286	.109286	.109286	0.000000	0.000000	0.000000	-.000000		
		-.018050	-.050126	.977944	.977944	.977944	.977944	.977944	.977944	.977944	-.337518	-.337518	-.337518	-.940587	-.940587	-.940587	.106317		

WSQF TEST PROBLEM FOR THE DUGLFT CODE

UNIFORM ONSET FLOW = ( .984810E+00, 0. , .173650E+00 )

		ON - BODY POINTS			FINAL OUTPUT					
N	M	X0	VX	VT	DCX	NX	SIG	YN	AREA	
		Y0	VY	VTSQ	DCY	NY				
		Z0	VZ	CP	DCZ	NZ				
13	6	1.050000	1.728045	1.837238	.940567	-.339552	-.154148			
		3.000000	.012035	3.375442	.006551	0.000000	-.000000			
		.018050	.623824	-2.375442	.339545	.940587	.106317			
7		1.200000	1.395135	1.398528	.997574	-.069333	-.139951			
		3.000000	.008799	1.955880	.062292	0.000000	-.000000			
		.043050	.096962	-.995880	.069331	.997594	.200482			
8		1.450000	1.170401	1.171808	.998799	0.48941	-.145558			
		3.000000	.002473	1.373133	.002110	0.000000	-.000000			
		.042650	-.057350	-.373133	-.048941	.998802	.300360			
9		1.725000	1.034171	1.036137	.996190	.087266	-.154607			
		3.000000	-.003443	1.077729	-.003316	0.000000	-.000000			
		.024350	-.090593	-.077729	-.087265	.996185	.250957			
10		1.925000	.944503	.948272	.996025	.088979	-.173960			
		3.000000	-.003998	.899220	-.004216	0.000000	-.000000			
		.006700	-.084376	.100780	-.088978	.996034	.150597			

\*\*\*\*\*

THE FORCE COMPONENTS OF THIS STRIP ARE     -.569644E-01     0.     .749739E+00  
 THE MOMENT COMPONENTS OF THIS STRIP ARE     .224922E+01     -.900956E+00     .170893E+00

		*****			*****			*****		
14	1	1.925000	.947142	.950916	.996031	.088979	.203855			
		2.000000	.002055	.904241	.002161	0.000000	-.000000			
		-.006700	.084611	.095759	.088979	-.996034	.150597			
2		1.725000	.967307	.971026	.996170	.087266	.174824			
		2.000000	.005313	.942892	.005471	0.000000	-.000000			
		-.024350	.084736	.057108	.067265	-.996185	.250957			
3		1.450000	.939474	.940636	.998765	.048941	.166262			
		2.000000	.008084	.884795	.008594	0.000000	-.000000			
		-.042650	.046034	.115205	.048939	-.998802	.300360			
4		1.200000	.765653	.767531	.997553	-.069333	-.181792			
		2.000000	.006327	.569104	.009025	0.000000	-.000000			
		-.043050	-.053213	.410896	-.069330	-.997594	.200482			

PROGRAM DUGLFT DOUGLAS CRAFT COMPANY  
 MODIFIED BY H.G.NORMENT, ATMOSPHERIC SCIENCE ASSOCIATES, BEDFORD, MASS.

CASE WSQF

WSQF TEST PROBLEM FOR THE DUGLFT CODE

UNIFORM ONSET FLOW = ( .984810E+00, 0. , .173650E+00 )

		GN - BODY POINTS						FINAL OUTPUT												
N	M	XO	YO	ZO	VX	VY	VZ	VT	VTSQ	CP	DCX	DCY	DCZ	NX	NY	NZ	SIG	VN	AREA	
14	5	1.050000	2.000000	-.018050	-.028109	.003955	.010147	.030145	.009099	.999091	-.932456	.131208	.336617	-.339552	0.000000	-.940587	0.000000	-.259392	-.000000	.106317
6		1.050000	2.000000	.018050	1.897615	.001935	.685039	2.017479	4.070223	-3.070223	.940587	.000959	.339552	-.339552	0.000000	.940587	0.000000	-.191321	-.000000	.106317
7		1.200000	2.000000	.043050	1.469389	.001018	.102123	1.472934	2.169535	-1.169535	.997593	.006691	.069333	-.069333	0.000000	.997594	0.000000	-.169723	-.000000	.200482
8		1.450000	2.000000	.042650	1.209217	.000551	-.059252	1.210668	1.465718	-1.465718	.998802	.000455	-.048941	.048941	0.000000	.998802	0.000000	-.176530	-.000000	.300360
9		1.725000	2.000000	.024350	1.051679	.000229	-.092127	1.055707	1.114517	-1.114517	.996185	.000217	-.087266	.087266	0.000000	.996185	0.000000	-.190048	-.000000	.250957
10		1.925000	2.000000	.006700	.947144	.000554	-.084612	.950916	.904242	-.057558	.996033	.000583	-.088979	.088979	0.000000	.996034	0.000000	-.217841	-.000000	.150597
*****																				
THE FORCE COMPONENTS OF THIS STRIP ARE												THE MOMENT COMPONENTS OF THIS STRIP ARE								
- .814695E-01												.940201E+00								
.188040E+01												-.113644E+01								
*****																				
15	1	1.925000	1.000000	-.006700	.947082	.004211	.084606	.950863	.904141	.095859	.996024	.004421	.088978	.088979	0.000000	-.996034	0.000000	-.229277	-.000000	.150597
2		1.725000	1.000000	-.024350	.961793	.005720	.084253	.965493	.932177	.067823	.996168	.005924	.087264	.087266	0.000000	-.996185	0.000000	-.197443	-.000000	.250957
3		1.450000	1.000000	-.042650	.921522	.004833	.045155	.922640	.851264	.148736	.998788	.005239	.048941	.048941	0.000000	-.998802	0.000000	-.188269	-.000000	.300360

PROGRAM DUGLFT DOUGLAS AIRCRAFT COMPANY  
 MODIFIED BY H.G.NORMENT, ATMOSPHERIC SCIENCE ASSOCIATES, BEDFORD, MASS.

CASE WSQF

WSQF TEST PROBLEM FOR THE DUGLFT CODE

UNIFORM ONSET FLOW = ( .984810E+00, 0. , .173650E+00 )

ON - BODY POINTS FINAL OUTPUT

N	M	X0	Y0	Z0	VX	VY	VZ	VT	VTSQ	CP	DCX	DCY	DCZ	NX	NY	NZ	SIG	VN	AREA
15	4	1.200000	1.000000	-.043050	.719936	.001335	-.050036	.721674	.520814	.479186	.997592	-.001850	-.069333	-.069333	0.000000	-.997594	-.205266	-.000000	.200482
5	1	1.050000	1.000000	-.018050	-.156508	-.001902	.056500	.166405	.07691	.972309	-.640526	-.011432	.339530	-.339552	0.000000	-.940587	-.289984	-.000000	.106317
6	1	1.050000	1.000000	.018050	2.023847	-.004418	.730609	2.151689	4.629766	-.3.629766	.940585	-.002053	.339551	-.339552	0.000000	.940587	-.221969	-.000000	.106317
7	1	1.200000	1.000000	.043050	1.509769	-.004230	.104929	1.513417	2.290430	-.1.230430	.997590	-.002795	.069332	-.069333	0.000000	-.997594	-.193189	-.000000	.200482
8	1	1.450000	1.000000	.042650	1.221134	-.000300	-.059836	1.222599	1.494748	-.494748	.988802	-.000245	-.048941	.048941	0.000000	.998802	-.198508	-.000000	.300360
9	1	1.725000	1.000000	.024350	1.054746	-.002504	-.092396	1.058788	1.121031	-.1.21031	.996182	-.032365	-.087266	.087266	0.000000	.996185	-.212666	-.000000	.250957
10	1	1.925000	1.000000	.006700	.947086	.003236	-.084606	.950863	.904141	-.003404	.996028	-.003404	-.088978	.088979	0.000000	.996034	-.243269	-.000000	.150597

\*\*\*\*\*  
 THE FORCE COMPONENTS OF THIS STRIP ARE                   -1.03528E+00   0.                   .105439E+01  
 THE MOMENT COMPONENTS OF THIS STRIP ARE               .105439E+01   -.127284E+01                   .103528E+00

\*\*\*\*\*  
 THE FORCE COMPONENTS OF THE SECTION ARE               -.241962E+00   0.                   .274433E+01  
 THE MOMENT COMPONENTS OF THE SECTION ARE             .518401E+01   -.331023E+01                   .437360E+00

PROGRAM DUGLFT DOUGLAS AIRCRAFT COMPANY PAGE 24.  
CASE WSQF MODIFIED BY H.G.NORMENT, ATMOSPHERIC SCIENCE ASSOCIATES, BEDFORD, MASS.

WSQF TEST PROBLEM FOR THE DUGLFT CODE

UNIFORM ONSET FLOW = ( .984810E+00, 0. , .173650E+00 )

ON - BODY POINTS FINAL OUTPUT  
-----

THE FORCE COMPONENTS OF THE ENTIRE BODY ARE -.241962E+00 .177195E+00 .309166E+01  
THE MOMENT COMPONENTS OF THE ENTIRE BODY ARE .516046E+01 -.364205E+01 .563370E+00

\*\*\*\*\*  
\*\*\*\*\*  
\*\*\*\*\*

PROGRAM DUGLFT DOUGLAS AIRCRAFT COMPANY  
 CASE WSQF MODIFIED BY H.G.NORMENT, ATMOSPHERIC SCIENCE ASSOCIATES, BEDFORD, MASS.

WSQF TEST PROBLEM FOR THE DUGLFT CODE  
 UNIFORM ONSET FLOW = ( .984810E+00, 0. , .173650E+00 )

POINTS	OFF - BODY POINTS			FINAL OUTPUT								
	XO	YO	ZO	VX	VY	VZ	VT	VTSQ	CP	DCX	DCY	DCZ
1	.250000	.250000	1.000000	1.051998	-.022314	.142048	1.061780	1.127376	-.127376	.990788	-.021015	.133783
2	.250000	.250000	5.000000	.993506	-.000470	.168271	1.007655	1.015369	-.015369	.985958	-.000467	.166992
3	.250000	.250000	9.000000	.987845	-.00126	.171273	1.002583	1.005173	-.005173	.985300	-.000125	.170832
4	1.450000	2.000000	1.000000	1.053198	-.025967	.136255	1.062292	1.128465	-.128465	.991439	-.024444	.128265
5	1.450000	2.000000	3.000000	1.001623	-.010820	.160405	1.014443	1.029095	-.029095	.987362	-.010666	.158121
6	1.450000	2.000000	5.000000	.992640	-.004413	.166586	1.006531	1.013105	-.013105	.986199	-.004384	.165505

\*\*\*\*\*  
 \*\*\*\*\*  
 \*\*\*\*\*



FLOPNT

BODY IDENTIFIER IS WSQF    NUMBER OF SYMMETRY PLANES= 1    NUMBER OF LIFTING ELEMENTS= 52    NUMBER OF NONLIFTING ELEMENTS= 24

FLOPNT RUN ID --  
 WSO7 TEST PROBLEM FOR THE FLOPNT CODE

INPUT DATA --

INITIAL X= 2.5000E-01 INCREMENT= 0. NUMBER OF VALUES= 1  
 INITIAL Y= 2.5000E-01 INCREMENT= 0. NUMBER OF VALUES= 1  
 INITIAL Z= 1.0000E+00 INCREMENT= 4.0000E+00 NUMBER OF VALUES= 3

X AXIS IS INCREMENTED THIRD  
 Y AXIS IS INCREMENTED SECOND  
 Z AXIS IS INCREMENTED FIRST

\* INDICATES THE POINT IS INSIDE THE BODY

X	Y	Z	VX	VY	VZ	V	CP
.2500000	.2500000	1.0000000	1.0520E+00	-2.2314E-02	1.4205E-01	1.0616E+00	-1.2738E-01
.2500000	.2500000	5.0000000	9.9351E-01	-4.7043E-04	1.6827E-01	1.0077E+00	-1.5369E-02
.2500000	.2500000	9.0000000	9.8785E-01	-1.2573E-04	1.7127E-01	1.0026E+00	-5.1729E-03

\* INDICATES THE POINT IS INSIDE THE BODY

INPUT DATA --

INITIAL X= 1.4500E+00 INCREMENT= 0. NUMBER OF VALUES= 1  
 INITIAL Y= 2.0000E+00 INCREMENT= 0. NUMBER OF VALUES= 1  
 INITIAL Z= 1.0000E+00 INCREMENT= 2.0000E+00 NUMBER OF VALUES= 3

X AXIS IS INCREMENTED THIRD  
 Y AXIS IS INCREMENTED SECOND  
 Z AXIS IS INCREMENTED FIRST

\* INDICATES THE POINT IS INSIDE THE BODY

X	Y	Z	VX	VY	VZ	V	CP
1.4500000	2.0000000	1.0000000	1.0532E+00	-2.5967E-02	1.3625E-01	1.0623E+00	-1.2846E-01
1.4500000	2.0000000	3.0000000	1.0016E+00	-1.0820E-02	1.6049E-01	1.0144E+00	-2.9095E-02
1.4500000	2.0000000	5.0000000	9.9264E-01	-4.4128E-03	1.6659E-01	1.0065E+00	-1.3105E-02

\* INDICATES THE POINT IS INSIDE THE BODY

## APPENDIX A

### PRANDTL-GLAUERT COMPRESSIBILITY CORRECTION

Sears (ref. 15) shows that application of the small perturbation approximation to Euler's equation for subsonic flow results in

$$\beta^2 \phi_{xx} + \phi_{yy} + \phi_{zz} = 0 \quad (A1)$$

where the velocity potential function  $\phi$  is given by

$$\phi = -Ux - \phi \quad (A2)$$

$U$  is uniform free stream speed in the positive  $x$  axis direction,  $\phi$  is perturbation velocity potential function, and if  $N_M$  is free stream Mach number, then

$$\beta^2 = 1 - N_M^2 \quad (A3)$$

Subscripts indicate partial differentiation, for example,  $\phi_{xx} = \partial^2 \phi / \partial x \partial x$ . In terms of perturbation velocity ( $u, v, w$ ), eq. (A1) is

$$\beta^2 u_x + v_y + w_z = 0 \quad (A4)$$

If the body surface is defined by the function  $S(x,y,z) = 0$ , then the surface boundary condition is satisfied by

$$(U + u)S_x + vS_y + wS_z = 0. \quad (A5)$$

The Prandtl-Glauert transformation stretches the coordinate system  $(x,y,z)$  and velocity  $(u,v,w)$  to  $(x,y,z)$  and  $(u,v,w)$  according to

$$\begin{aligned} x &= x/\beta \\ y &= y \\ z &= z \end{aligned} \quad (A6)$$

and

$$\begin{aligned}u &= \beta^2 u \\v &= \beta v \\w &= \beta w\end{aligned}\tag{A7}$$

and the transformed partial derivatives of  $S$  are

$$\begin{aligned}S_x &= \beta S_x \\S_y &= S_y \\S_z &= S_z\end{aligned}\tag{A8}$$

In terms of the transformed quantities eqs. (A4) and (A5) are

$$u_x + v_y + w_z = 0\tag{A9}$$

and

$$(U + u/\beta^2)S_x + vS_y + wS_z = 0\tag{A10}$$

Use and significance of these results in the context of the Hess flow calculation method are as follows. We apply the eq. (A6) transformation to all body surface coordinates as they are first input to the code. This amounts to stretching the body along the  $x$  axis by a factor of  $1/\beta$ . Velocities  $(u, v, w)$  then are calculated for the stretched body, and source strengths are determined for the quadrilateral panels subject to the boundary condition of eq. (A10). From eq. (A9) we see that these velocities satisfy the continuity equation for potential flow. Finally, when velocities in the original coordinate system are recovered, via application of the inverse transformation

$$\begin{aligned}
u &= u/\beta^2 \\
v &= v/\beta \\
w &= w/\beta
\end{aligned}
\tag{A11}$$

they are already corrected as they stand for significant compressibility effects caused by the high Mach number free stream flow.

It should be understood that this compressibility correction is based on application of the small perturbation approximation. As such it assumes that perturbation velocity, pressure and density, and their derivatives, are small relative to the free stream. Thus, for example, the method does not treat compressibility effects caused by locally high Mach number flow.

In addition to the transformation above, there are others that are needed to calculate pressure force and moments on the body. Pressure force,  $\vec{F}$ , on a quadrilateral element is given by

$$\vec{F} = - \vec{n} C_p A
\tag{A12}$$

where  $\vec{n}$  is the unit vector normal to the element surface,  $A$  is the element area, and

$$C_p = 1 - \left| \vec{V}_0 \right|^2$$

where  $\vec{V}_0$  is flow velocity at the element centroid. Both  $\vec{n}$  and  $A$  must be calculated for the original, unstretched body, and they are recovered from quantities computed for the stretched body as follows.

Change our subscript notation such that  $(n_x, n_y, n_z)$  represents components of  $\vec{n}$  in the  $x$ ,  $y$  and  $z$  axis directions. Then we have

$$\begin{aligned}
n_x &= n_x/c \\
n_y &= n_y \beta/c \\
n_z &= n_z \beta/c
\end{aligned}
\tag{A14}$$

where

$$c^2 = n_x^2 + \beta^2(n_y^2 + n_z^2) \quad (A15)$$

Using the notation of Appendix B below, area for nonlifting elements,  $A_{NL}$ , and for lifting elements  $A_L$ , are calculated by the equations

$$A_{NL} = (\xi_3 - \xi_1)(\eta_2 - \eta_4)/2 \quad (A16)$$

and

$$A_L = (\xi_2 - \xi_1 + \xi_3 - \xi_4)(\eta_1 - \eta_3)/2 \quad (A17)$$

These equations can be evaluated from the following general equations for the  $\xi$  and  $\eta$  differences

$$\xi_i - \xi_j = \frac{1}{q} \left[ \beta^2 a_{11}(x_i - x_j) + a_{12}(y_i - y_j) + a_{13}(z_i - z_j) \right] \quad (A18)$$

$$\eta_i - \eta_j = \frac{1}{qc} \left[ \beta^2 a_{21}(x_i - x_j) + (\beta^2 n_z a_{11} - n_x a_{13})(y_i - y_j) + (n_x a_{12} - \beta^2 n_y a_{11})(z_i - z_j) \right] \quad (A19)$$

where

$$q^2 = \beta^2 a_{11}^2 + a_{12}^2 + a_{13}^2 \quad (A20)$$

and the  $a_{kl}$  are transformation matrix elements for transforming coordinates between the flow and element reference frames (see ref. 4, sec. 9.2).

APPENDIX B  
BODY PENETRATION TESTS

INTRODUCTION

A sequence of three sets of tests are applied to each on-body surface element for which the exact source and dipole contribution equations are required to determine if a particle trajectory has penetrated the element surface. In the event that the tests of the first two sequences (see pp. 67-68) fail to eliminate the possibility of penetration, then this means that the plane of the element has been intersected by the trajectory during the current integration time step, and it is the purpose of the sequence 3 tests, which are described in detail in this appendix, to determine if the intersection point lies within or on the boundaries of the element.

Since the particle is sufficiently close to the element centroid that the "exact" equations are being used for the velocity contribution calculations (see ref. 3, sec. 7.4 and ref. 4, sec. 9.52), all coordinates have been transformed to the element reference frame: origin at the element centroid, x and y axes in the plane of the element with the z axis normal to the element plane and positive toward the exterior of the body. Element corner points are defined differently in the element coordinate systems for nonlifting and lifting elements, and therefore, we treat these types of elements separately below.

First we find the line that connects the current particle position with its position at the previous time step, and find the point of intersection of this line in the element plane. Designate the current particle coordinates as  $(x_c, y_c, z_c)$  and the coordinates at the previous time step as  $(x_r, y_r, z_r)$ . Then the line that connects these points may be defined by the ratios,

$$\frac{x - x_c}{x_r - x_c} = \frac{z - z_c}{z_r - z_c} = \frac{y - y_c}{y_r - y_c} \quad (B1)$$

and since in the element coordinate system the element plane is defined by  $z = 0$ , the coordinates of the point of intersection,  $(x_p, y_p, z_p)$ , of this line with the element plane are

$$\left. \begin{aligned} x_p &= x_c - z_c (x_r - x_c)/(z_r - z_c) \\ y_p &= y_c - z_c (y_r - y_c)/(z_r - z_c) \\ z_p &= 0 \end{aligned} \right\} \quad (B2)$$

#### NONLIFTING ELEMENTS

Nonlifting elements are configured as shown in Figure B1 in which the corner points are numbered in accordance with the convention shown on p. 30 above. The element coordinate system is defined such that points 1 and 3 lie on the x axis; point 2 or 4, but not both, also may lie on the x axis.

To determine if point P (Fig. B2) is within or on the element boundaries, consider the m and n<sup>th</sup> neighboring element corner points, and define vectors  $\vec{v}_{mn}$  between these points and  $\vec{v}_{mP}$  between the points m and P as

$$\vec{v}_{mn} = (\xi_n - \xi_m)\vec{i} + (\eta_n - \eta_m)\vec{j} \quad (B3)$$

$$\vec{v}_{mP} = (x_p - \xi_m)\vec{i} + (y_p - \eta_m)\vec{j} \quad (B4)$$

where  $\vec{i}$  and  $\vec{j}$  are unit vectors in the directions of the x and y axes, and the pair (m,n) has values (1,2), (2,3), (3,4) or (4,1). If we take the vector product of  $\vec{v}_{mn}$  with  $\vec{k}$ , the unit vector in the direction of the z axis, we obtain a vector,  $\vec{N}_{mn}$ , in the element plane that is normal to  $\vec{v}_{mn}$

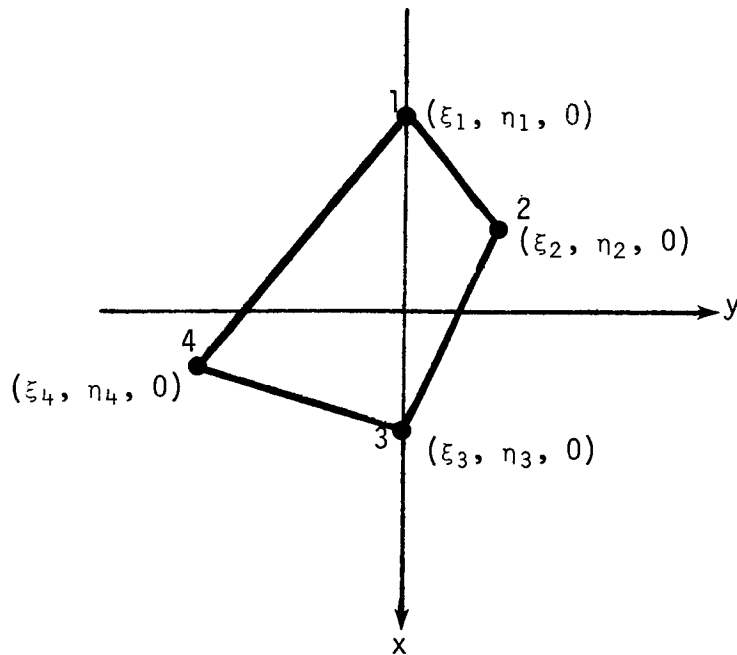


Figure B1. Configuration of a nonlifting element in the element coordinate system. The positive  $z$  axis direction is up from the paper.

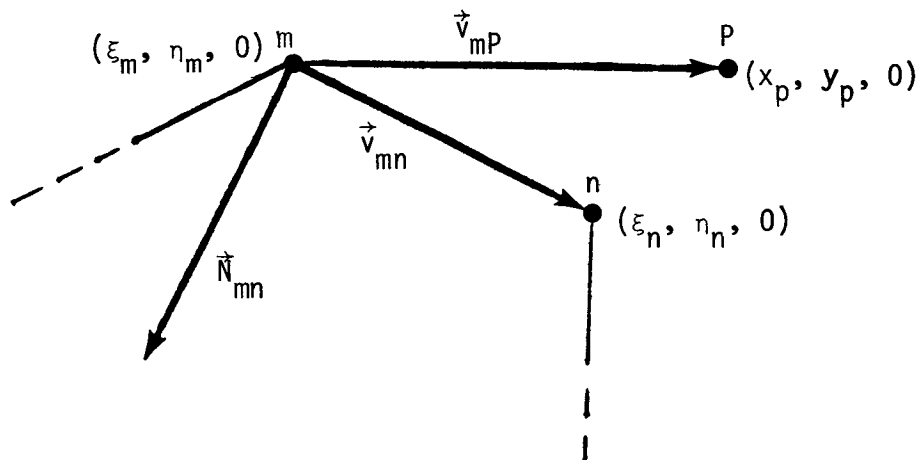


Figure B2. Relationship of element corner points  $m$  and  $n$ , the point  $P$  of intersection of the particle trajectory with the element plane, and vectors  $\vec{v}_{mn}$ ,  $\vec{v}_{mP}$  and  $\vec{N}_{mn}$ .

and is directed toward the interior of the element, given by

$$\vec{N}_{mn} = (\eta_n - \eta_m)\vec{i} - (\xi_n - \xi_m)\vec{j} \quad (B5)$$

Now, if the scalar product,  $S_{mn}$ , of  $\vec{N}_{mn}$  with  $\vec{v}_{mP}$  is negative, the point P must be exterior to the element. Thus we compute

$$S_{mn} = (x_p - \xi_m)(\eta_n - \eta_m) - (y_p - \eta_m)(\xi_n - \xi_m) \quad (B6)$$

successively for the (m,n) pairs given above, and if the relation

$$S_{mn} < 0 \quad (B7)$$

is valid for any (m,n), point P cannot lie on or within the element boundaries. If relation (B7) fails for all of the (m,n), we have proved that P lies on or within the element boundaries, and thus, we have proved that the trajectory intersects the body surface.

#### LIFTING ELEMENTS

Lifting elements are configured in the element coordinate system as shown in Figure B3, with sides 1-2 and 3-4 parallel with the x axis. Thus, it is immediately apparent that point P cannot lie inside or on the element boundaries if  $(y_p - \eta_1) > 0$  or  $(y_p - \eta_3) < 0$ . These tests are combined in the code such that if

$$(y_p - \eta_1)(y_p - \eta_3) > 0 \quad (B8)$$

there can be no impaction.

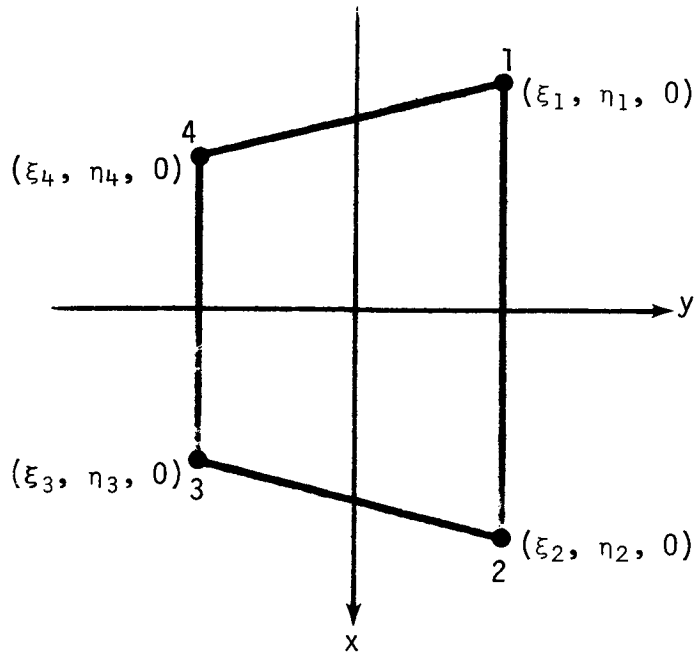


Figure B3. Configuration of a lifting element in the element coordinate system. The positive  $z$  axis is directed up from the paper. The  $x$  axis is approximately parallel with the streamwise direction, and the  $y$  axis is approximately parallel with the spanwise direction of an airfoil.

If relation (B8) is not satisfied,  $P$  lies on or between the line defined by points 1 and 2 and the line defined by points 3 and 4. Then we proceed to see which sides of the lines 2-3 and 4-1  $P$  lies on by applying essentially the same method as was used for the nonlifting element. In terms of the slope,  $M = \Delta x / \Delta y$ , of lines 2-3 and 4-1, we test the relations

$$M_{23} (y_p - y_3) - x_p + \xi_3 < 0 \quad (B9)$$

$$M_{41} (y_p - y_1) - x_p - \xi_1 > 0 \quad (B10)$$

and if either is satisfied,  $P$  cannot lie inside or on the element boundaries. If neither is satisfied, we have proved that  $P$  lies inside or on the boundaries of the element, and thus, we have proved that the trajectory has intersected the body surface.

## APPENDIX C

### SPECIAL SOURCE AND DIPOLE CONTRIBUTION CALCULATIONS

#### INTRODUCTION

Unless precautions are taken numerical problems can arise when velocities are calculated at points very close to element surfaces, to element edges, and for lifting elements, at points close to extensions of element edges. This is because some of the equation terms for exact calculation of source and dipole contributions become infinite at such points. In this appendix we identify the troublesome terms, and describe how the numerical problems are handled in the velocity calculations. The notations of Hess (ref. 3) and Hess and Smith (ref. 4) are used. Our frame of reference is the element coordinate system in which nonlifting and lifting elements are defined as illustrated in Figures B1 and B3 above. Additional definitions are given in Figure C1.

#### GENERAL

If the coordinates of the point for which the velocity calculation is desired are  $(x, y, z)$ , then the distance of this point from the  $i^{\text{th}}$  element corner point is

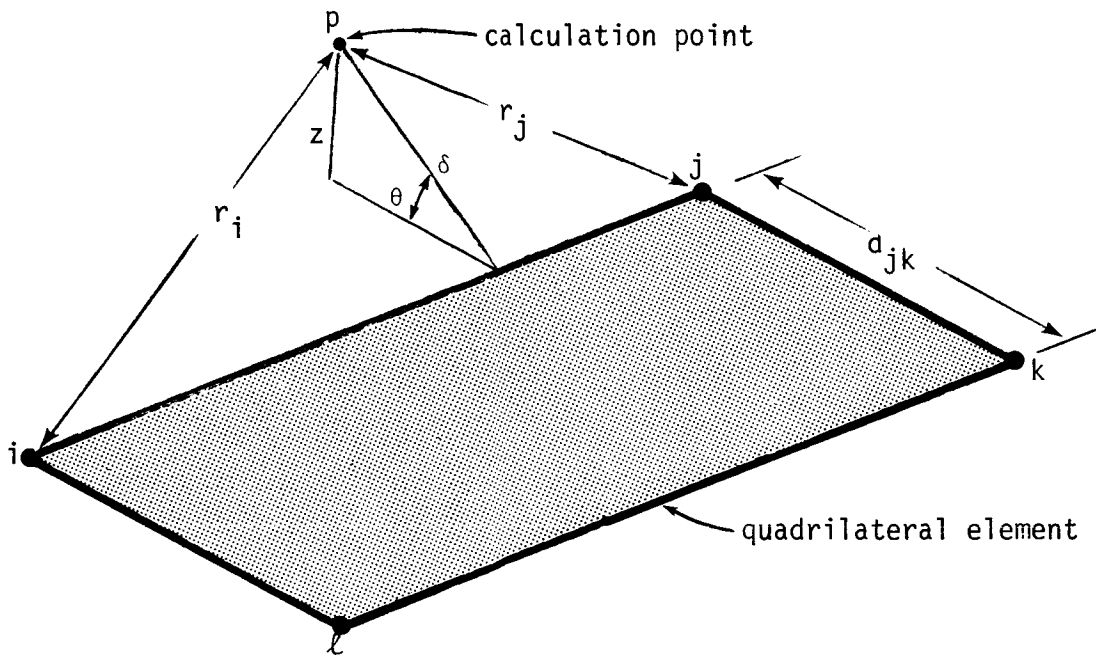
$$r_i = \sqrt{(x - \xi_i)^2 + (y - \eta_i)^2 + z^2} \quad (\text{C1})$$

and for certain purposes the calculation point coordinates relative to the corner point are defined as

$$\alpha_i = (x - \xi_i)/r_i$$

$$\beta_i = (y - \eta_i)/r_i \quad (\text{C2})$$

$$\gamma_i = z/r_i$$



- $z$  Perpendicular distance from calculation point to the plane of the element.
- $\delta$  Perpendicular distance from calculation point to the element edge.
- $\theta$  Angle of perpendicular  $\delta$  with the element plane.
- $r_i$  Distance of calculation point from element corner point  $i$ .
- $d_{jk}$  Distance between corner points  $j$  and  $k$ .

Figure C1. Definitions of some geometric quantities.

If  $r_i$  is very small equations (C2) may blow up, therefore if  $r_i$  is calculated by equation (C1) to be less than  $10^{-3}t$ , where  $t$  is the maximum diagonal of the element, then we set  $r_i = 10^{-3}t$ . That is, we impose the restriction

$$(r_i)_{\min} = 10^{-3}t. \quad (C3)$$

Define quantity  $h_k^{(ij)}$ , which applies to nonlifting (NL) elements, and  $H_k^{(ij)}$  which applies to lifting (L) elements, as

$$h_k^{(ij)} = m_{ij}\alpha_k - \beta_k \quad (C4NL)$$

where

$$m_{ij} = \frac{\eta_j - \eta_i}{\xi_j - \xi_i} \quad (C5NL)$$

and

$$H_k^{(ij)} = M_{ij}\beta_k - \alpha_k \quad (C4L)$$

where

$$M_{ij} = \frac{\xi_j - \xi_i}{\eta_j - \eta_i} \quad (C5L)$$

and  $k = i$  or  $k = j$ . For equations (C4L) and (C5L) we are restricted to (ij) pairs (32) and (41). (See Figures B1 and B3.)

It is easy to show that, as the projection of point  $(x, y, z)$  in the  $z = 0$  plane approaches the straight line that passes through both the  $i^{\text{th}}$  and  $j^{\text{th}}$  element corner points,  $h_k^{(ij)}$  (or  $H_k^{(ij)}$ ) approaches zero. For lifting

elements, as the projection of point  $(x, y, z)$  in the  $z = 0$  plane approaches one of the straight lines that pass through points 1 and 2 or 3 and 4, we have  $\beta_k \rightarrow 0$ .

Finally, it is obvious that as point  $(x, y, z)$  approaches the element plane,  $z \rightarrow 0$ , and usually  $\gamma_k \rightarrow 0$ .

#### SOURCE CONTRIBUTION TERMS

The Hess-Smith method of velocity calculation requires that potential sources be uniformly distributed over the surface of each on-body element. In calculating source velocity contributions from individual elements numerical problems are encountered at points very close to or on element edges, and at general points close to or in the plane of the element.

The  $x$  component of velocity contributed by the distributed source on an element consists of a summation of terms of the form

$$\frac{\eta_j - \eta_i}{d_{ij}} L(ij)$$

where

$$L(ij) = \ln \left( \frac{r_i + r_j - d_{ij}}{r_i + r_j + d_{ij}} \right) \quad (C6)$$

and the  $y$  component consists of a sum of terms of the form

$$\frac{\xi_j - \xi_i}{d_{ij}} L(ij)$$

where

$$d_{ij} = \sqrt{(\xi_j - \xi_i)^2 + (\eta_j - \eta_i)^2} \quad (C7)$$

is the distance between the neighboring  $i^{\text{th}}$  and  $j^{\text{th}}$  element corner points. From equation (C6) it is apparent that as point  $(x, y, z)$  approaches the line connecting the  $i^{\text{th}}$  and  $j^{\text{th}}$  points,  $L^{(ij)} \rightarrow -\infty$ . Thus, we impose the restriction that the minimum value of  $(r_i + r_j - d_{ij})/(r_i + r_j + d_{ij})$  be  $10^{-3}$ ; that is

$$(L^{(ij)})_{\min} = \ln(10^{-3}) \quad (\text{C8})$$

Contribution to the  $z$  component of velocity from an element consists of a summation of terms

$$T_k^{(ij)} = \tan^{-1} \left( \frac{m_{ij} \gamma_k^2 + \alpha_k h_k^{(ij)}}{\gamma_k} \right) \quad (\text{C9NL})$$

$$T_k^{(ij)} = \tan^{-1} \left( \frac{M_{ij} \gamma_k^2 + \beta_k H_k^{(ij)}}{\gamma_k} \right) \quad (\text{C9L})$$

Thus as the point  $(x, y, z)$  approaches the plane of the element,  $\gamma_k \rightarrow 0$  and  $T_k^{(ij)} \rightarrow \pm \pi/2$ . If  $\alpha_k h_k^{(ij)}$  (or  $\beta_k H_k^{(ij)}$ ) also approaches zero, then  $T_k^{(ij)}$  is indeterminate, but the summation is such that indeterminate terms of equal magnitude but opposite sign cancel, so that we simply set the  $T_k^{(ij)}$  to zero. In summary, the following restrictions are imposed.

$$T_k^{(ij)} = \pm \frac{\pi}{2} \quad ; \quad |\gamma_k| < \epsilon, \quad \left. \begin{array}{l} \alpha_k h_k^{(ij)} \\ \beta_k H_k^{(ij)} \end{array} \right\} \geq \epsilon \quad (\text{C10a})$$

$$T_k^{(ij)} = 0 \quad ; \quad |\gamma_k| < \epsilon, \quad \left. \begin{array}{l} \alpha_k h_k^{(ij)} \\ \beta_k H_k^{(ij)} \end{array} \right\} < \epsilon \quad (\text{C10b})$$

where  $\epsilon$  is specified to be  $10^{-4}$  for nonlifting elements and  $10^{-3}$  for lifting elements: the different values being imposed more for convenience than necessity. In equation (C10a) the sign of  $\pi/2$  is taken to be the sign of the product  $\gamma_k \alpha_k h_k^{(ij)}$  (or  $\gamma_k \beta_k H_k^{(ij)}$ ).

It can be shown that the sum of  $T_k^{(ij)}$  terms results in the following values of the z component of velocity,  $v_z$ , contributed by the element for the following calculation points which are a small distance  $\epsilon$  from the plane of the element:

<u>Location of (x, y, <math>\epsilon</math>)</u>	<u><math>v_z</math></u>
1. Inside the boundaries of the element	(sign of $\epsilon$ ) $2\pi$
2. On a line connecting two element corner points	(sign of $\epsilon$ ) $\pi$
3. On an element corner point	(sign of $\epsilon$ ) $\pi/2$
4. Outside the element boundaries	0

The restrictions imposed by equations (C10a) and (C10b) automatically ensure that these results are obtained.

#### DIPOLE CONTRIBUTION TERMS

Hess uses distributed dipoles to represent lift vorticity sheets, and he finds that space partial derivatives of various moments of the dipole distributions are required in computing velocity contributions from the lift vorticity. Numerical problems may arise in computing space derivatives of  $L^{(ij)}$ , which are required for the evaluation of the space derivatives of the  $\phi_{01}$  and  $\phi_{10}$  potential dipole moments, and in computing space derivatives of  $T_k^{(ij)}$ , which are required to evaluate space derivatives of the  $\phi_{00}$  potential dipole moment.

The derivatives of  $L^{(ij)}$  are

$$\frac{\partial L^{(ij)}}{\partial x} = D_{ij}(\alpha_i + \alpha_j), \quad \frac{\partial L^{(ij)}}{\partial y} = D_{ij}(\beta_i + \beta_j), \quad \frac{\partial L^{(ij)}}{\partial z} = D_{ij}(\gamma_i + \gamma_j)$$

where

$$D_{ij} = \frac{2d_{ij}}{(r_i + r_j)^2 - d_{ij}^2} \quad (C11)$$

As point  $(x, y, z)$  approaches the line connecting element corner points  $i$  and  $j$ ,  $D_{ij}$  blows up. Consistent with equation (C8) we impose the restriction that

$$\left[ (r_i + r_j)^2 - d_{ij}^2 \right]_{\min} = 10^{-3} (r_i + r_j + d_{ij})^2 \quad (C12)$$

Space derivatives of  $T_k^{(ij)}$  are given by

$$\frac{\partial T_k^{(ij)}}{\partial x} = -\frac{\gamma_k}{r_k} \left( \frac{\beta_k + \alpha_k P_k^{(ij)}}{\gamma_k + [P_k^{(ij)}]^2} \right) \quad (C13a)$$

$$\frac{\partial T_k^{(ij)}}{\partial y} = \frac{\gamma_k}{r_k} \left( \frac{\beta_k [M_{ij} - P_k^{(ij)}] + H_k^{(ij)}}{\gamma_k + [P_k^{(ij)}]^2} \right) \quad (C13b)$$

$$\frac{\partial T_k^{(ij)}}{\partial z} = \frac{1}{r_k} \left( \frac{[M_{ij} - P_k^{(ij)}] \alpha_k^2 - \beta_k H_k^{(ij)}}{\gamma_k + [P_k^{(ij)}]^2} \right) \quad (C13c)$$

where

$$P_k^{(ij)} = M_{ij} \gamma_k^2 + \beta_k H_k^{(ij)} \quad (C14)$$

It is easily seen for points  $(x, y, \epsilon)$ , where  $\epsilon$  is small or zero, that are not on or very close to element boundary lines or their extensions, (i.e.,  $|\beta_k| \gg 0$  and  $|H_k^{(ij)}| \gg 0$ ), that equations (C13) can be used as given without any trouble. If the calculation point approaches an extension of an element edge line (i.e.,  $\gamma_k \rightarrow 0$ ,  $\beta_k \rightarrow 0$  or  $H_k^{(ij)} \rightarrow 0$ , and  $r_i^2 + r_j^2 - d_{ij}^2 \gg 0$ ), then special equations can be used. However, if an element edge is approached, the only practical response seems to be to set the partial derivatives of eq. (C13) to zero, as is shown below.

The general equation for the derivative of  $\phi_{00}$  with respect to space coordinates  $\Omega$  ( $= x, y$  or  $z$ ) is

$$\frac{\partial \phi_{00}}{\partial \Omega} = - \frac{\partial T_2^{(32)}}{\partial \Omega} + \frac{\partial T_3^{(32)}}{\partial \Omega} + \frac{\partial T_1^{(41)}}{\partial \Omega} - \frac{\partial T_4^{(41)}}{\partial \Omega} \quad (C15)$$

The terms in this equation are most conveniently considered in pairs as is indicated by the  $\psi_{\Omega}^{(ij)}$ . For example,

$$\psi_{\Omega}^{(34)} = \frac{\partial T_3^{(32)}}{\partial \Omega} - \frac{\partial T_4^{(41)}}{\partial \Omega}$$

and so forth. In the following we assume that the line that passes through quadrilateral points  $(ij)$  is very closely approached, where  $(ij)$  is the superscript on  $\psi$ . The quantities  $\delta$  and  $\theta$  are as defined in Figure C1.

Case 1. Calculation point approaches an extension of an element edge:

$$\psi_{\Omega}^{(ij)} = 0 \text{ for } \Omega = x \text{ and } y.$$

$$\psi_z^{(12)} = \left( M_{41} |x - \xi_1|^{-1} - M_{32} |x - \xi_2|^{-1} \right) \sin^2 \theta$$

$$\psi_z^{(34)} = \left( M_{32} \left| x - \xi_3 \right|^{-1} - M_{41} \left| x - \xi_4 \right|^{-1} \right) \sin^2 \theta$$

$$\psi_z^{(ij)} = M_{ij} \left( \left| y - \eta_j \right|^{-1} - \left| y - \eta_i \right|^{-1} \right) \sin^2 \theta; (ij) = (32) \text{ or } (41)$$

(Note: The factor  $\sin^2 \theta$  is missing from these equations, (7.8.5), in reference 3.)

Case 2. Calculation point approaches an element edge:

$$\psi_x^{(ij)} = 0 \text{ for } (ij) = (12) \text{ and } (34).$$

$\delta$  appears in the denominator of the equations for all other  $\psi_{\Omega}^{(ij)}$ .

To accommodate these problems without seriously compromising overall accuracy, for example for particle trajectory calculations, we have selected the following sequence of tests which are applied in order:

1. If  $\left| z/t \right| \geq 10^{-3}$ , bypass the following tests and use equations (C13). Here, as elsewhere,  $t$  is the maximum diagonal of the element.
2. If  $\left| r_{k\beta_k}/t \right| \geq 10^{-3}$  and  $\left| r_{kH_k}^{(ij)}/t \right| \geq 10^{-3}$  use equations (C13).
3. If both of the above tests are negative, then set

$$\frac{\partial T_k^{(ij)}}{\partial x} = \frac{\partial T_k^{(ij)}}{\partial y} = \frac{\partial T_k^{(ij)}}{\partial z} = 0.$$

One additional special calculation is required for semi-infinite wake elements (see section 7.10 of reference 3) which may be needed in calculating space derivatives of  $L^{(ij)}$  such as

$$\frac{\partial L^{(34)}}{\partial x} = \frac{\alpha_4 - 1}{r_4 - (x - \xi_4)} \quad (C16)$$

To prevent blow-up when the denominator becomes very small, we impose the restriction

$$\left[ r_k - (x - \xi_k) \right]_{\min} = 10^{-3} t \quad (C17)$$

where  $t$  is the maximum diagonal of the element.

## REFERENCES

1. Aircraft Icing. A workshop held at Lewis Research Center, Cleveland Ohio, July 19-21, 1978. NASA Conference Publication 2086. FAA-RD-78-109.
2. Norment, H. G.: Calculation of Water Drop Trajectories To and About Arbitrary Three-Dimensional Bodies in Potential Airflow, NASA CR 3291, Aug. 1980.
3. Hess, John L.: Calculation of Potential Flow About Arbitrary Three-Dimensional Lifting Bodies, Report No. MDC J5679-01, Oct. 1972. AD-755 480.
4. Hess, J. L. and Smith, A.M.O.: Calculation of Non-Lifting Potential Flow About Arbitrary Three-Dimensional Bodies, McDonnell Douglas Report E. S. 40622, Mar. 15, 1962. AD-282 255.
5. Hess, J. L. and Smith, A.M.O.: Calculation of Potential Flow About Arbitrary Bodies, Progress in Aeronautical Sciences, Vol. 8, edited by D. Kuchemann, Pergamon Press, New York, 1967.
6. Mack, Dun-Pok: Calculation of Potential Flow About Arbitrary Three-Dimensional Lifting Bodies. Users Manual, Report No. MDC J5679-02, Oct. 1972. AD-755 933.
7. Krogh, F. T.: Variable Order Integrators for Numerical Solutions of Ordinary Differential Equations, Jet Propulsion Lab Technology Utilization Document No. CP-2308, Nov. 1970.
8. Hull, T. E., Enright, W. H., Fellen, B. M. and Sedgwich, A. E.: Comparing Numerical Methods for Ordinary Differential Equations, SIAM J. Numer. Anal., Vol. 9, 1972, p. 603.
9. Davies, C. N.: Definitive Equations for the Fluid Resistance of Spheres, Proc. Phys. Soc. London, Vol. 57, 1945, pp. 259-270.
10. Keim, S. R.: Fluid Resistance to Cylinders in Accelerated Motion, J. Hydraulics Div., Proc. Amer. Soc. Civil Eng., Vol. 6, 1956, paper 1113.
11. Crowe, C. T., Nicholls, J. A. and Morrison, R. B.: Drag Coefficients of Inert and Burning Particles Accelerating in Gas Streams, Ninth Symp. (Int'l) on Combustion, Academic Press, 1963, pp. 395-405.

12. Gunn, R. and Kinser, G. D.: The Terminal Velocity of Fall for Water Droplets in Stagnant Air, J. Meteor., Vol. 6, 1949, pp. 243-248.
13. Beard, K. V.: Terminal Velocity and Shape of Cloud and Precipitation Drops Aloft, J. Atm. Sci., Vol. 33, 1976, p. 851.
14. Norment, H. G.: Collection and Measurement Efficiencies of the EWER Cloud Water Meter for Hydrometeors, AFGL-TR-79-0122, May 11, 1979.
15. Sears, W. R.: Small Perturbation Theory in High Speed Aerodynamics and Jet Propulsion. Vol. VI. General Theory of High Speed Aerodynamics, W. R. Sears, editor, Princeton University Press, 1954.
16. Norment, H. G. and Zalosh, R. G.: Effects of Airplane Flowfields on Hydrometeor Concentration Measurements, AFCRL-TR-74-0602, Dec. 6, 1974. AD-A006 690.
17. Gelder, T. F., Smyers, W. H. and von Glahn, U.: Experimental Droplet Impingement on Several Two-Dimensional Airfoils with Thickness Ratios of 6 to 16 Percent, NACA TN 3839, Dec. 1956.
18. Brun, R. J., Gallagher, H. M., Vogt, D. E.: Impingement of Water Droplets on NACA 65A004 Airfoil and Effect of Change in Airfoil Thickness from 12 to 4 Percent at 4° Angle of Attack, NACA TN 3047, Nov. 1953.



1. Report No. NASA CR-3935		2. Government Accession No.		3. Recipient's Catalog No.	
4. Title and Subtitle  Calculation of Water Drop Trajectories To and About Arbitrary Three-Dimensional Lifting and Nonlifting Bodies in Potential Airflow				5. Report Date October 1985	
				6. Performing Organization Code	
7. Author(s)  Hillyer G. Norment				8. Performing Organization Report No.  None	
				10. Work Unit No.	
9. Performing Organization Name and Address  Atmospheric Science Associates 363 Great Road, P.O. Box 307 Bedford, Massachusetts 01730				11. Contract or Grant No. NAS3-22146	
				13. Type of Report and Period Covered Contractor Report	
12. Sponsoring Agency Name and Address  National Aeronautics and Space Administration Washington, D.C. 20546				14. Sponsoring Agency Code 505-45-54 (E-2687)	
15. Supplementary Notes  Final report. Project Manager, Robert J. Shaw, Propulsion Systems Division, NASA Lewis Research Center, Cleveland, Ohio 44135.					
16. Abstract  Subsonic, external flow about nonlifting bodies, lifting bodies or combinations of lifting and nonlifting bodies is calculated by a modified version of the Hess lifting code. Trajectory calculations can be performed for any atmospheric conditions and for all water drop sizes, from the smallest cloud droplet to large raindrops. Experimental water drop drag relations are used in the water drop equations of motion and effects of gravity settling are included. Inlet flow can be accommodated, and high Mach number compressibility effects are corrected for approximately. Seven codes are described: (1) a code used to debug and plot body surface description data; (2) a code that processes the body surface data to yield the potential flow field; (3) a code that computes flow velocities at arrays of points in space; (4) a code that computes water drop trajectories from an array of points in space; (5) a code that computes water drop trajectories and fluxes to arbitrary target points; (6) a code that computes water drop trajectories tangent to the body; (7) a code that produces stereo pair plots which include both the body and trajectories. Code 1 and codes 3-7 are essentially identical to those described in NASA CR-3291. Code descriptions include operating instructions, card inputs and printouts for example problems. Accuracy of the calculations is discussed, and trajectory calculation results are compared with prior calculations and with experimental data.					
17. Key Words (Suggested by Author(s))  Water drop trajectories; Three-dimensional potential flow; Computer programs; Tangent trajectories; Water drop fluxes; Aircraft icing			18. Distribution Statement  		
19. Security Classif. (of this report) Unclassified		20. Security Classif. (of this page) Unclassified		21. No. of pages 166	22. Price